

INFORMATION TO USERS

The most advanced technology has been used to photograph and reproduce this manuscript from the microfilm master. UMI films the text directly from the original or copy submitted. Thus, some thesis and dissertation copies are in typewriter face, while others may be from any type of computer printer.

The quality of this reproduction is dependent upon the quality of the copy submitted. Broken or indistinct print, colored or poor quality illustrations and photographs, print bleedthrough, substandard margins, and improper alignment can adversely affect reproduction.

In the unlikely event that the author did not send UMI a complete manuscript and there are missing pages, these will be noted. Also, if unauthorized copyright material had to be removed, a note will indicate the deletion.

Oversize materials (e.g., maps, drawings, charts) are reproduced by sectioning the original, beginning at the upper left-hand corner and continuing from left to right in equal sections with small overlaps. Each original is also photographed in one exposure and is included in reduced form at the back of the book.

Photographs included in the original manuscript have been reproduced xerographically in this copy. Higher quality 6" x 9" black and white photographic prints are available for any photographs or illustrations appearing in this copy for an additional charge. Contact UMI directly to order.



University Microfilms International
A Bell & Howell Information Company
300 North Zeeb Road, Ann Arbor MI 48106-1346 USA
313 761-4700 800 521-0600

Order Number 9110954

**Permeability of endothelial monolayers under stationary and
flow conditions**

Casnocha, Susan Amelia, Ph.D.

Rice University, 1990

U·M·I

300 N. Zeeb Rd.
Ann Arbor, MI 48106

NOTE TO USERS

**THE ORIGINAL DOCUMENT RECEIVED BY U.M.I. CONTAINED PAGES
WITH SLANTED AND POOR PRINT. PAGES WERE FILMED AS RECEIVED.**

THIS REPRODUCTION IS THE BEST AVAILABLE COPY.

RICE UNIVERSITY

PERMEABILITY OF ENDOTHELIAL MONOLAYERS
UNDER STATIONARY AND FLOW CONDITIONS

by

SUSAN AMELIA CASNOCHA

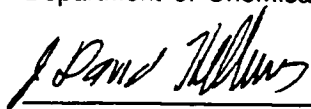
A THESIS SUBMITTED
IN PARTIAL FULFILLMENT OF THE
REQUIREMENTS FOR THE DEGREE

DOCTOR OF PHILOSOPHY

APPROVED, THESIS COMMITTEE



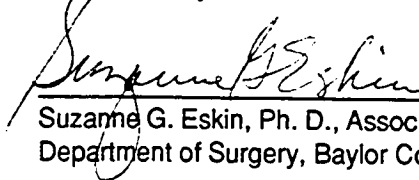
Larry V. McIntire, Ph.D.,
E.D. Butcher Professor, Director
Department of Chemical Engineering, Rice University



J. David Hellums, Ph.D., A.J. Hartsook Professor
Department of Chemical Engineering, Rice University



Kathleen S. Matthews, Ph.D., Chair and Wiess Professor
Department of Biochemistry and Cell Biology,
Rice University



Suzanne G. Eskin, Ph. D., Associate Professor
Department of Surgery, Baylor College of Medicine

Houston, Texas
April, 1990

PERMEABILITY OF ENDOTHELIAL MONOLAYERS

UNDER STATIONARY AND FLOW CONDITIONS

by

SUSAN CASNOCHA

ABSTRACT

In vivo and *ex vivo* studies with whole vessels demonstrated that the endothelium comprises the major permeability barrier in the blood vessel wall. As a lining between the blood and the underlying tissue, the endothelium is exposed to biochemical components of the blood and wall shear stress. The endothelium responds to these biochemical and mechanical agonists both metabolically and morphologically. Using a model system consisting of human umbilical vein endothelial cells cultured on a permeable polycarbonate membrane, the permeability barrier function of endothelial monolayers was characterized quantitatively by determination of permeability coefficients. The effect of biochemical agonists and wall shear stress on permeability was assessed by the extent to which the agonists modulated the baseline permeability coefficient.

Permeability increased nearly 10-fold over baseline values in the presence of 0.1 U/ml thrombin. Using altered forms of thrombin, it was shown that both proteolytic activity and binding to the endothelium are necessary for thrombin to increase permeability. Permeability was unaltered in the presence of 1 μ M bradykinin. Permeability decreased to 25% of baseline during treatment with 6 nM iloprost, a

stable functional analog of the vasodilator and anti-platelet aggregating agent prostacyclin. Prostacyclin often acts through the second messenger cAMP. The permeability also decreased in cells treated with combinations of cAMP analogs and phosphodiesterase inhibitors which act in concert to increase intracellular cAMP concentrations. Another anti-platelet aggregating agent and vasodilator, endothelial derived relaxing factor, acts by increasing intracellular cGMP concentrations. The cGMP analog dibutyl cGMP also decreased endothelial permeability. Pretreatment of endothelial monolayers with iloprost, cAMP analog/phosphodiesterase inhibitor combinations or dibutyl cGMP diminished the permeability increasing effect of thrombin.

A parallel plate flow chamber was used to subject endothelial monolayers cultured on permeable membranes to steady, laminar flow under the condition of no volume flux across the membrane. After 1 hour of 7 dynes/cm² shear stress, permeability increased 7-fold in a partially reversible manner. When cells were pretreated with 6 nM iloprost, the effect of shear stress was diminished to a 2-fold increase which was completely reversible.

ACKNOWLEDGEMENTS

I would like to take this opportunity to thank the people who have helped me during my graduate school career:

Dr. L.V. McIntire for serving as my thesis advisor and providing the setting necessary to accomplish this research,

Dr. J.D. Hellums for serving on my thesis committee,

Dr. K.S. Matthews for serving on my thesis committee,

Dr. S.G. Eskin for providing tissue culture facilities and serving on my thesis committee,

Dr. B. Gillard for tissue culture discussions and advice, Dr. D. Carney for helpful discussions about thrombin and for sharing his supply of modified thrombins, Dr. E. Hall for discussions about prostacyclin and for providing iloprost, Dr. M. Phillips for providing ethylene oxide sterilization facilities, and Dr. G. Downey for providing expertise on polycarbonate membrane coating procedures,

Ms. L. Sturgis for my training in tissue culture techniques and flow loop operation,

Ms. N. Turner, Ms. M. Estrella and Ms. E. Preisinger for assistance in preparing for and performing experiments,

my fellow dark room users, Scott Diamond and Dr. Thomas Chow, for helping me set up my fluorescence detection system,

and most importantly, I thank my husband Keith Jones for his support and encouragement, and my son Evan for making me smile, and both of them for all the times they managed without me.

TABLE OF CONTENTS

Chapter 1: General Introduction

1. A. General Introduction	1
1. B. Physiology Review	8
1. C. Cell Biology Review	11
1. D. Mass Transport Review	18
1. E. Tissue Culture Review	25

Chapter 2: Methods

2. A. Endothelial Cell Culture	29
2. B. Experimental Apparatus	32
2. C. Agonists and Dosage	38
2. D. Experimental Protocol	44
2. E. Scanning Electron Microscopy	49
2. F. LDH Determination	49
2. G. Prostacyclin Determination	50
2. H. Determination of Permeability Coefficients	50
2. I. Percent Recovery Calculation	54
2. J. Statistics	55

Chapter 3: Results

3. A. Substrate Choice	56
------------------------	----

3. B. Time Course of Permeability Coefficient	59
3. C. Permeability Changes in Iloprost-Treated Monolayers	59
3. D. Effect of Thrombin on Permeability	62
3. E. Effect of Bradykinin on Permeability	67
3. F. Cyclic Nucleotide Analog/Phosphodiesterase Inhibitor Permeability Alterations	69
3. G. Inhibition of Thrombin-Induced Permeability Increase	69
3. H. Recovery of Albumin	71
3. I. Effect of Shear Stress on Permeability	71
3. J. Polarity of Prostacyclin Expression	73
Chapter 4: Discussion	
4. A. Model Verification and Application	79
4. B. The Effect of Biochemical Agonists on Permeability	86
4. C. Polarity of Prostacyclin Expression	97
4. D. The Effect of Flow on Permeability	98
4. E. In Vivo Implications	102
Chapter 5: Potential Future Work	
5. A. Co-Culture Systems	107
5. B. Endothelial Derived Relaxing Factor	109
5. C. More Flow Studies	110
5. D. Morphology and Polarity	111
5. E. Practical Applications	112

References	113
Appendix: Transwell permeability coefficient program and sample printout	125

LIST OF FIGURES AND TABLES

Fig. 1. D. 1	Concentration Profile	20
Fig. 1. D. 2	Possible Transendothelial Transport Mechanisms	22
Fig. 1. D. 3	Diffusion Pathway	23
Fig. 2. B. 1	SEM of Polycarbonate Membrane	33
Fig. 2. B. 2	Transwell System	34
Fig. 2. B. 3	Permeable Membrane Flow Chamber	36
Fig. 2. B. 4	Electronics for Fluorescence Detection	37
Fig. 2. C. 1	Flow Loop	41
Fig. 3. A. 1	SEM of HUVEC	57
Fig. 3. A. 2	SEM of BAEC on 3.0 μ m Pore Diameter Membrane	58
Fig. 3. B. 1	Time Course of HUVEC Permeability	60
Fig. 3. B. 2	Time Course of BAEC Permeability	61
Fig. 3. C. 1	Effect of Iloprost on Permeability	63
Fig. 3. D. 1	Effect of Thrombin on Permeability	64
Table 3. D. 1	Effect of Inactivated Thrombins on Permeability	66
Table 3. E. 1	Effect of Bradykinin on Permeability	68
Fig. 3. F. 1	Effect of cAMP on Permeability	70
Fig. 3. I. 1	Effect of Shear Stress on Permeability	72
Fig. 3. I. 2	Shear Stress Controls	74

Fig. 3. J. 1	Polarity of Prostacyclin Expression	75
Fig. 3. J. 2	Polarity by Cord Pool	77
Fig. 3. J. 3	Polarity Controls	78
Table 4. A. 1	In Vitro Permeability Coefficient Comparison	80

CHAPTER ONE: INTRODUCTION

1. A. General Introduction

Endothelial cells line the blood vessel in a single layer, forming an interface between the blood and the underlying tissue. The endothelium is metabolically active, serving important roles in hemostasis, controlling vascular smooth muscle tone (thereby regulating blood pressure), regulating transport of blood components into the tissue, and mediating transendothelial migration of other cell types (i.e. leukocytes (Doukas et al., 1986; Furie and McHugh, 1989; Lawrence et al., 1990) and metastasizing cancer cells (Orr et al., 1988; Castronovo et al., 1989; Knuchel et al., 1988)). The endothelium accomplishes these functions by its capacity to respond to its environment, i.e., through its signal transduction mechanisms, which allow external stimuli to affect changes in gene expression, morphology, and metabolite production and release.

The dynamic endothelium responds to both biochemical and mechanical stimuli provided by the flowing blood. An example of a powerful biochemical stimulus is thrombin, which elicits release of endothelial products such as von Willebrand Factor (vWF, Levine et al., 1982), tissue plasminogen activator (tPA, Levin et al., 1984), prostacyclin (PGI_2 , Weksler et al., 1978), and endothelial derived relaxing factor (EDRF, DeMey and Vanhoutte, 1982). The mechanical stimulus of wall shear stress has also been shown to affect endothelial metabolism, i.e. by increasing PGI_2 (Frangos et al., 1985; Grabowski et al., 1985) and tPA (Diamond et al., 1989) release, upregulating tPA mRNA (Diamond et al., 1990), down regulating endothelin production (S.L. Diamond, personal communication), increasing pinocytosis (Davies et al., 1984), increasing LDL uptake (Sprague et al., 1987), increasing cytosolic calcium (Ando et

al., 1988), and activating a potassium current (Olesen et al., 1988). *Ex vivo* studies have also implicated flow in stimulating increased production of EDRF (Miller et al., 1986; Rubanyi et al., 1986); however, this phenomenon has not been investigated under well-defined fluid dynamic conditions. In addition to metabolic modulations, physiological shear stress results in morphological changes such as alignment in the direction of flow (Eskin et al., 1984), cell migration (Eskin et al., 1989), and alterations in attachment plaque configurations (Eskin et al., 1989). Chronic reductions in blood flow rate result in a significant, endothelium-dependent reduction in artery diameter (both internal and external) which cannot be attributed to long term smooth muscle contraction (Langille and O'Donnell, 1986).

The time course for these flow-dependent effects varies widely. For example, the rate of PGI₂ production is maximal almost instantaneously with the onset of flow. Long term increases in PGI₂ production rates are further enhanced by pulsatile flow of 1 hertz frequency when compared to steady flow at the same mean magnitude (Frangos et al., 1985). Alternately, the increased tPA production is associated with upregulation of that gene (Diamond et al., 1990), requiring four to six hours of shear stress before increased protein synthesis leads to a detectable increase in the rate of release (Diamond et al., 1989). This increased rate of protein synthesis is not affected by pulsatile flow of 1 hertz frequency. Decreased arterial diameters are observed after two weeks of reduced blood flow (Langille and O'Donnell, 1986).

In addition to the above mentioned responses to chemical and mechanical stimuli, alterations in endothelial permeability also occur. The permeability barrier function of the endothelium, assessed by monitoring transendothelial albumin transport, is the focus of this study. The permeability barrier function of the endothelium is important since the blood supplies nutrients to the tissues and removes wastes. Increased permeability to macromolecules and fluid has pathological implications such as

atheroscleotic plaque formation (Navab et al., 1986; Menzoian et al., 1987), brain edema during space flight (Dr. P.A. Whitson, personal communication), and edema during cancer chemotherapy involving IL-2 (Bucana et al., 1988). Alternately, variations in endothelial permeability may be exploited in a positive sense to improve drug delivery. Enhanced drug delivery can be accomplished in a site specific manner by taking advantage of unique organ specific endothelial surface glycoproteins (Belloni and Nicolson, 1988). Drugs intended for specific organs could be conjugated to antibodies for these surface antigens, and their uptake could be further enhanced by designing the drugs with a permeability modulating factor.

This study investigates the role of physiological agonists (both biochemical and mechanical) in permeability alterations, and compares the agonists' effects in a relative manner. No specific disease state was modeled. There was an interest in the permeability barrier function specifically of the endothelium because whole blood vessel studies have demonstrated that the endothelium comprises the major permeability barrier in the vessel wall (Bell et al., 1974; Bratzler et al., 1977; Ramirez et al., 1984). These studies were accomplished by injecting test animals with radiolabelled albumin and allowing this tracer to circulate for a fixed time period before sacrificing the animals. The aorta walls were then serially sectioned and radioactivity determined by gamma counting. From the counts, transmural concentration profiles were determined. Both Bell et al. (1974) and Bratzler et al. (1977) utilized aorta with intact endothelium. They showed that for up to four hours circulating time the concentration gradients from the luminal surface to the media-adventitial border had the greatest slope across the intima. This steep gradient indicates that the endothelium functions as a diffusion barrier. From estimates of intima and media permeability coefficients, Bratzler et al. (1977) concluded that the diffusive resistance of the intimal endothelium is about an order of magnitude greater

that that of the media. This was further demonstrated by Ramirez et al. (1984), who repeated these tracer studies with both endothelial-intact and balloon catheter-deendothelialized rabbit aorta. In the deendothelialized aorta, relatively flat concentration profiles from the luminal surface to the media-adventitial border were seen, indicating a domination of convective flux over diffusive flux. In addition to the altered shape of the concentration profiles, the absolute tissue concentrations of tracer were at least an order of magnitude higher in the deendothelialized vessels.

Since the endothelium is in intimate contact with the blood, there is interest in assessing how blood-borne agonists alter endothelial permeability. For example, *in vivo* and *ex vivo* studies demonstrated increased permeability in response to bradykinin (Mullins, 1986), and histamine (Majno and Palade, 1961), and decreased permeability in response to noradrenaline (Caro and Lever, 1983). However, these studies describe modulation of vascular permeability in which several cell types or vessel wall components may contribute to the permeability barrier, metabolize marker macromolecules, or mediate agonist-induced permeability changes. *In vitro* cell culture systems allow detection of the role of the intimal cellular elements in permeability modulations by studying direct effects of agonists on endothelial permeability (Alexander et al., 1988; Garcia et al., 1986; Killackey et al., 1986; Mizuno-Yagyu et al., 1987). The knowledge gained from such a system can be applied to understanding the more complex issues of vascular permeability.

Using an *in vitro* cell culture permeability model the following items were investigated: post-seeding time dependence of *in vitro* permeability, effects of vasoactive agonists and the second messengers 3',5'-cyclic adenosine monophosphate (cAMP) and 3',5'-cyclic guanosine monophosphate (cGMP) on permeability, effect of physiological wall shear stress on permeability, and permeability modulation interactions between agonists manifesting opposite effects on permeability. Central to

this investigation is the vasodilator and anti-platelet aggregating agent prostacyclin, which is produced by the endothelium in response to bradykinin, thrombin, and wall shear stress stimulation, and which causes increased intracellular cAMP concentration via activation of adenylate cyclase.

Permeability assays were conducted with an *in vitro* system consisting of a monolayer of human umbilical vein endothelial cells (HUVEC) cultured on a permeable polycarbonate substrate. This system served as a simplified model of the blood vessel wall and contained luminal and subluminal compartments. The tracer molecule albumin, a plasma protein, appears to cross the endothelium via cell junctions, as shown by Bottaro et al. (1986a), using glutaraldehyde fixed cells and cells at 4 °C. However, this subject is currently under investigation by at least two groups (Rivero-Hudec and Williams at Thomas Jefferson University, and Kaska and Colton at MIT) using ultrastructural studies. Transendothelial albumin transport was monitored, allowing sequential determinations of mass flux. From the mass flux and concentration gradients, permeability coefficients were calculated. Two systems were used, a system operated under static conditions and a parallel plate flow system operated under steady laminar flow driven by a constant hydrostatic head.

In the static system a post-seeding time exhibiting the lowest baseline permeability was determined for HUVEC, and all subsequent experiments were conducted with monolayers at this time in culture. This dependence on time in culture was verified using another cell line, bovine aortic endothelial cells (BAEC). The effect of PGI₂ on permeability was assessed utilizing a stable PGI₂ analog, iloprost, since PGI₂ has a 3.5 minute half-life in aqueous solutions (Cho and Allen, 1978). Permeability alterations in the presence of compounds which stimulate HUVEC synthesis of PGI₂, thrombin (native and modified forms) and bradykinin, were determined. These agonists also affect many other cell functions. The effect of increased intracellular cAMP on

permeability was determined by treating monolayers with lipid soluble analogs of cAMP (dibutyl cAMP and 8-bromo cAMP) in conjunction with phosphodiesterase inhibitors (IBMX and theophylline). Dibutyl cGMP was used to determine the effect of increased cGMP on permeability. In the flow system, the effect of wall shear stress in the absence of transendothelial convective solute flux was studied.

Endothelium in culture can exhibit a luminal-subluminal polarity which is demonstrated at the level of integral membrane proteins (Muller and Gimbrone, 1986), protein secretion (Unemori et al., 1990; Sporn et al., 1989; Zerwes and Risau, 1987), and fatty acid release (Stoll and Spector, 1987). Because of the differing environments associated with each side of the cell, it is not unexpected for this polarity to exist. The polarity of membrane proteins is favored by the presence of cell junctions, which serve to limit the lateral transport of membrane lipids by the limiting the available "diffusion area" (Tournier et al., 1989).

The polarity of endothelial product release can differ in response to different stimuli. For example, constitutive secretion of vWF and thrombin-stimulated vWF release had no apparent polarity. However, stimulation with calcium ionophore A23187 resulted in 90% release subluminally (Sporn et al., 1989). These investigators have not ruled out the possibility that the lack of polarity in response to thrombin is at least partially due to disruption of the integrity of the monolayer.

Polarity often correlates with function of the product. vWF, which is secreted in both directions, binds to basement membrane constituents and serves as a carrier for factor VIII in the blood. However, extracellular matrix components collagen and fibronectin, and matrix degrading enzymes are polarized in the subluminal direction (Unemori et al., 1990). Polarity was not observed with other vascular cell types, i.e., smooth muscle cells with respect to cell membrane proteins (Muller and Gimbrone, 1986) and fibroblasts with respect to protein secretion (Unemori et al., 1990).

Since endothelial cells exhibit polarity with respect to hemostatic and cell attachment functions, do they also exhibit polarity related to factors used to communicate with smooth muscle cells? A smooth muscle cell and fibroblast chemotactic factor is secreted almost exclusively basolaterally (Zerwes and Risau, 1987). Stoll and Spector (1987) investigated fatty acid transfer between endothelial cells and smooth muscle cells in a co-culture system. They reported polarized release of oleic and arachidonic acids to the lumen and a comparatively slow uptake of these compounds by the smooth muscle cells. However, their experiments were not controlled for fatty acid modulation of endothelial permeability, which could have a significant impact on transport during the 24 hour experiments.

There is evidence that EDRF is released both luminally and subluminally (Bassenge et al., 1987), although the relative amounts have not been quantified. This result does, however, indicate a signal transduction mechanism between endothelial cells and smooth muscle cells. The subject of communication between these cell types has recently been reviewed by Davies et al. (1988). Both humoral and direct contact (through endothelial-smooth muscle gap junctions) mechanisms of communication are discussed. It is unknown which is the dominant transport mechanism for EDRF.

An underlying interest in this study is the possible transport of prostacyclin from the endothelium to the smooth muscle cells, a form of humoral cell-cell communication. Prostacyclin, a vasodilator and anti-platelet aggregating agent, acts synergistically with EDRF (also a vasodilator and anti-platelet aggregating agent) in its anti-thrombogenic function (Radomski et al., 1987b). In addition to the permeability studies, polarity of prostacyclin expression by the endothelium in response to bradykinin was investigated.

As stated earlier, the model system was comprised of human umbilical vein endothelial cells cultured on a permeable polycarbonate substrate. This substrate is

chosen for many *in vitro* transport studies (Aldelda et al., 1988; Garcia et al., 1986; Cooper et al., 1987; Shasby and Shasby, 1986) because it is non-protein binding, has cylindrical straight through pores for rapid transport, is manufactured to consistent standards, and supports good cell growth. However, another widely used support for *in vitro* permeability studies has been Cytodex 3 (Pharmacia, Inc., Piscataway, NJ) microcarrier beads (Killacky et al., 1986; Bottaro et al, 1986a, b), Alexander et al., 1988; Boiadjeva et al., 1984). This technique has the advantage of direct visualization of the cells by light microscopy, but cannot be used for well-defined fluid flow studies.

The findings of this study include: permeability decreases with increasing time in culture; thrombin and wall shear stress increase permeability; and prostacyclin, combinations of cAMP analogs/phosphodiesterase inhibitors, and dibutyryl cGMP decrease permeability. In addition, pretreatment with agents that elevate cAMP inhibit the effect of thrombin and shear stress. Also, bradykinin induced prostacyclin production by HUVEC is not polarized.

1. B. Physiology Review

There are three major types of blood vessels: arteries, which carry blood away from the heart; capillaries, which allow for exchange of nutrients and wastes between the blood and the tissue; and veins, which return blood to the heart. The principal cellular component of capillaries is the endothelium. However, the arteries and veins are comprised of three layers: the intima, consisting of the endothelium and the subendothelial matrix; the media, consisting of smooth muscle cells, elastin, collagen and proteoglycans; and the adventitia, consisting of collagen and elastin fibers and, in larger vessels, the vasa vasorum (small blood vessels that nourish the adventitia).

The endothelium, common to all vessels, presents the major barrier to transport

in large blood vessel walls, as confirmed by *in vivo* and *ex vivo* studies. Using endothelialized and balloon catheter-deendothelialized rabbit descending thoracic aorta, Ramirez et al. (1984) showed that the intact endothelium is the dominant mass transfer resistance for albumin transport across the blood vessel wall. This permeability barrier function varies with location in the vasculature. *In vivo* studies with Yorkshire pigs showed greater radiolabeled albumin uptake in the aortic arch than in the abdominal aortic segments (Bell et al., 1974). Tissue culture studies have shown that while bovine aortic endothelial cells and pulmonary microvessel endothelial cells have similar permeability barrier characteristics, cerebral microvessel endothelial cells are significantly less permeable (Bottaro et al., 1986a). This "form follows function" architecture of the human body is evident in the fenestration of glomerular endothelium versus the formidable blood-brain barrier.

The endothelium must withstand (and react to) many forces and factors within the body, including transmural pressure gradients, shear stress, pulsatile flow and the resulting wall compliance, volume fluxes, and sometimes locally high concentrations of blood-borne components. Mass transport across the blood vessel wall is a function of the magnitude of these various environmental factors. Mass transport studies can be conducted at the level of diffusive transport, active transport, and convective transport. Albumin is not actively transported across the endothelium, and pressure gradients across the monolayers can be eliminated to abolish convective transport. Therefore, passive diffusive transport alone can be studied.

In the work presented herein, both static and dynamic (flow) permeability studies were performed with the dominant transport mechanism being passive diffusion. The static system contained no significant pressure gradients or fluid induced mechanical forces. The flow system was operated with no significant transmural pressure gradients; however, the cells were subjected to 7 dynes/cm² shear stress. This

corresponds approximately to a shear stress level of arterioles. The reason it is interesting to study shear stress is that it is a force uniquely experienced by the endothelium. Other mechanical forces may also influence non-endothelial components of the blood vessel wall. Therefore observed modulations in vascular permeability with these other forces may not directly result from an effect on the endothelium.

A related function to the permeability barrier function of the endothelium is that of regulation of hemostasis. The endothelium prevents blood loss from intact vessels and reduces blood loss from injured vessels. Other vascular cells, especially the platelets, have important functions in hemostasis as well as interacting with the endothelium to help maintain structural integrity (Lo et al., 1988).

The non-thrombogenic endothelium presents an unfavorable surface for platelet adhesion and deposition due to its negative charge, constitutive prostacyclin and EDRF secretion (which act synergistically to inhibit platelet aggregation (Radomski et al., 1987b)), and heparin-like molecules (heparan sulfate) on its surface. In the event of an injury to the blood vessel wall, platelet adhesion and deposition occurs caused by exposure of extracellular matrix proteins (such as collagen, fibronectin, and vWF) and by activation of the coagulation cascade (both intrinsic and extrinsic pathways). The final steps of coagulation, common to both the extrinsic and intrinsic pathways, are activation of thrombin from prothrombin, and the subsequent platelet aggregation and cleavage of soluble fibrinogen to insoluble fibrin. The fibrin polymerizes, and these fibrin polymers provide structural integrity for the clot. The clot is eventually dissolved by the fibrinolytic process, and the injured vessel site is re-endothelialized by cell migration and division.

Damage to the endothelium can initiate both the extrinsic and intrinsic pathways. Release of thromboplastin (a tissue phospholipid) from damaged endothelium activates the extrinsic pathway, and exposure of the subendothelium, rich in collagen and vWF,

promotes the intrinsic pathway. The thrombin produced by the common pathway interacts with the endothelium both in pro-coagulatory and anti-coagulatory ways. First, thrombin stimulates release of endothelial products favorable to coagulation, i.e. vWF, and unfavorable to coagulation, i.e. prostacyclin, EDRF, and tPA (which activates production of the fibrinolytic agent plasmin). Second, receptor-mediated binding of thrombin to the endothelium inhibits further thrombin production and facilitates the deactivation of thrombin by anti-thrombin. There are three receptors on the endothelial surface to which thrombin may bind: thrombomodulin, heparan sulfate, and a 30,000 dalton protein. Thrombin binds reversibly to thrombomodulin. This binding facilitates thrombin activation of protein C and restricts the activity of thrombin toward fibrinogen, factor V, and platelets. Activated protein C, facilitated by protein S on the activated platelet surface, inactivates activated factors V and VIII, resulting in inhibition of thrombin production from prothrombin. Thrombin also binds reversibly to heparan sulfate, which facilitates thrombin inactivation by antithrombin III. Thrombin binds covalently to the 30,000 dalton protein. This receptor-thrombin complex is then endocytosed and degraded (Machovich, 1986).

Therefore, the endothelium acts as more than a predetermined diffusion barrier. It actively responds to its environment in ways that will affect its permeability barrier function. By studying the basic permeability characteristics of the isolated endothelium, a foundation is provided for future, more complex, models of mass transport at the blood vessel wall.

1. C. Cell Biology Review

Endothelial cells are dynamic elements of the blood vessel wall. To serve in the roles of permeability barrier and regulation of hemostasis, the endothelium maintains structural integrity, replicates, migrates, and actively responds to and regulates

factors involved in coagulation and fibrinolytic processes. In addition, endothelial products form the subendothelial matrix and influence smooth muscle tone, growth and metabolism. The subendothelial matrix is composed of the endothelial-produced glycosaminoglycans, such as heparan sulfate and chondroitin sulfate (Wang et al., 1985), and the endothelial produced proteins collagen, laminin and fibronectin (Unemori et al., 1990). Endothelial cells also secrete vasodilators such as PGI_2 and EDRF, the vasoconstrictor peptide endothelin (Yanagisawa et al., 1988), a heparin-like smooth muscle cell growth inhibitor (Castellot et al., 1982), a smooth muscle cell mitogen (Gajdusek et al., 1980), and a humoral factor which results in increased smooth muscle cell metabolism of low density lipoprotein (LDL) in co-culture (Davies et al., 1985).

In order to accomplish these functions, the endothelium senses chemical and mechanical stimuli. The transduction of external stimuli to intracellular signals leads to formation of second messengers (i.e. cyclic AMP, cyclic GMP, calcium ions, inositol trisphosphate (IP_3) and diacylglycerol (DG)), which propagate the signal within the cell. When a stimulus either binds to an external receptor or otherwise perturbs the cell membrane, membrane bound G proteins can be activated (Sibley et al., 1987). G proteins are a family of proteins with many members as yet poorly characterized. There are two G proteins associated with adenylate cyclase, G_s (stimulatory G protein) and G_i (inhibitory G protein) which serve to regulate intracellular cAMP levels. Another set of G proteins regulate the rate of hydrolysis of phosphoinositides, possibly by phospholipase C activation. Phosphoinositide hydrolysis leads to generation of two second messengers: IP_3 , which mobilizes intracellular Ca^{2+} ; and DG, which activates protein kinase C. The second messengers act within the cell, through mechanisms that are just beginning to be elucidated, to cause some observable change in cell metabolism, morphology, or other cell function. One link often involved in this signal transduction

system is the family of protein kinases, which are activated via phosphorylation by different second messengers or at least different concentrations or combinations of second messengers. Regulation of signal transduction can occur at any level within the signal transduction mechanism, from binding of the external receptor to activation/deactivation of the protein kinase. In addition to transmitting external signals in "cellular language", signal transduction mechanisms can give rise to long term effects in the cell initiated by unstable stimulus such as PGI_2 or EDRF.

In the case of cAMP regulation, the following mechanisms have been elucidated (Gilman, 1984). An external stimulus, such as acetylcholine, binds to an external surface receptor, resulting in a conformational change. This change allows membrane bound G_s to bind to the substrate guanosine 5'-triphosphate (GTP). The resulting conformational change is responsible for activation of adenylate cyclase, the enzyme which produces cAMP. The cAMP then activates a cAMP-dependent protein kinase (also known as protein kinase A), which ultimately results in a cellular response to the external signal. The second messenger cAMP can be amplified approximately 1000 fold over an against eliciting a full response since one receptor activates about 10 adenylate cyclase, and the G_s -GTP-adenylate cyclase complex produces approximately 100 molecules before GTP is hydrolyzed (Levitzki, 1988). The complete mechanism can be regulated at many steps in the process. The transduction element of the mechanism can be inhibited by GTPase, which hydrolyzes GTP to guanosine 5'-diphosphate (GDP). In turn, GTPase can be inhibited by cholera toxin. The hydrolysis can also be inhibited by treating the cell with the nonhydrolyzable GTP analog guanosine-5'-[β,γ -imino]triphosphate. An inhibitory external signal can bind to a receptor which activates the G_i protein, leading to inhibition of adenylate cyclase. Adenylate cyclase can be activated directly by forskolin, and cAMP can be added to the cell in the form of lipid soluble analogs such as dibutyryl cAMP and 8-bromo cAMP.

Enzymatic degradation of cAMP is antagonized by inhibitors of phosphodiesterase (i.e. theophylline and 3-isobutyl-1-methylxanthine (IBMX)). The cAMP dependent protein kinase can be inhibited by H-8, H-9 or Rp-cAMPs or stimulated by S-9, S-10 or Sp-cAMPs.

The endothelial products PGI_2 and EDRF are known to inhibit platelet aggregation and induce smooth muscle relaxation by increasing cyclic nucleotide levels in these cells. The mechanism of EDRF production has not been elucidated. PGI_2 is an arachidonic acid metabolite produced by the cyclooxygenase mediated pathway of the arachidonic acid cascade. The principal arachidonic acid metabolites produced in HUVEC are PGI_2 and $\text{PGF}_{2\alpha}$ (both cyclooxygenase products). HUVEC subjected to shear stress preferentially secrete PGI_2 over $\text{PGF}_{2\alpha}$ (Nollert et al., 1989a). Cyclooxygenase is inhibited by aspirin (acetylsalicylic acid) or indomethacin.

The effects of PGI_2 are mediated by cAMP and can be mimicked by treating the cells with lipid soluble cAMP analogs, IBMX, forskolin or cholera toxin. PGI_2 and PGI_2 analogs also increase cAMP levels in endothelial cells. The effects of EDRF on platelets and smooth muscle cells are mediated by cGMP. Increased intracellular cGMP concentration is one of the three bioassays for EDRF (the other two are antiplatelet aggregating activity and smooth muscle relaxation activity). These bioassays were the only methods to detect EDRF prior to its identification as nitric oxide (NO, Palmer et al., 1987), and still serve as important tools in the study of EDRF related phenomena. EDRF and PGI_2 are secreted by the endothelium, indicating a humoral form of communication with the target cells. However, the short half lives of these compounds (EDRF, 6 seconds, and PGI_2 , 3.5 minutes) indicate a limited realm of activity from their point source. These small molecules (EDRF (NO), molecular weight 30, and PGI_2 , molecular weight ~350) may also be transmitted to the smooth muscle cells via gap junctions between the endothelium and smooth muscle cells. Gap junctions form 3

nm channels, allowing diffusion of molecules up to a molecular weight of about 1000 (Davies et al., 1988). Gap junctions between the endothelium and between the smooth muscle cells may also serve to propagate the signals of vasoactivity. It has been shown that endothelial gap junctions allow electronic, nucleotide and dye (Lucifer Yellow CH) transfer in the lateral plane (Larson and Sheridan, 1982).

The signal transduction mechanisms of shear stress in endothelial cells are currently under investigation. Inositol triphosphate, diacylglycerol and Ca^{2+} have all been implicated as second messengers for this mechanical stimuli. A transient (~1 minute) increase in cytoplasmic-free Ca^{2+} was detected using Fura 2 in shear stressed (6-10 dynes/cm²) BAEC (Ando et al., 1988). This phenomenon was observed in both calcium containing and calcium depleted medium, indicating that calcium is released from intracellular stores. Another laboratory reported that elevated Ca^{2+} concentrations concomitant with shear stress (22 dynes/cm²) -induced prostacyclin production in HUVEC are mobilized from both intracellular and extracellular Ca^{2+} (Bhagyalakshmi and Frangos, 1989). The same group has also suggested shear stress activation of phospholipase C, resulting in increased formation of DG. Shear stress at 22 dynes/cm² has been reported to increase IP_3 concentrations in HUVEC 2-fold (Nollert et al., 1989b). It is interesting to note that shear stress does not increase cAMP levels in HUVEC (Dr. J.A. Frangos, personal communication).

The permeability barrier function of the endothelium depends on the structural integrity of the monolayer. It is believed that the majority of albumin which crosses the endothelium does so through intercellular junctions (Bottaro et al., 1986a). Alterations in contractile activity of the endothelium may disrupt or enhance monolayer integrity. For this reason, the cytoskeleton has an important role in maintaining the permeability barrier function. The cytoskeleton is comprised of three filamentous polymers: microfilaments (5-7 nm diameter), intermediate filaments (8-10 nm),

and microtubules (~25 nm). The microfilaments consist of polymerized actin and associated proteins which can regulate polymerization/depolymerization. Approximately half of the millimolar concentration of actin in each cell is not polymerized, but is available to respond to cell stimulation (Stossel, 1989). Microfilaments participate in cell motility, cytokinesis, cytoplasmic structure, membrane topology regulation and intracellular transport (Clarkson et al., 1986). Microfilaments also help maintain the endothelial permeability barrier function. The role of microfilaments was first demonstrated by Shasby et al. (1982). They disrupted monolayers with cytocholasin B and D (inhibitors of actin polymerization), which resulted in increased transendothelial albumin transport. More recently Alexander et al. (1988) showed that phalloidin (a polymerized actin stabilizer) enhanced monolayer integrity, increased the concentration of stress fibers (large actin bundles), and decreased albumin permeability. PGI₂, serotonin and norepinephrine also increased actin stress fibers (Welles et al., 1985a, b), and serotonin and norepinephrine decrease endothelial permeability to albumin (Bottaro et al., 1986b).

Monolayer permeability is also influenced by calcium, and these modulations are at least partially due to concomitant cytoskeletal alterations. Chelation of extracellular calcium reversibly increased transendothelial albumin transport, reduced transendothelial electrical resistance (TEER), disrupted monolayer integrity, and produced retraction of the peripheral dense band (actin band) in porcine pulmonary artery endothelium (Shasby and Shasby, 1986). However, the disruption of monolayer integrity in a non-calcium medium may be due to decreased adhesion to the substratum. Treatment of HUVEC with histamine is associated with a biphasic rise in Ca²⁺ consisting of an initial transient peak followed by a sustained elevation 2-3 fold above resting levels (Rotrosen and Gallin, 1986). The initial rise in cytosolic calcium, present even in the absence of extracellular Ca²⁺, is most likely due to mobilization of intracellular

stores, and the sustained elevation could be due to calcium influx or inhibition of calcium efflux. Histamine also increased permeability to albumin and decreased filamentous actin. The F-actin and permeability effects of histamine were mimicked by treating the cells with calcium ionophore ionomycin. The permeability-increasing effect of thrombin has also been reported to be dependent on Ca^{2+} influx and intracellular Ca^{2+} mobilization in bovine pulmonary arterial endothelial cells (Lum et al., 1989). The transient shear stress-induced Ca^{2+} increase (Ando et al., 1988) may be an important mediator of shear stress-induced permeability increases. The mechanism by which Ca^{2+} influences permeability is unknown. Calcium ions may interact directly with elements of the cytoskeleton similar to the Ca^{2+} -calmodulin activation of myosin light chain kinase which results in actin-myosin contraction in smooth muscle cells (Exton, 1985). Alternatively, Ca^{2+} could indirectly cause cytoskeletal changes through activation of a protein kinase (perhaps calmodulin dependent) mediated pathway.

Shear stress has been shown to influence stress fiber formation in cultured endothelium over the time course of hours to days. Stress fiber formation may also be a mechanism for shear stress mediated permeability, although it is probably not an important factor in our short term (1-2 hour) experiments. BAEC subjected to 8 dynes/cm² for 72 hours were oriented in the direction of flow with prominent stress fibers also aligned in the direction of flow (Dewey et al., 1981). The appearance of shear stress-induced stress fibers correlates with decreased non-stress fiber associated actin (White et al., 1982). In HUVEC, shear stress at 2 dynes/cm² induced stress fiber formation by the third hour of shear; however, neither the fibers nor the cells were aligned in the direction of flow during this time interval (Franke et al., 1984). Increased flow is also associated with the induction of stress fibers *in vivo* and *ex vivo* (Herman et al., 1987). The same group reported increased cholesterol uptake

in *ex vivo* canine carotid arteries subjected to stress fiber inducing increased flow for 24 hours.

The maintenance and regulation of the permeability barrier function of the endothelium is influenced by cytoskeletal modulations. These modulations are the result of biochemical and mechanical stimuli which the cell perceives through its signal transduction mechanisms.

1. D. Mass Transport Review

The governing principle for one dimensional mass transport of species A in species B is Fick's first law of diffusion

$$J_{Ax} = -D_{AB} \frac{dC_A}{dx} \quad 1. D. 1.$$

where: J_{Ax} = mass flux of A in the x-direction

D_{AB} = diffusion coefficient of A in B

dC_A/dx = concentration gradient of A

This equation is a simplified form of Fick's law, valid for ideal dilute binary solutions of constant density. Because of these assumptions, the concentration gradient dC_A/dx can be used instead of the more rigorous chemical potential gradient. (The chemical potential refers to the change in Gibbs free energy of a species with respect to the change in the number of moles of that species, with temperature, pressure and number of moles of all other species constant). When this form of Fick's law is applied to a multicomponent system, species B includes all components other than species A.

This equation can be applied to transendothelial albumin transport *in vitro* in the absence of significant hydrostatic or oncotic pressure gradients. It has also applied to transmural albumin transport, *in vivo* and *ex vivo*, where all mass flux is assumed to

be due to the concentration gradient, and pressure, thermal and forced diffusion are ignored. Because such systems are multicomponent, the diffusion coefficient is an effective binary diffusion coefficient, D_{Am} with m referring to multicomponent.

From the equations of continuity for a binary mixture, Fick's second law of diffusion is derived:

$$\frac{\delta C_A}{\delta t} = D_{Am} \frac{\delta^2 C_A}{\delta x^2} \quad 1. D. 2$$

For a steady state system the derivative with respect to time is zero; therefore, equation 1. D. 2 reduces to:

$$\frac{d^2 C_A}{dx^2} = 0 \quad 1. D. 2(a)$$

Solving for C_A with the boundary conditions $C_A = C_L$ (luminal solution albumin concentration) at $x = h$ (Fig. 1. D. 1), and $C_A = C_S$ (subluminal solution albumin concentration) at $x = 0$, yields a straight line concentration profile through the cells and the membrane.

$$C_A(x) = \frac{C_L - C_S}{h} x + C_S \quad 1. D. 3$$

This concentration profile, shown in Figure 1. D. 1, assumes the same solubility of albumin in the bilayer of endothelial cells and membrane as in the surrounding media, which is probably not correct. A distribution coefficient indicates the relative solubility in a membrane to the solubility in the surrounding media. If this quantity is

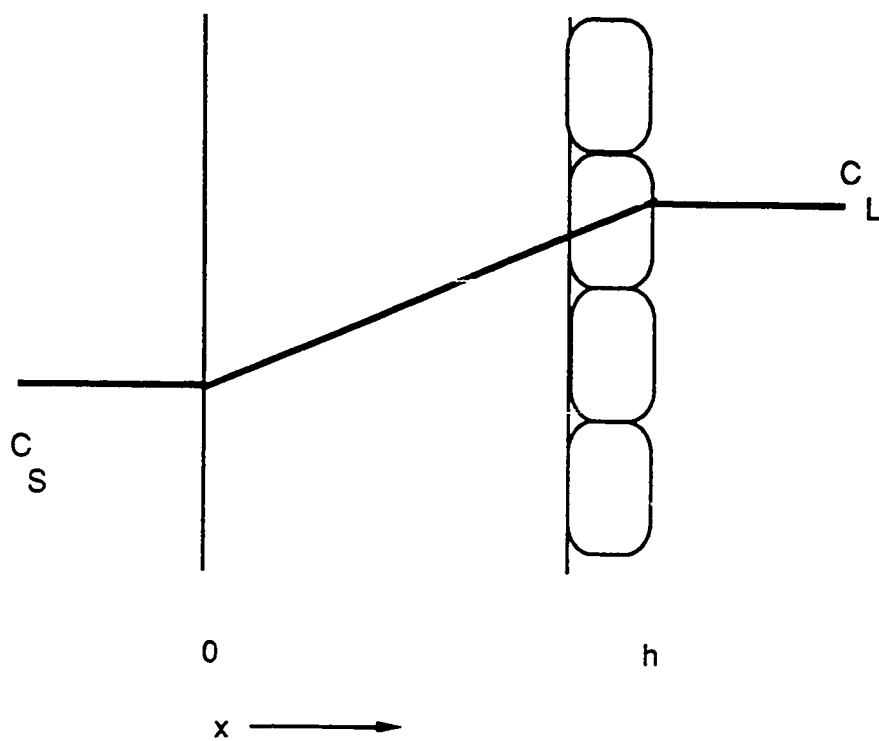


Figure 1. D. 1: A cross section of the membrane-monomer composite showing the system geometry and the albumin concentration profile. The subluminal membrane surface is at $x=0$ and the luminal endothelial surface is at $x=h$. The luminal albumin concentration, C_L , is greater than the subluminal concentration C_S .

not equal to one, then the right hand side of equation 1. D. 3 should be multiplied by the distribution coefficient α . Hindered diffusion occurs in the endothelial layer, and some reasons for this will be discussed in the next paragraph. Differentiation of equation 1. D. 3 with respect to x and substitution into equation 1. D. 1 yields:

$$J_{Ax} = -D_{Am} \frac{\alpha(C_L - C_S)}{h} \quad 1.D. 1(a)$$

The straight line concentration profile depicted in Figure 1. D. 1 is not strictly applicable in our system. Albumin crosses the endothelium by multiple pathways that do not represent the shortest route across the thickness of the endothelium. Figure 1. D. 2 shows three possible pathways for solute transfer across the endothelium: receptor mediated transport, non-specific endocytosis, and junctional transport. Endothelial cells do not have receptors for albumin, and non-specific endocytosis has been shown to make only a small contribution to transendothelial albumin transport (Bottaro et al., 1986a). Therefore, the majority of albumin crosses the monolayer through cell junctions. These junctions vary in length and width due to the varying degree of interdigitation between adjacent cells and to the number and complexity of cell junctions. The presence of interendothelial posts, composed of a single chain macromolecule, with the purpose of stabilizing the width of the cleft between cells, has been hypothesized (Silberberg, 1988). In addition, the endothelial glycoprotein/glycolipid outer layer is negatively charged. Therefore, the albumin molecule traversing the endothelium may interact ionically with the endothelial surface, may collide with interendothelial posts or the endothelial surface, and has a diffusion pathway much longer than the actual thickness of a cell (Fig. 1. D. 3). These factors, separately and combined, hinder diffusion of albumin across the endothelium.

The effective diffusion coefficient D_{Am} can be used to characterize the mass

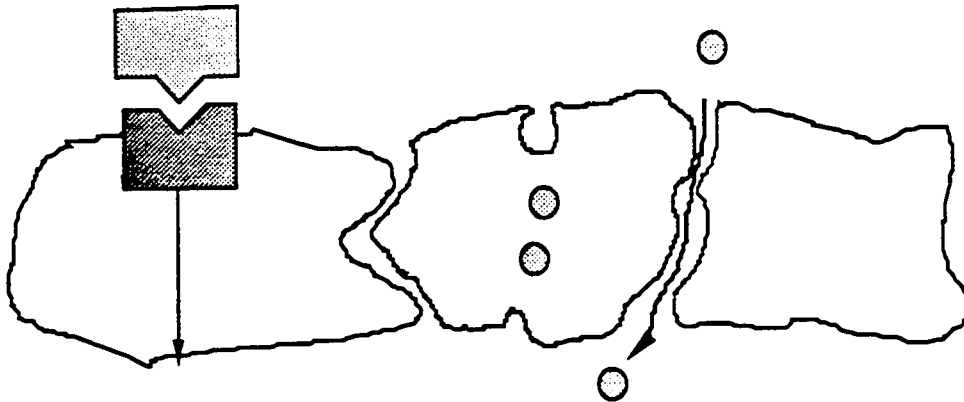


Figure 1. D. 2: Possible pathways for solute transport across the endothelium. On the left, a molecule binds to an external receptor, becomes internalized, and if not catabolized by the cell, may diffuse or be directed through the cell. In the middle, non-specific endocytosis of a small volume entrapped in a vesicle formed by the cell membrane. The vesicle is internalized and may diffuse through the cell, ultimately fusing again with the cell membrane and releasing the vesicle contents extracellularly. Both receptor-mediated transport and endocytosis require cellular energy. On the right, interjunctional transport. A solute molecule passes through the space between cells. Because the molecule does not enter the cell, this process is not energy requiring.

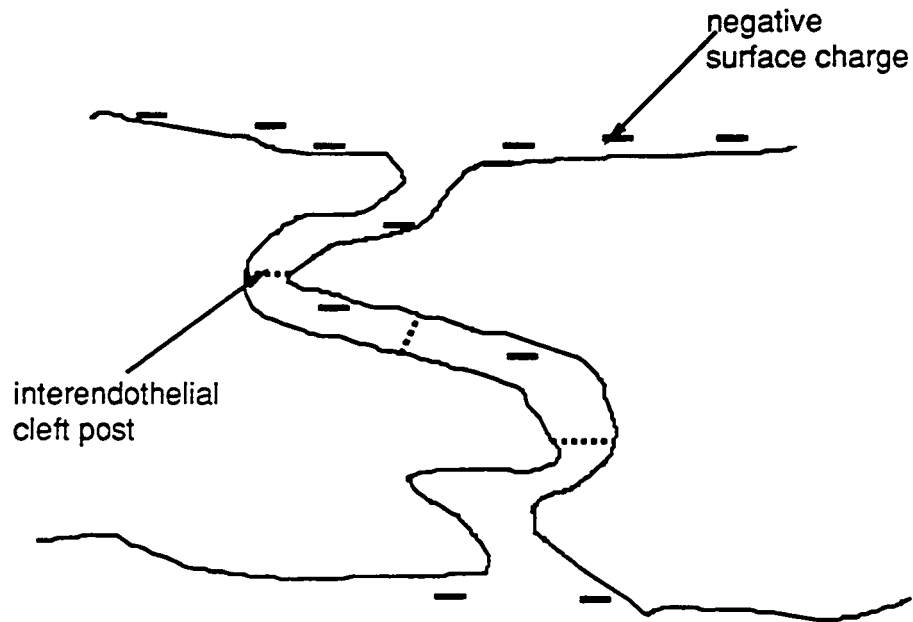


Figure 1. D. 3: Diffusion pathway. A solute traversing the endothelium through the junctions between cells may interact ionically with negatively charged molecules on the membrane surface, or collide with interendothelial posts or the surface itself. The diffusion pathway may be much greater than the thickness of the cells due to the interdigitation of cellular junctions.

transport property of the endothelium; however, it does not provide information regarding the mechanism of transport. In order to calculate D_{Am} from equation 1. D. 1(a), the flux J_{Ax} , $(C_L - C_S)$, α and h must be known. The flux and the concentration difference can be calculated from at least two determinations of C_L and C_S , the time interval of sampling, and the geometry of the system. The distribution coefficient and the diffusion pathway are more difficult to determine; however, their absolute values are not as important as their use in calculating a coefficient to characterize the endothelium. Therefore, an alternate coefficient PC is defined as:

$$PC = \frac{\alpha D_{Am}}{h} = \frac{J_{Ax}}{C_L - C_S} \quad 1. D. 4$$

which is the permeability coefficient, with units of length/time. The permeability coefficient can be calculated from the experimentally determined mass flux and concentration difference across the membrane.

In this experimental system, which contains a monolayer of endothelial cells cultured on a polycarbonate substrate, the permeability coefficient calculated is an equivalent permeability coefficient for the endothelial-membrane composite. In order to obtain a permeability coefficient for the endothelial monolayer alone, a permeability coefficient for the membrane alone must be determined. Then, assuming continuity of flux across the composite, it can be written:

$$\Delta C_{\text{endothelium}} + \Delta C_{\text{membrane}} = \Delta C_{\text{composite}}$$

$$\frac{J}{PC_{\text{endothelium}}} + \frac{J}{PC_{\text{membrane}}} = \frac{J}{PC_{\text{composite}}}$$

or,

$$\frac{1}{PC_{\text{endothelium}}} = \frac{1}{PC_{\text{composite}}} - \frac{1}{PC_{\text{membrane}}} \quad 1. D. 5$$

The permeability coefficient of the endothelium alone can be calculated from equation 1. D. 5. This coefficient will be used to describe the baseline permeability characteristic of endothelial monolayers as well as the modulations produced by the biochemical and mechanical stimuli. Permeability coefficients can be compared between and within groups of *in vivo* and *in vitro* permeability models. However, in *in vivo* systems other factors, such as convective diffusion and enhanced diffusion, may contribute to solute flux although the permeability coefficient only considers ordinary diffusion.

The concept of a permeability coefficient is used analogously in polymer science and engineering when solubilities in membranes and diffusion pathways are unknown. As in our experimental system, these quantities are not of primary importance as long as a method to quantitatively characterize the permeability properties of a polymer is available. Such is the case in characterizing mass flux through transdermal patches for drug delivery, synthetic wound coverings for drug delivery and maintenance of sterility (Behar et al., 1986), and oxygen through permeable or semi-permeable contact lenses.

1. E. Tissue Culture Review

With the advent of the Gimbrone (1976) and Jaffe et al. (1973) papers on human umbilical vein culturing techniques, the scientific community quickly embraced this new cell type for tissue culture. HUVEC are used for metabolic studies, adhesion assays, permeability studies, and more recently, due to the availability of polymerase chain reaction technology, molecular biology studies.

Once harvested from the umbilical vein, the presence of a pure culture of

endothelial cells can be verified by various immunohistochemical techniques, morphological appearance, or angiotensin converting enzyme (ACE) activity. Two widely used immunohistochemical techniques use fluorescently labeled antibodies for Factor VIII, which binds in a punctate pattern the Weibel-Palade bodies unique to endothelial cells (Cole et al., 1986), and for acetylated-low density lipoprotein (LDL), which binds to the endothelium with an order of magnitude greater affinity than to smooth muscle cells or pericytes (Voyta et al., 1984). The acetylated-LDL technique may be used nondestructively, since it binds to an external receptor; it can therefore be used without a membrane permeabilizing factor required by immunofluorescent techniques for intracellular antigens. HUVEC are also identified by their cobblestone morphology of contact inhibited growth. Another biochemical assay for HUVEC verification is that for ACE activity, an enzyme which deactivates bradykinin. One or more of these methods may be used to verify authenticity of endothelial cultures.

HUVEC in primary cultures are adhesive enough to be seeded directly onto tissue culture plastic or NaOH treated glass. Subcultured HUVEC grow best on surfaces treated with some attachment factor such as collagen (sometimes denatured in the form of gelatin), human fibronectin, or attachment peptides (such as the RGD (Arginine-Glycine-Aspartic acid) sequence). The substrate not only affects cell attachment, but also influences cell metabolism. Seeding density also affects cell viability and perhaps also cell function. Passaged HUVEC grow best in the presence of a growth factor. The most commonly used HUVEC growth factors are derived from bovine neural tissue, although other compounds can influence their growth. Growth factors are commercially available or may be isolated from bovine neural tissue according to Burgess et al. (1985). Growth factors derived in this manner are heparin binding, and act synergistically with heparin in heparin supplemented medium (Thorton et al., 1983).

Tissue culture techniques for culturing cells on permeable membranes are not as well established as those for tissue culture plastic. Cells are typically seeded at higher densities (sometimes greater than a 1:1 seeding ratio), and often with an albumin pretreatment for attachment to non-specific binding sites, followed by treatment with an adhesion protein. Permeable membranes commonly used are polycarbonate (i.e. Nuclepore, Pleasanton, CA or Transwell, CoStar, Cambridge, MA), microcarrier beads (i.e. Cytodex 3), and to a lesser extent, (due to its protein binding properties, tortuous pore structure, and 150 μm thickness which give the membrane undesirable transport properties), nitrocellulose based membranes (i.e. Millicell-HA, Millipore, Bedford, MA). The advantages of polycarbonate membranes are their low protein binding characteristic, the straight through cylindrical pores, the pore size of 0.4 μm which permits macromolecular transport without allowing cell migration, the consistency in manufacturing standards, the thinness of the membrane (10 μm), and the ability of cultures to form confluent monolayers on these membranes. In the past two years many new materials have appeared on the market. These membranes, the composition of which is proprietary, offer the desirable feature of transparency at the price of demonstrating a formidable permeability barrier compared to that of the monolayers themselves. For example, the thickness of the CoStar transparent membrane product, Transwell-COL, available in 0.4 and 3.0 μm pore sizes, varies from 25 - 50 μm , presenting a greater and more variable diffusion barrier than the Transwell polycarbonate product. The Cellagen permeable transparent collagen membrane (ICN Biomedicals, Inc., Cleveland, OH) will not allow passage of macromolecules commonly used as tracers (i.e. albumin or LDL) since its molecular weight cut-off is 10,000.

Endothelial cells in culture exhibit many morphological characteristics and synthetic capabilities seen *in vivo* which serves to justify their use in tissue culture models. Cultured endothelial cells form junctional complexes similar to those in

freshly isolated endothelial monolayers; however, the number and complexity of the junctions is not as extensive (Larson and Sheridan, 1982). Endothelial cells migrate in culture, allowing their use in wound healing and angiogenesis models. Endothelial cells in static culture and in low flow regions *in vivo* do not exhibit elongation, rather they are polygonal. However, elongation can be induced *in vitro* by subjecting cultures to shear stress (Ives et al., 1983; Eskin et al., 1984) or by culturing endothelial cells with smooth muscle cells (van Buul-Wortelboer et al., 1986). Elongation is also seen *in vivo* in high flow rate arterial vessels in areas away from bifurcation (Nerem et al., 1981). Endothelial cells in culture retain many important synthetic capabilities; prostacyclin, vWF, tPA, plasminogen activator inhibitor, type 1 (PAI-1), and EDRF comprise only a partial list of these products. Endothelial cells also respond to agonists in culture, resulting in modulation of metabolism and morphology. Thrombin, a proteolytic enzyme which initiates platelet aggregation and fibrin formation, will stimulate endothelial release of all the above mentioned metabolites as well as stimulate changes in endothelial morphology.

The use of a tissue culture model for permeability studies depends on three major features of the model. First, the cells must form confluent monolayers on the permeable substrate. Second, the permeability of such a monolayer (which is indicative of the integrity of the monolayer) must be characterizable in a quantitative manner. Third, the quantitative characterization of permeability must be sensitive enough to quantify modulations in permeability induced by agonists or experimental conditions. In the remaining chapters of this thesis, these issues will be discussed as they apply to the model developed herein.

CHAPTER TWO: METHODS

2. A. Endothelial Cell Culture

i. Human Umbilical Vein Endothelial Cells.

Human umbilical vein endothelial cells (HUVEC) were harvested using collagenase digestion (Gimbrone, 1976), pooled and seeded in T-25 flasks (Falcon, Oxnard, CA) which had been incubated with 5 mls of 0.2% tissue culture grade gelatin (Sigma, St. Louis, MO) for 30 minutes. Briefly, two or more umbilical cords, obtained within approximately 8 hours of delivery (preferably Ceasarian section), were canulated, gently rinsed with 100 ml volume of PO_4 , filled with approximately 55 U/ml collagenase (Worthington Biochemical Corporation, Freehold, NJ, 231 U/mg, type CLS) in phosphate-buffered saline (PBS, GIBCO Laboratories, Grand Island, NY) and incubated for 30 minutes. After the incubation, the collagenase solution was collected and the cords perfused quickly with 100 ml of PO_4 . The collagenase solution and PO_4 perfusate were combined and centrifuged at $100 \times g$ for 10 minutes. The resulting pellet was resuspended in complete medium (described below).

Complete culture medium was M199 (GIBCO) containing 20% heat-inactivated fetal bovine serum (HyClone Laboratories, Logan, UT), penicillin, streptomycin and neomycin (PSN, 2% by volume, Gibco), 1% glutamine (GIBCO), 0.1 $\mu\text{g/ml}$ heparin (Sigma) and 20 $\mu\text{g/ml}$ endothelial mitogen (Biomedical Technologies, Inc., Stoughton, MA). When confluent, cells were subcultured with 0.05% trypsin in 1:5000 EDTA

(GIBCO) and seeded in a 1:3 split on gelatin-coated flasks. Verification of endothelial origin of cultures from representative cord pools was accomplished by positive immunofluorescence of Weibel-Palade bodies (anti-Factor VIII, Atlantic Antibodies, Scarborough, Maine) or LDL receptors (1,1'-dioctadecyl-1-3,3,3',3'-tetramethyl-indo-carbocyanine perchlorate acetylated LDL, Biomedical Technologies). Confluent first passage cells were subcultured and seeded at approximately 4×10^4 cells/cm² (1:1) onto permeable polycarbonate membranes (Transwell, Co-Star, Cambridge, MA, described below in 2. B. Experimental Apparatus). The membranes were preincubated with 1 ml of complete medium for one hour and then with 0.5 ml of 100 µg/ml human fibronectin (New York Blood Center, Inc., New York, NY) for one hour. Culture medium was changed three times a week. Cell cultures were used in experiments at 15-day post-seeding, except for time-course experiments when 7 and 11-day post-seeding cultures were also used. Prior to static experiments, cell monolayers were washed three times in PBS (GIBCO). The PBS used for washing and experimental solutions contained 2.5 mM calcium.

For polarity and flow experiments, the following changes in tissue culture techniques were implemented. The serum used was bovine calf serum, iron supplemented (HyClone Laboratories, Catalog No. A-2151). Endothelial cell growth factor was obtained from Collaborative Research (Bedford, MA, Catalog No. 40006) and used in a concentration of 15 mg/500 ml. Heparin was no longer added to the medium. Fibronectin was purchased from Calbiochem (La Jolla, CA, Catalog No. 341635). The concentration of PSN was reduced to 0.5 volume %. Also, only passage number 1 cells were used in these experiments. Prior to flow experiments, cells were incubated for

approximately 45 minutes in the experimental solution consisting of M199, 1% bovine serum albumin, and 25mM HEPES (GIBCO).

ii. Bovine Aortic Endothelial Cells.

Endothelial cells were harvested using 0.05% collagenase (Worthington, type CLS) from bovine aorta according to Eskin et al. (1978). The resulting primary cells were maintained in Dulbecco's modification of Eagle's medium (DME, GIBCO), supplemented with 10% fetal calf serum (HyClone), and 100 µg/ml each penicillin and streptomycin. Cells were then cloned using Microtest II plates (Falcon). Cloned cells were maintained in Eagle's minimal essential medium with Earle's salts (MEM) containing 10% fetal calf serum (HyClone), 1% glutamine (GIBCO), PSN (0.1% by volume, GIBCO). Cells were subcultured when confluent with 0.05% trypsin in 1:5000 EDTA (GIBCO).

For experiments, cells in passages five through ten were seeded onto permeable polycarbonate membranes (approximately 5×10^4 cells/cm²) and incubated in complete MEM for either 3, 7, 11 or 15 days. Medium was changed at least twice a week. Just prior to an experiment, complete medium was removed from the cells and the permeable membrane by washing with phosphate buffered saline.

iii. Staining

Wright's stain (Sigma) was used for a gross indication of cell coverage in some experiments due to the non-transparent nature of the membrane. Since this is a destructive procedure, it was performed at the conclusion of an experiment. Briefly, after rinsing twice with PBS, 1 ml of stain was added to each membrane and incubated for 3 minutes. Then 0.5 ml of deionized water was added and mixed with the stain by a gentle swirling motion. After a 9 minute incubation, the membrane was rinsed three

gentle swirling motion. After a 9 minute incubation, the membrane was rinsed three times with deionized water and allowed to air dry.

iv. Cell Counting.

In some experiments cells were counted by hemacytometer after removal from the membrane with trypsin-EDTA and staining with trypan blue (Sigma).

2. B. Experimental Apparatus

i. Transwell System for Static Experiments

Cells were cultured and experiments were performed in Transwells, a six-well tissue culture tray containing six polycarbonate bottomed inserts set in the wells. The membrane, which originated from Nuclepore, has 0.4 μm diameter pores, 15-20% porosity, and is 10 μm thick and 24 mm in diameter (Fig. 2. B. 1). The insert is designated the luminal chamber and outer well the subluminal chamber (Fig. 2. B. 2). The sample ports allowed independent sampling from either chamber. During experiments a wire collar was placed beneath the rim of the Transwell insert to accommodate placement of a 2 mm x 7 mm magnetic stirring bar in the subluminal chamber. The modified Transwell trays were placed on a magnetic stirrer (Bellco Biotechnology, Vineland, NJ) set at approximately 60 RPM in a 37 $^{\circ}\text{C}$ dry incubator.

ii. Permeable Membrane Flow Chamber

Cells were cultured on the Transwell membrane which had been carefully removed from its support, glued (Silastic Medical Adhesive, Silicon Type A, Dow Corning, Midland, MI) to an annular silastic gasket, which was glued to the subluminal section of the flow chamber. The assembled permeable membrane flow chamber was sterilized by

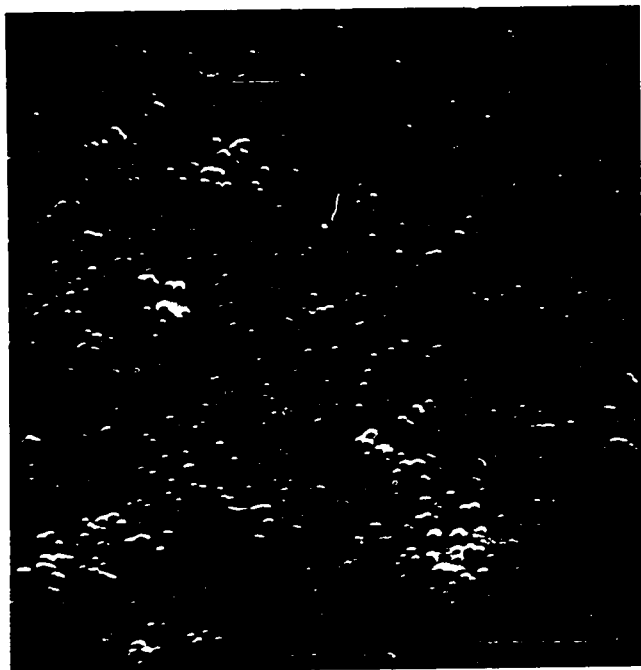


Figure 2. B. 1: Scanning electron micrograph of bare 0.4 μm pore diameter polycarbonate membrane (x3000). Note the uniformity of the pore size and distribution.

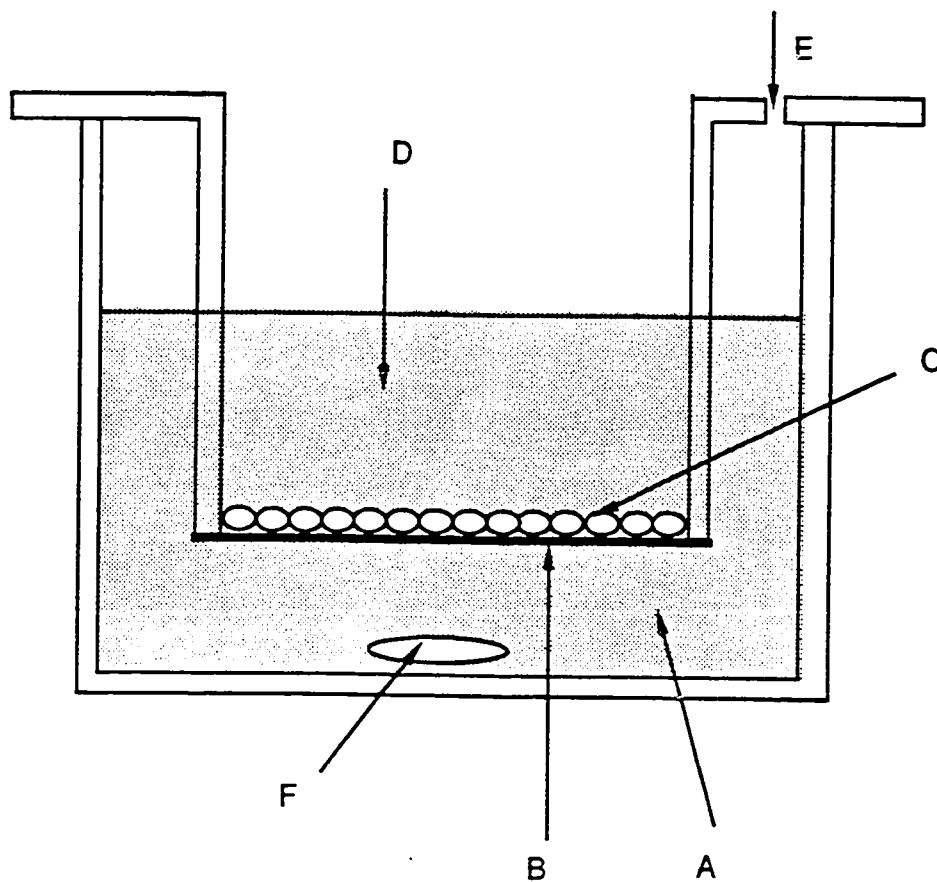


Figure 2. B. 2: Schematic of experimental apparatus. Components include: A, subluminal chamber; B, polycarbonate membrane; C, HUVEC monolayer; D, luminal chamber; E, sample port; and F, magnetic stirring bar.

exposure to ethylene oxide. The flow chamber was machined from a solid block of polycarbonate (Lexan, General Electric Plastics, Inc. Mt. Vernon, IN). It features a ledge on which the annular gasket is fixed, a 2.4 ml subluminal chamber, a well to accommodate a 7mm x 2mm magnetic stir bar, and a tapered port for a three way stopcock which is connected to the subluminal manometer leg (Fig. 2. B. 3). The permeable membrane flow chamber comprises one plate of the parallel plate flow chamber, described further in section 2. C. ii..

The permeable membrane flow chamber has a polished surface on one outer face of the subluminal chamber which is used for detection of fluorescently labeled albumin. The single end of a bifurcated fiber optic cable is fixed in place next to this polished surface by an aluminum holder which also holds the permeable membrane flow chamber in place (Fig. 2. B. 4). One leg of the double end of the bifurcated fiber optic cable is connected to a mercury lamp (Oriel Corporation, Stratford, CT) operated by a 100 W power supply. The other leg of the cable is fixed to a photomultiplier tube (PMT, model 1P21, Hamamatsu Corporation, Bridgewater, NJ) in a light-tight housing (model 3150, Pacific Precision Instruments, Concord, CA) powered by a Pacific Precision Instruments high voltage power supply. From the PMT the signal is amplified by a variable amplifier (United Detector Technology, Hawthorne, CA) and converted by an analog to digital converter (Strawberry Tree Computers, Inc., Sunnyvale, CA) installed in a Macintosh SE. Data were stored by the Macintosh as digitized volts.

The excitation light is filtered by a 495 nm center wavelength (CWL) 20 nm half-bandwidth (HBW) narrow bandpass interference filter (Discriminating Filter Series, Omega Optical, Inc. Brattleboro, Vermont) installed in the mercury lamp. The

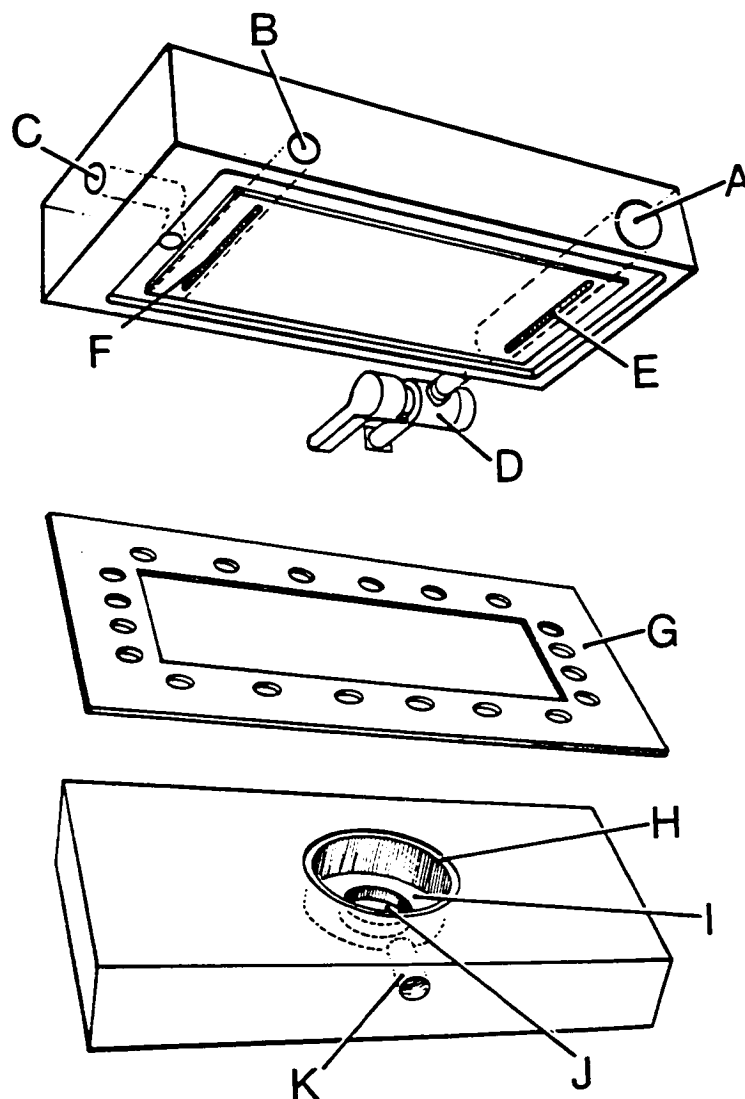


Figure 2. B. 3: Permeable membrane flow chamber. In the upper section, medium enters through A, the inlet port, to E, the inlet slit, and flows across the channel before exiting at F, the outlet slit, to B, the outlet port. The valve D is used as necessary to remove air bubbles trapped in the inlet port. C is a port for vacuum, used to hold the three components of the assembled chamber together. The gasket G forms the four sides of the flow channel and determines its thickness. Onto the recessed ledge H is glued the permeable membrane, glued to an annular gasket which covers the ledge. The membrane is mounted flush with the surface of this bottom section of the flow chamber. Directly beneath the membrane is the subluminal chamber I, containing a well for a magnetic stir bar, J. The subluminal chamber also contains a port, K, for the subluminal manometer leg used to control the subluminal chamber pressure.

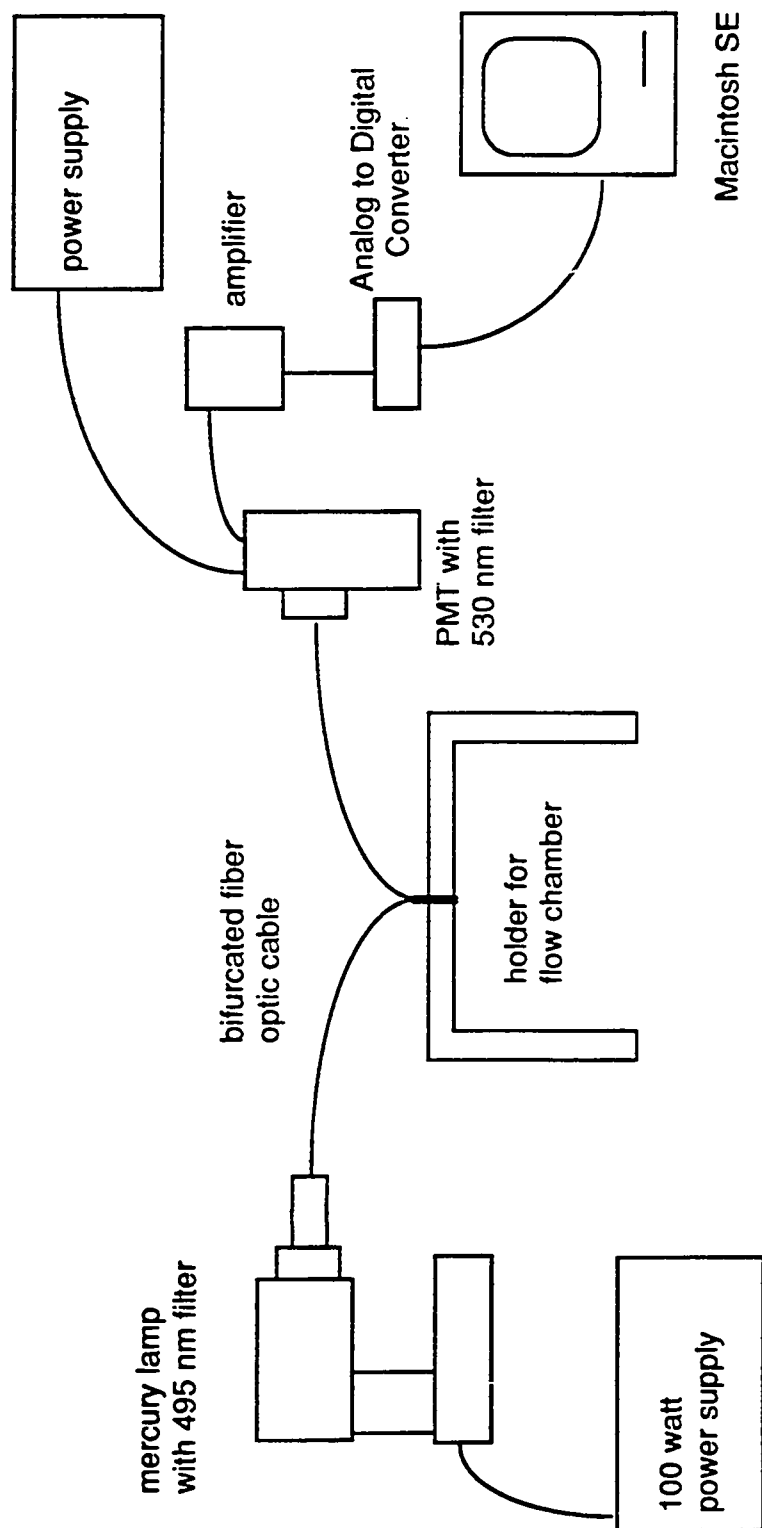


Figure 2. B. 4: Electronic system for fluorescence detection. The flow chamber is fixed in place by an aluminum holder which also holds the single end of a bifurcated fiber optic cable adjacent to a polished surface on the exterior of the subluminal chamber. Excitation light, filtered at 495 nm, is provided by a mercury lamp powered by a 100 W power supply. Emission light is filtered at 530 nm before entering a photomultiplier tube (PMT). The resulting analog signal is amplified (10⁵ gain), converted to a digital signal, and stored as volts on a Macintosh SE.

emission light is filtered by a 530 nm CWL 30 nm HBW narrow band interference filter (Discriminating Filter Series, Omega Optical, Inc.) installed in the PMT.

2. C. Agonists and Dosage

i. Static Permeability Experiments

All agonist solutions were prepared in PBS unless otherwise noted. The prostacyclin analog iloprost, (a gift from Schering, West Germany) was used at 6 nM final concentration. Biological activity of iloprost (inhibition of thrombin-induced platelet aggregation) was verified in the concentration range 0.6-6 nM. Agonist stimulated prostacyclin production in this system is approximately 1.5 nM after 10 minutes. A somewhat higher concentration of iloprost was chosen because there were no data available regarding the kinetics of endothelial metabolism of iloprost.

Bradykinin, (Calbiochem) was used at 1 μ M. This concentration is approximately one order of magnitude higher than that required for maximal prostacyclin stimulation in HUVEC (Hong, 1980; Alhenc-Gelas et al., 1982) to ensure cell stimulation. Bradykinin was used in the presence of captopril, 0.1 μ M, (a gift from E. R. Squibb & Sons, Princeton, NJ), which inhibits angiotensin converting enzyme degradation of bradykinin.

The cyclic AMP analogs dibutyryl cAMP, 0.5 mM, and 8-bromo cAMP, 0.5 mM, (Sigma) were usually used in combination with a phosphodiesterase inhibitor to sustain the elevated intracellular cAMP concentrations. Two phosphodiesterase inhibitors used were 3-isobutyl-1-methylxanthine (IBMX), 0.1mM, and theophylline, 0.5 mM, (Sigma). The values correspond to concentrations reported to cause increased cAMP

accumulation or to induce cAMP mediated effects in endothelium (Lloyd et al., 1987; Schafer et al., 1980; Leitman et al., 1986; Hopkins and Gorman, 1981; Laposata et al., 1983). The cyclic GMP analog dibutyryl cGMP (Sigma) was also used at 0.5 mM.

The concentration of thrombin, 0.15 U/ml, (45 ng/ml of 3200 U/mg, Calbiochem) corresponds to that which will induce gap formation in confluent HUVEC cultured on a solid, impermeable substrate (Laposata et al., 1983). Alpha-thrombin, 1 nM, (46 ng/ml of 2900 U/mg) and altered thrombins: γ -thrombin, 1 nM (46 ng/ml), diisopropylfluorophosphate- α -thrombin (DIP- α -thrombin, 1 nM (45 ng/ml)) and D-Phe-Pro-Arg-CH₂- α -thrombin (PPACK- α -thrombin, 1 nM (45 ng/ml)), were gifts from Dr. John Fenton, New York State Department of Health, Albany, NY). The DIP, PPACK and γ thrombins were prepared by Dr. Fenton from his α -thrombin. The concentrations of altered thrombins were determined based on equivalent unit concentrations of the Calbiochem α -thrombin and Dr. Fenton's α -thrombin. The α -thrombin donated by Dr. Fenton was used in experiments with PPACK- α -thrombin and DIP- α -thrombin pretreated monolayers, otherwise Calbiochem thrombin was used.

In some experiments, prior to stimulation with thrombin or bradykinin, the cells were incubated with 5 μ M aspirin (Sigma) or 50 μ M indomethacin (Sigma) in PBS for 30 minutes prior to washing with PBS. Aspirin and indomethacin are inhibitors of cyclooxygenase, the enzyme which initiates production of prostacyclin from arachidonic acid. Cyclooxygenase inhibition was carried out to determine if the permeability modulations observed in the presence of thrombin and bradykinin were mediated by

their stimulation of HUVEC prostacyclin production. Experiments conducted with indomethacin pretreated monolayers were carried out in the presence of 50 μ M indomethacin in the albumin solution and PBS. Aspirin and indomethacin were dissolved in ethanol then diluted in PBS to yield a final ethanol concentration of 0.0345 vol% in solutions containing these inhibitors.

ii. Flow Experiments

For these experiments, flow was the major agonist. Steady laminar flow through the flow chamber was provided by a flow loop (Fig. 2. C. 1). The upper section of the flow chamber, shown in detail in Fig. 2. B. 3, features an inlet slit, an outlet slit, a plane surface which forms the upper plate of the parallel plate geometry, a recessed ledge which fits a rectangular silastic gasket, and a vacuum port. The lower section of the flow chamber, containing the HUVEC monolayer, is held in place by vacuum. The rectangular silastic gasket separates the upper from the lower flow chamber sections, and forms the four sides of the flow channel.

The basic flow loop, described in detail elsewhere (Frangos et al., 1988), consists of upper and lower reservoirs for experimental medium and associated tubing to provide circulation to and from the flow chamber. The vertical distance between the reservoirs determines the hydrostatic pressure which drives the flow through the chamber. Recirculation of medium from lower to upper reservoir is achieved by a roller pump (Masterflex, Cole Parmer, Chicago, IL). The volumetric flowrate at the chamber outlet was determined by timing flow into a graduated cylinder. From the flowrate, combined with a knowledge of the chamber geometry and viscosity of the experimental medium, the wall shear stress is calculated. The defining equation for

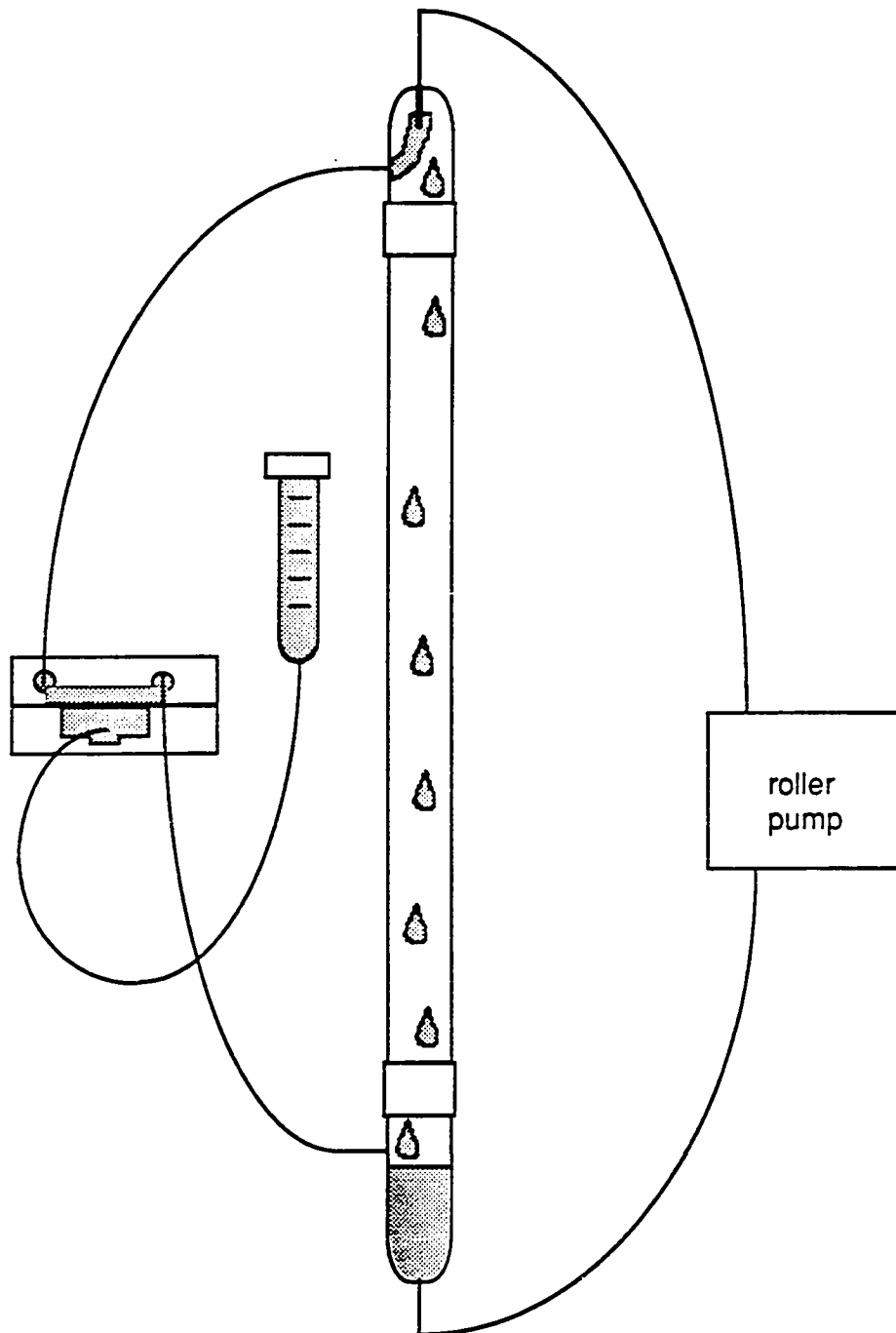


Figure 2. C. 1: Flow loop schematic. The assembled flow chamber is connected to a flow loop and a subluminal manometer leg. The flow loop consists of an upper reservoir and a lower reservoir. The vertical distance between these reservoirs determines the hydrostatic head which drives flow through the chamber. The roller pump serves only to recirculate medium from the lower to the upper reservoir, with any excess medium pumped allowed to freely overflow back to the lower reservoir. The height of the subluminal manometer leg can be adjusted to offset the pressure in the flow channel.

shear stress, τ , for a Newtonian fluid is:

$$\tau = \tau_{yx} = -\mu \frac{dv_x}{dy}$$

Where velocity is in the x-direction (the long axis of the chamber) and is a function only of the slit height of the chamber, along the y-axis (defined by the thickness of the gasket). Assuming that the experimental medium is a Newtonian fluid, and that due to the large aspect ratio (b/h) the flow chamber can be modeled by parallel plate geometry, and that there is no volume flux through the permeable membrane, a momentum balance can be written and solved for τ_{yx} at the endothelial surface ($y=h$).

$$\tau = \frac{6 Q \mu}{b h^2}$$

where: τ = wall shear stress in dynes/cm²
 Q = volumetric flowrate in ml/sec
 μ = viscosity of medium in dynes-sec/cm² (0.01 dynes-sec/cm²)
 b = slit width (2.5 cm)
 h = channel height (.0203 cm)

A wall shear stress of 7 dynes/cm², corresponding to a low arterial level, was used in these experiments. This shear stress was achieved by adjusting the height difference between the upper and the lower reservoirs so that the pressure drove flow at a rate of

approximately 7.2 ml/min.

The Reynolds number, used to determine whether flow is laminar or turbulent, for flow through the chamber is:

$$Re = Uhp/\mu$$

where: U = mass average linear velocity (cm/sec)

ρ = Density of experimental medium (1 gm/cm³)

This equation can be re-written in terms of the volumetric flow rate, Q , as:

$$Re = \frac{Q\rho}{\mu b}$$

Therefore, for the flow rate used in these experiments, the Reynolds number was approximately 5, which is well within the laminar flow regime.

A potential flow disturbance can be caused by entrance length effects. An empirical equation for the entry length (l) for plane Poiseuille flow is given by Schlichting (1968) as:

$$l = 0.04 (h) Re$$

For the flow rate and channel height used in these experiments, the entry length is 4 μ m. The total channel length of 6 cm indicates that the entry length was negligible for these experiments.

In some flow experiments the monolayers were treated with iloprost, 6 nM, prior

to and during flow to expose the cells to a biologically active concentration of prostacyclin.

iii. Polarity of Expression of PGI₂ Experiments

Stimulation of prostacyclin production was achieved by treating HUVEC with 1 μ M bradykinin. At this concentration bradykinin stimulates prostacyclin production without directly affecting permeability.

Controls for these experiments were run with tritiated iloprost (Amersham, Chicago, IL) at a concentration of 0.1 nM (97,900,000 dpm/ml) to determine the extent of diffusion of iloprost (or prostacyclin) during the time course of the experiment.

2. D. Experimental Protocol

Due to the relatively short experimental period (<4 hours), none of these experiments were performed under aseptic conditions.

i. Static Permeability Time Course Experiments

The procedures for BAEC and HUVEC time course studies are essentially the same. One ml of 4% bovine serum albumin (Sigma) in PBS was added to the luminal chamber and 4 mls of PBS were added to the subluminal chamber. This produced equal liquid levels in both chambers and served to prevent hydrostatic pressure gradients across the monolayer. The 4 ml subluminal chamber was sampled every 20 minutes for two hours and the 1 ml luminal chamber was sampled at two hours. Sample volumes, 300 μ l, were replaced with PBS. For BAEC studies, albumin content of the

samples was determined by a Lowry assay (Sigma protein assay kit number P5656). For HUVEC studies, the Coomassie Blue Protein Assay (#23200, Pierce Chemical Co., Rockford, IL) was used. All time course experiments were performed with BAEC from the same cloned line or HUVEC from the same cell harvest.

ii. Static Agonist Permeability Experiments

All agonist experiments followed the protocol outlined above for baseline permeability determination with the following differences in albumin tracer, sample size, and sample time. The 4% albumin solution in the luminal chamber contained a tracer of ^{14}C -albumin (75 nCi (2.8 kBq) or 166,500 dpm, DuPont, NEN Research Products, Boston, MA) . Subluminal samples, 200 μl , were taken every eight minutes for 32 minutes to establish the baseline permeability characteristic of the monolayer. Then agonist(s) were added in equal concentrations to the existing solutions in both chambers. Five subluminal samples, 200 μl , were taken at eight minute intervals, beginning 12 minutes after agonists were added. All sample volumes were replaced with PBS or, after agonist addition, PBS containing agonist(s). The luminal chamber was sampled at the completion of each experiment. Samples were mixed with Hydrofluor (National Diagnostics, Manville, NJ) and counted for ten minutes in a liquid scintillation counter using disintegrations per minute (dpm) software (TRI-CARB 4430, Packard Instrument Co., Laguna Hills, CA). Background counts determined from the mean of a pentad of PBS samples were subtracted from each sample. Over the course of the study background averaged 207.9 ± 26.68 (n=17) dpm/ml and net first sample counts (the lowest radioactivity levels of all samples) averaged 358.6 ± 35.22 (n=98) dpm/ml. These agonist studies were conducted with HUVEC from 9 cell

harvests.

iii. Polarity of Expression of PGI₂ Experiments

Baseline permeability determinations were conducted with radiolabeled albumin as described in section 2. D. ii. above, except that the experimental medium for both luminal and subluminal chambers was 1% albumin in M199 with 25mM HEPES. Equal concentrations of albumin in both chambers were used because control experiments demonstrated an albumin gradient dependence of prostacyclin (iloprost) mass flux across the monolayer. After the baseline permeability determination, bradykinin was added to the luminal chamber in a final concentration of 1 μ M. Samples (200 μ l) were taken from both luminal and subluminal chambers at t<0, and t= 3.5, 7.0 and 10.5 minutes. A ten minute sampling period was chosen because *in vitro* studies on the kinetics of bradykinin-induced prostacyclin production have shown that production peaks at approximately 3 minutes and returns to baseline values by ten minutes. Sample volumes were replaced with experimental medium.

A two-point assessment of monolayer integrity following bradykinin stimulation was made by taking subluminal samples at a newly defined t=0 and t=8 minutes and a luminal sample at t=8 minutes.

The polarity experiments were conducted with HUVEC from 4 cell harvests. Passage 1 cells were used exclusively since prostacyclin production declines with increasing population doublings (Ingerman-Wojenski and Silver, 1988). Also, the culture medium did not contain heparin because of the adverse affect of heparin on prostacyclin production (Hasegawa et al., 1988).

Controls were run with tritiated iloprost to assess the rate of transport of iloprost across the monolayer.

iv. Flow Experiments

These experiments followed the protocol of baseline permeability determination, agonist permeability determination, and recovery permeability determination. A detailed protocol for each phase of the experiment follows later in this section.

The experimental medium was M199 (15mM HEPES), de-gassed by exposure to ambient air under a sterile laminar flow hood at room temperature for approximately 2 days. After addition of albumin and HEPES for final concentrations of 1% and 25mM, respectively, the pH of the medium was adjusted to 7.4. The medium was sterilized by filtration with a low protein binding filter (Corning, Inc., Coring, NY). The tracer molecule for these experiments was fluorescein conjugated albumin (Molecular Probes, Eugene, OR) used at 500 μ g/ml concentration in the luminal (loop) medium.

In the presence of only red light, the flow loop was filled with 18 ml of the medium containing fluorescently labeled albumin. A clamp on the inlet line prevented flow through the chamber; however, the roller pump recirculated medium from the lower to upper reservoirs. The subluminal manometer leg was filled with approximately 15 ml of non-labeled experimental medium. The subluminal chamber, which contained a 7mm x 2mm magnetic stir bar, was filled with 2.4 ml of non-labeled experimental medium before attaching the filled manometer leg by means of a 3-way stop-cock.

The two halves of the flow chamber were assembled by gently holding them in place, with the vacuum greased rectangular silastic gasket between them, while applying vacuum generated by a vacuum pump. Gentle, short term release of the inlet

line clamp was used to fill the flow chamber channel, exit slit, and exit tubing with labeled medium. The manometer leg was positioned so that the liquid level was equal to the liquid level of the flow chamber exit tubing, with the clamp remaining in the inlet tubing. A 30 minute incubation period followed.

The baseline permeability determination, repeated 3 to 5 times, was made as follows. The inlet clamp was gently released 10 - 15 times to fill the flow channel with fresh medium of known label concentration. Sample points were taken by unshuttering the mercury lamp at fixed time intervals for five seconds and recording volts at a frequency of 1 hertz. The five observations for each 5 second sampling period were then averaged. Five 5 second samples were taken at 30 to 90 second intervals, depending on the sensitivity of the fluorescent detection system to the increasing fluorescent concentration in the subluminal chamber. At other times the lamp was shuttered to prevent photobleaching of the dye fluorescein.

Flow was started by releasing the clamp on the inlet tubing. At the same time the manometer leg was raised so that the pressure in the subluminal chamber was equalized with that in the flow channel. The liquid levels of the manometer leg and the subluminal chamber were carefully monitored to ensure no volume flux across the membrane. Between 45 to 60 minutes post onset of flow, at least five 5 second samples with a sampling frequency of 1 hertz were taken. The data from each five second sample were averaged and treated as one sample point. The sampling periods were the only times that the lamp was unshuttered. At 60 minutes, a 4 ml sample was removed from the loop in order to determine its concentration fluorometrically, and the inlet to the chamber resealed.

After a 30 minute incubation period under no flow conditions, the recovery permability determination was made following the same procedure as the baseline permeability determination described above.

A multipoint calibration was performed for each experiment by filling the subluminal chamber with known concentrations of fluorescently labeled albumin. Also, after some experiments, the concentration of the manometer leg medium and the flow loop medium were determined for the purpose of calculating the % recovery of label.

After some experiments, the cells were counted (Section 2. A. iv.) or the membrane stained (Section 2. A. iii.) for an indication of cell coverage.

2. E. Scanning Electron Microscopy

Confluency of HUVEC and BAEC was assessed by scanning electron microscopy of representative samples of 7, 11 and 15-day post-seeding. Membranes were washed three times with PBS and then fixed in 2% glutaraldehyde in phosphate buffer (pH 7.2). Membranes were dehydrated in an ethanol series, critical point dried from CO₂, coated with gold-palladium and examined at 10 kV in an ETEC Autoscan.

2. F. LDH Determination

Lactate dehydrogenase (LDH) activity of supernatants and cell lysates was determined with LDH-P Reagent Assay (Gilford Systems, Oberlin, Ohio). Supernatant samples were taken from cultures in the presence and in the absence of thrombin at the conclusion of static agonist experiments. Control monolayers were treated with 1%

Triton X-100 (Sigma) to lyse cells. LDH activity is expressed as the activity of the supernatant normalized to the activity of the lysed monolayer.

2. G. Prostacyclin Determination

Prostacyclin (PGI_2) production was determined by radioimmunoassay (RIA) of 6-keto-prostaglandin $\text{F}_{1\alpha}$ (6-keto- $\text{PGF}_{1\alpha}$), the stable hydrolysis product of PGI_2 , using a ^{125}I -6-keto- $\text{PGF}_{1\alpha}$ RIA kit (NEK-025, NEN). This RIA is based on competitive binding, where the non-radioactive 6-keto- $\text{PGF}_{1\alpha}$ antigen of the samples competes with a known quantity of radiolabeled antigen for a fixed, limited number of antibody binding sites. The lower detection limit of this RIA is 60 pM. Samples were taken at the conclusion of an experiment and analyzed in duplicate.

Each group of RIA samples was run with a multipoint calibration. Duplicate determinations were averaged. The average blank counts (radioactive tracer only, no antibody) were subtracted from the averaged determination of each standard or sample. The net standard or sample counts were divided by the net zero standard counts to give a B/B_0 number. A standard curve was plotted as a semi-log graph of B/B_0 versus standard concentrations. The resulting curve was used to determine the concentrations of the samples.

2. H. Determination of Permeability Coefficients

The defining equation for the permeability coefficient (PC) first shown as equation

1. D. 4 is repeated below:

$$PC \equiv \frac{\text{Mass Flux of Albumin from Luminal to Subluminal Chamber}}{[\text{Albumin}]_{\text{luminal chamber}} - [\text{Albumin}]_{\text{subluminal chamber}}}$$

Depending on the physical parameters of each experimental set-up, this equation can be written in terms of known quantities. Abbreviations common to each situation are:

A = area of membrane

V = volume of chamber

C = concentration of chamber

TP = total protein in solution for time course experiments,

total labeled albumin for other experiments

t = sample time

The subscript S refers to the subluminal chamber and the subscript L to the luminal chamber.

i. Transwell System

The known quantities V_S , V_L , $C_S(t)$, $TP(t)$, and A at each time point t can be substituted into the previous equation. Assuming that the total protein in the system varies only due to the step changes caused by sampling and that the albumin in the subluminal chamber at t=0 is 0, integration and rearrangement yields:

$$\ln \left[\frac{1}{1 - (V_S + V_L) C_S(t) / TP(t)} \right] = PC \left[A \frac{(V_S + V_L)}{V_L V_S} t \right] \quad 2.H. 1$$

A plot of the known quantities in the above equation with t as the independent variable should yield a straight line, if the assumptions made above are correct. The slope of this line, calculated by least squares linear regression, is the PC. Each PC is determined from five samples representing the mass of protein in the subluminal chamber at five different time points. The dilution effect due to sampling is adjusted for by subtracting the amount of albumin removed with the previous sample ($C_S(t) \times$ sample volume) from $TP(t)$. Therefore, the time dependence of TP refers to the step change resulting from sample removal, and the time dependence of C_S accounts for both diffusion and the sampling step changes. For consistency, a computer program was used to calculate PC from the primary dpm data. (Appendix, Transwell permeability coefficient program and sample printout)

The PC is corrected for the contribution from the membrane as described by equation 1. D. 5, repeated below :

$$\frac{1}{PC_{\text{endothelium}}} = \frac{1}{PC_{\text{composite}}} - \frac{1}{PC_{\text{membrane}}} \quad 2. H. 2$$

based on continuity of flux across the monolayer and membrane. The PC of the membrane alone was determined using membranes pretreated with complete medium and fibronectin as described earlier.

For agonist experiments, normalized monolayer PC are expressed as the ratio of the agonist PC to the baseline PC for the same monolayer. Control or baseline

normalized PC are by definition equal to 1. For monolayers pretreated with aspirin or indomethacin, the baseline PC was determined after the pretreatment.

ii. Flow Experiments

In these experiments, different assumptions are made starting from equation 1. D. 4, resulting in a different algebraic form of the permeability equation for the flow and non-flow portions of the experiment.

For the flow permeability coefficient, the loop volume is much greater than that of the subluminal chamber; therefore, the loop concentration (C_L) is treated as a constant. There is no change in the overall mass of the label since no samples are removed from the system. Also, the initial concentration in the subluminal chamber is not necessarily zero, as in the static system. The defining equation for the permeability coefficient under these conditions takes the form:

$$\ln \left[\frac{C_L - C_S(t)}{C_L - C_S(t=0)} \right] = - PC \frac{A t}{V_S} \quad 2. H. 3$$

For the baseline and recovery portions of the experiments (non-flow), the subluminal volume is much greater than the luminal volume, both concentrations change with time, the overall mass of the label remains constant, the initial concentration in the subluminal chamber is not necessarily zero, and the initial concentration of the luminal channel is the same as that of the loop. For these conditions, the defining equation for the permeability coefficient is similar to that for the static system:

$$\ln \left[\frac{TP - (V_S + V_L)C_S(t)}{TP - (V_S + V_L)C_S(0)} \right] = -PC \frac{A(V_S + V_L)t}{V_L V_S} \quad 2. H. 4$$

For a $V_L:V_S$ ratio <1 , as is in this system (0.13), equation 2. H. 4 can be simplified with only a few percent error to:

$$\ln \left[\frac{C_L(t)}{C_L(0)} \right] = -PC \frac{At}{V_L} \quad 2. H. 5$$

2. I. Percent Recovery Calculation

i. Transwell System

The TP(t) at the conclusion of each experiment and the final luminal ($C_L(t)$) and subluminal ($C_S(t)$) concentrations were used to calculate the percent recovery of albumin as follows:

$$\left[\frac{C_S(t) \times V_S + C_L(t) \times V_L}{TP(t)} \right]_{t=\text{final}} \times 100 = \% \text{ recovered} \quad 2. H. 6$$

ii. Flow Loop System

For the flow loop experiments, this calculation takes the form:

$$\frac{[C_S(t) \times V_S + C_L(t) \times V_S + C_M(t) \times V_M]_{t=final}}{C_L(t=0) \times V_L} \times 100 = \% \text{ recovered} \quad 2. H. 7$$

where the subscript M refers to the manometer.

2. J. Statistics

Normalized PC (mean \pm SEM (n)) were determined for each agonist experiment.

Significance ($p < .05$) of PC in the presence or absence of an agonist was determined by

the paired Student's t-test. Analysis of variance (ANOVA) was used to determine

significance ($p < .05$) of differences between agonist treatments.

CHAPTER THREE: RESULTS

3. A. Substrate Choice

i. Material

The substrate of choice for these experiments was polycarbonate. This substrate demonstrates low protein binding as evidenced by the nearly complete recovery of radiolabeled albumin ($95.2 \pm 1.96 \%$, $n=98$). The substrate had straight through cylindrical pores which allowed for nearly an order of magnitude difference in the permeability coefficient for the membrane (3.5×10^{-5} cm/sec) versus that of the baseline endothelial monolayer (5×10^{-6} cm/sec). Finally, the cells grew well on this membrane, forming complete monolayers as shown by scanning electron microscopy (Fig. 3. A. 1) and as indicated by the low baseline permeability coefficients.

ii. Pore Size

Data are not shown for experiments utilizing BAEC cultured on $3.0 \mu\text{m}$ pore size Transwells. Cells cultured on membranes with this pore size proved to be a poor model for studying endothelial monolayer permeability. Permeability coefficients were not related to time in culture, and scanning electron microscopy revealed pores blocked or partially blocked with cell extensions. Staining with Wright's stain showed cells attached to the bottom well of the Transwells, indicating that cells migrated through the membrane. This was confirmed by the presence of cells on both sides of the membrane by SEM (Fig. 3. A. 2). The $0.4 \mu\text{m}$ membranes did not allow this cell migration.

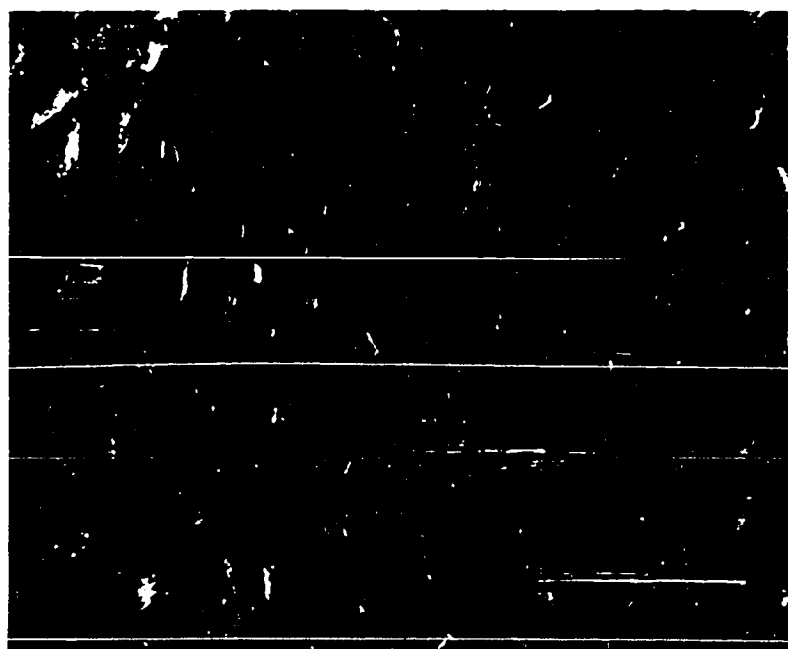


Figure 3. A. 1: Scanning electron micrograph (SEM) of HUVEC, 15 days post seeding, on 0.4 μm pore diameter permeable polycarbonate membrane (x300). Note confluent nature of the monolayer.

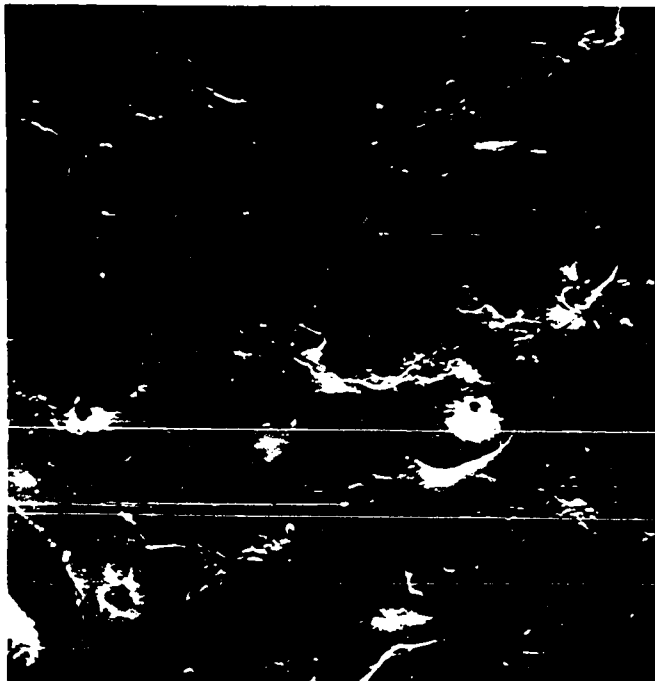


Figure 3. A. 2: Scanning electron micrograph (SEM) of BAEC, 7 days post seeding, on 3.0 μm pore diameter permeable polycarbonate membrane (x150). Note cellular extensions migrating through pores.

3. B. Time Course of Permeability Coefficient

i. HUVEC

The permeability decrease of a single cord pool of HUVEC with increasing time in culture is shown in Figure 3. B. 1. Figure 3. B. 1a represents the transport of albumin across both the monolayer and the permeable membrane. From these data and equation 2. H. 1, permeability coefficients were calculated, then corrected for the membrane permeability coefficient ($3.9 \times 10^{-5} \pm 4.2 \times 10^{-6}$ (n=8) cm/sec) using equation 2. H. 2. The 7-day mean permeability coefficient ($1.1 \times 10^{-5} \pm 2.8 \times 10^{-6}$ (n=4) cm/sec) is significantly greater than either the 11-day ($1.1 \times 10^{-6} \pm 3.4 \times 10^{-7}$ (n=6) cm/sec) or 15-day ($5.5 \times 10^{-7} \pm 3.3 \times 10^{-8}$ (n=6) cm/sec) permeability coefficients. For agonist experiments, monolayers exhibiting a baseline permeability coefficient greater than the mean 7-day post-seeding permeability coefficient of 1.1×10^{-5} cm/sec were rejected. The mean baseline PC for non-flow agonist experiments was $4.8 \times 10^{-6} \pm 3.4 \times 10^{-7}$ (n=98) cm/sec.

ii. BAEC

BAEC permeability coefficients also decreased with increasing time in culture (Fig. 3. B. 2). The 3-day PC is not significantly different from the membrane PC. Each of the higher time points represents a significant decrease in permeability from the previous time point. Scanning electron micrographs show a subconfluent monolayer at 3-days and a confluent monolayer at 11-days post seeding.

3. C. Permeability Changes in Iloprost-Treated Monolayers

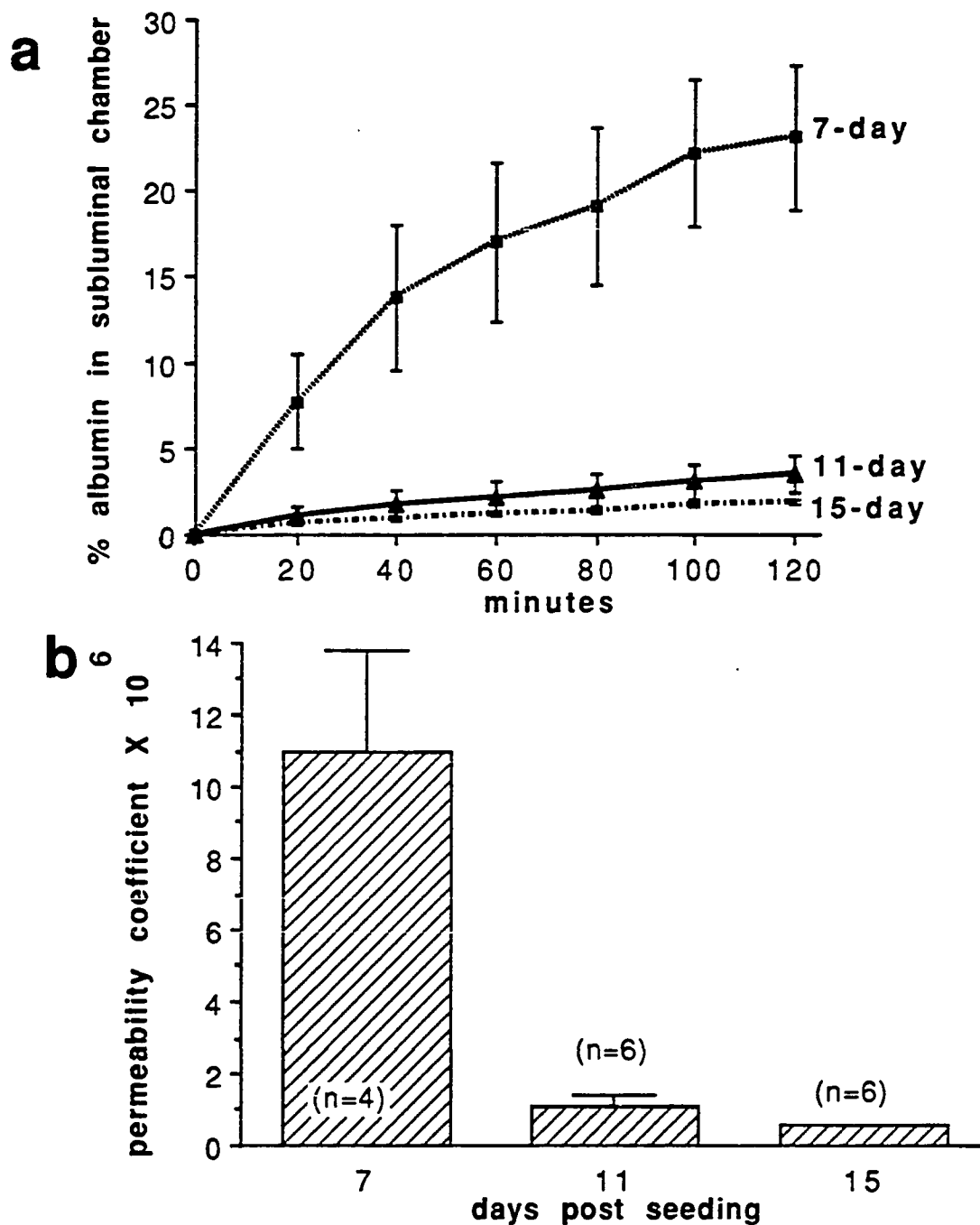


Figure 3. B. 1: Effect of time in culture on permeability. P2 HUVEC are derived from the same cell harvest. The absolute value of the permeability coefficients may vary with cell harvest. a) The mass of albumin (as percent of total system albumin) transported across the monolayer is plotted versus time. b) Permeability coefficients (cm/sec) are shown for each post-seeding time point, corrected for the permeability of the membrane as described in Methods. Error bars represent standard error of the mean.

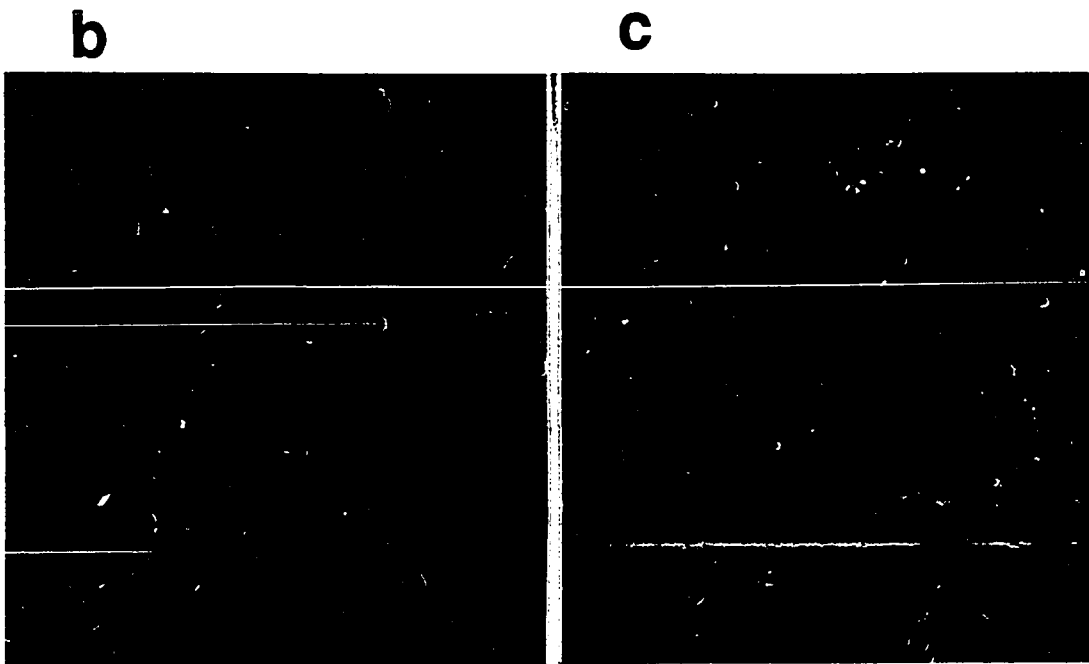
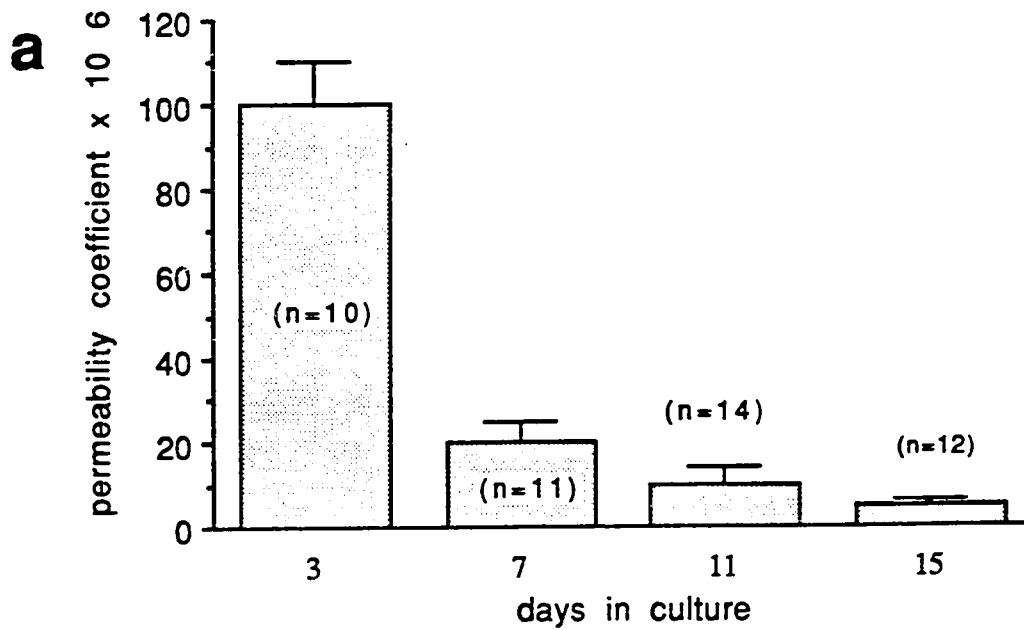


Figure 3. B. 2: Time course of BAEC permeability. a) Permeability coefficients for 3, 7, 11, and 15 days post seeding. b) SEM of BAEC 3 days post seeding on 0.4 μm pore diameter polycarbonate membrane (x120). At this time point the permeability coefficient was no significantly different from that of the membrane alone. c) SEM of BAEC 11 days post seeding on 0.4 μm pore diameter polycarbonate membrane (x120).

Treatment of monolayers with 6 nM iloprost resulted in a decrease in permeability to $33\% \pm 4.8\%$ (n=7) of the baseline value. The mean baseline PC for iloprost experiments was $3.5 \times 10^{-6} \pm 4.6 \times 10^{-7}$ (n=7) cm/sec. Figure 3. C. 1a is a representative graph of albumin tracer concentration in the subluminal chamber versus time. In Figure 3. C. 1b, the data are plotted using coordinate axes defined by equation 2. H. 1. The decreased slope in the presence of iloprost represents decreased permeability. Similar reductions in permeability were observed with 30 nM and 60 nM iloprost. Functional activity of iloprost at 6 nM was verified by its ability to inhibit aggregation of thrombin-treated platelet rich plasma in a platelet aggregometer. The decrease in permeability was observed within 10 minutes of iloprost treatment and was constant thereafter throughout the permeability assay.

3. D. Effect of Thrombin on Permeability

Thrombin (0.15 U/ml) dramatically increased permeability of HUVEC monolayers 9.6-fold over the baseline values (Fig. 3. D. 1). The maximum effect of thrombin was observed within 10 minutes of treatment and remained constant throughout the permeability assay (40 minutes). Permeability after thrombin washout and approximately one hour incubation in complete medium was not significantly different

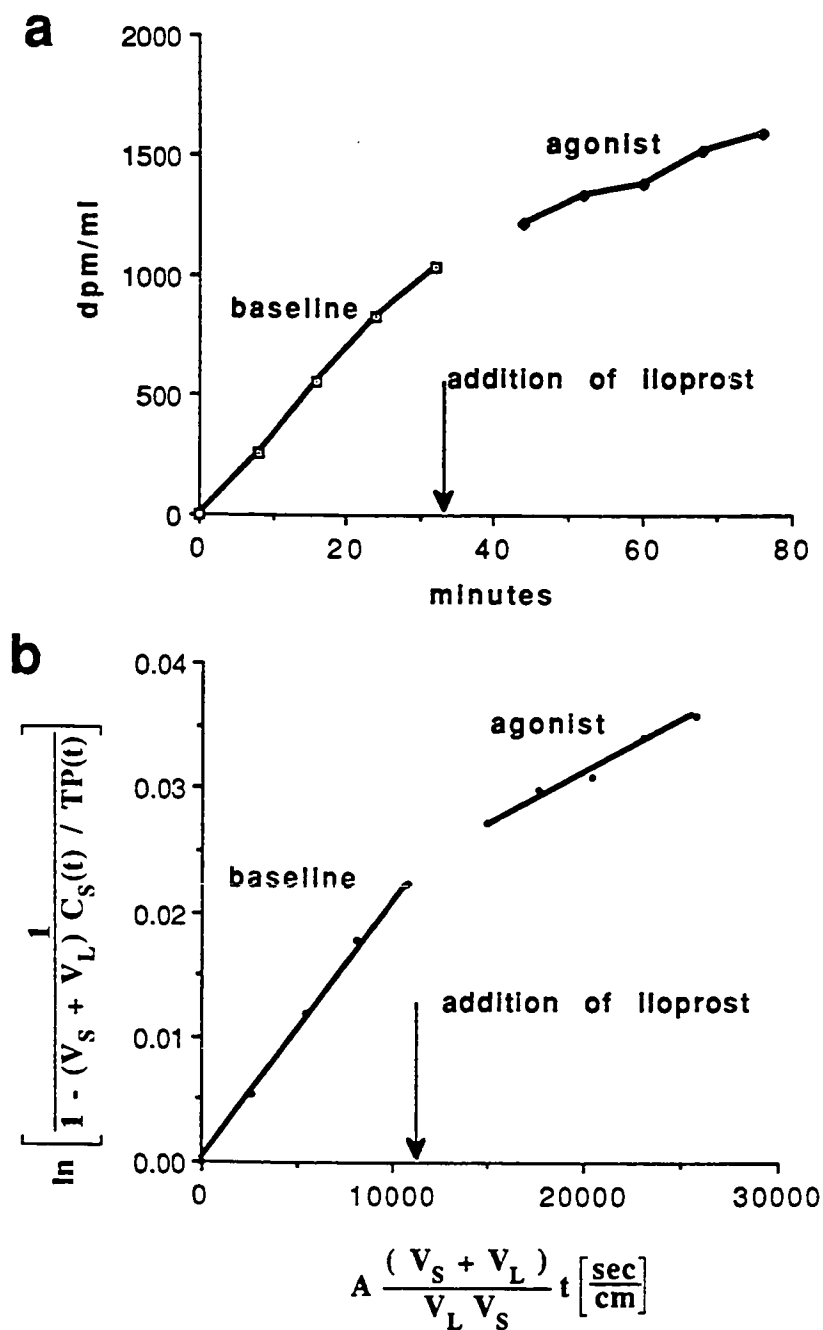


Figure 3. C. 1: Determination of PC from permeability assay data. a) The concentration of albumin tracer in the subluminal chamber is plotted against time. At approximately $t = 33$ minutes, iloprost was added to the system to achieve a 6 nM concentration in each chamber. b) The data for the baseline and the agonist portions of the experiment are plotted using coordinate axes defined by equation 2. H. 1 in Methods. The permeability coefficients are determined from the slopes of these lines by least squares linear regression.

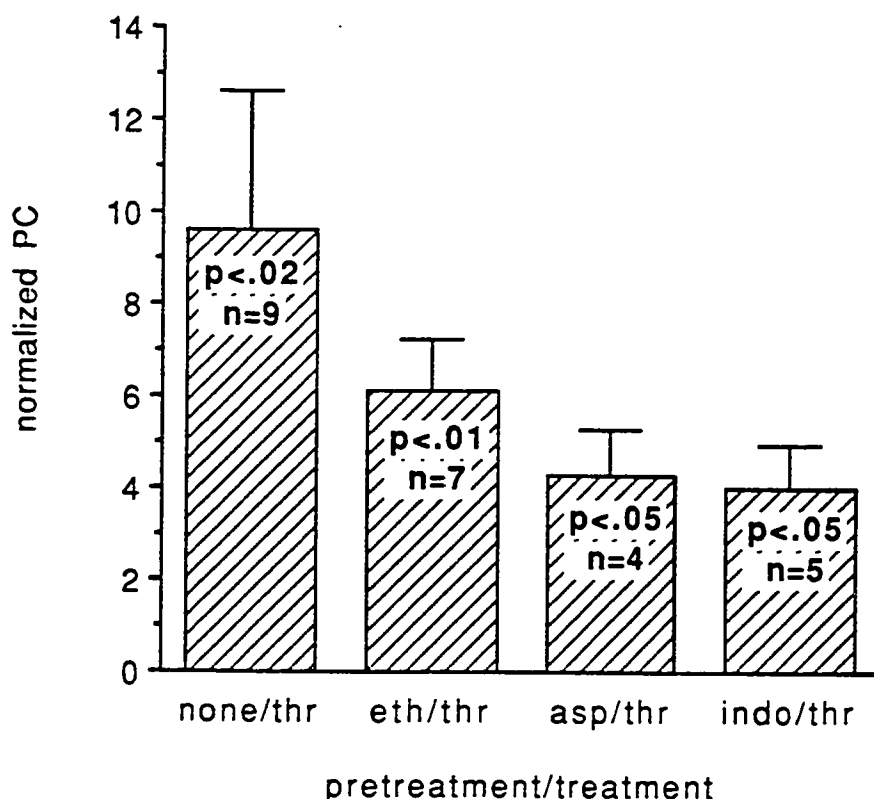


Figure 3. D. 1: Effect of thrombin on permeability of cyclooxygenase inhibited monolayers. Normalized PC are shown for thrombin (0.15 U/ml) treatment of non-pretreated, ethanol (eth, 0.0345 vol %), aspirin (asp, 5 μ M in 0.0345 vol % ethanol), and indomethacin (indo, 50 μ M in 0.0345 vol % ethanol) pretreated monolayers. P-values indicate significance of normalized PC from normalized baseline permeability (unity by definition) for each pretreatment group. The non-normalized baseline PC (cm/sec) for each group are: none/thrombin, $3.3 \times 10^{-6} \pm 1.1 \times 10^{-6}$ (n=9); ethanol/thrombin, $3.2 \times 10^{-6} \pm 7.3 \times 10^{-7}$ (n=7); aspirin/thrombin, $2.2 \times 10^{-6} \pm 3.8 \times 10^{-7}$ (n=4); and indomethacin/thrombin, $3.6 \times 10^{-6} \pm 1.2 \times 10^{-6}$ (n=5). These baseline PC were determined following a 30 minute incubation with complete medium, or complete medium containing ethanol, aspirin, or indomethacin, respectively. The groups of non-normalized baseline PC are not significantly different from each other by ANOVA.

from permeability in the presence of thrombin.

Thrombin also increased permeability in aspirin and indomethacin pretreated monolayers. Aspirin and indomethacin inhibit prostacyclin production by blocking cyclooxygenase activity. Pretreatment of monolayers with aspirin or indomethacin exposed the cells to 0.0345 volume % ethanol as a solvent vehicle for these inhibitors. Ethanol alone inhibited thrombin-induced permeability increases. The effect of thrombin on aspirin or indomethacin pretreated monolayers was not significantly different from the effect of thrombin on ethanol vehicle pretreated monolayers (Fig. 3. D. 1).

Neither DIP- α -thrombin nor PPACK- α -thrombin significantly altered permeability of monolayers versus baseline values (Table 3. D. 1). α -Thrombin added subsequent to incubation with DIP- α -thrombin or PPACK- α -thrombin did not significantly affect permeability. γ -thrombin, a form of thrombin which is proteolytically active but does not bind well to the endothelium, did not significantly increase permeability (normalized permeability coefficient of 1.72 ± 0.447 , $n = 4$).

LDH activity of supernatants from thrombin treated and non-thrombin treated monolayers were not significantly different. LDH activity was measured in samples taken from both chambers at the conclusion of some agonist experiments. LDH release, expressed as the percent of cell lysate release, is 8.45 ± 1.27 ($n=6$) for thrombin treated monolayers and 6.01 ± 1.01 ($n=6$) for non-thrombin treated monolayers.

Table 3. D. 1: Effect of proteolytically active and inactive thrombins on permeability

	<u>normalized permeability coefficient \pm sem</u>	
α -thrombin	9.6 ± 3.0	(n=9)
DIP- α -thrombin	0.54 ± 0.25	(n=3)
PPACK- α -thrombin	1.0 ± 0.052	(n=4)

Concentrations of agonists were: α -thrombin, 0.15 U/ml; DIP- α -thrombin, 1nM; and PPACK- α -thrombin, 1nM. Permeability in the presence of α -thrombin was significantly ($p < .02$) greater than normalized baseline permeability coefficient (PC, unity by definition). Inactivated thrombins did not significantly alter permeability. Non-normalized baseline PC (cm/sec) for each group are: α -thrombin, $3.3 \times 10^{-6} \pm 1.1 \times 10^{-6}$ (n=9); DIP- α -thrombin, $4.5 \times 10^{-6} \pm 8.3 \times 10^{-7}$ (n=3); and PPACK- α -thrombin, $7.5 \times 10^{-6} \pm 1.6 \times 10^{-6}$ (n=4). The groups of baseline PC are not significantly different from each other by ANOVA.

3. E. Effect of Bradykinin on Permeability

Bradykinin (1 μ M) had no significant effect on permeability of non-treated, aspirin-pretreated or ethanol-pretreated monolayers (Table 3. E. 1). There is no significant difference between the effect of bradykinin on ethanol versus aspirin pretreated endothelial cells. All bradykinin experiments were performed in the presence of 0.1 μ M captopril to inhibit degradation of bradykinin by endothelial angiotensin converting enzyme.

The effectiveness of aspirin or indomethacin inhibition of cyclooxygenase metabolite production was determined by RIA for 6-keto-PGF_{1 α} . No detectable production of 6-keto-PGF_{1 α} (< 60 pM) occurred in response to thrombin or bradykinin challenge of cyclooxygenase-inhibited monolayers. In non-inhibited monolayers, thrombin and bradykinin stimulation resulted in measurable concentrations of 1.8 nM and 0.20 nM 6-keto-PGF_{1 α} in the luminal chamber, respectively, and in the subluminal chamber, 0.64 nM and < 60 pM, respectively. These concentrations represent cumulative production during both the baseline and agonist stimulation periods; however, baseline production was non-detectable. These 6-keto-PGF_{1 α} concentrations can not be used to indicate polarity of prostacyclin expression for at least three reasons. First, the time scale of the agonist experiments (greater than one hour) is long enough to allow significant diffusion between the chambers. Second, subluminal samples were removed and the above concentrations do not take into account the resulting dilution effect because the 6-keto-PGF_{1 α}

Table 3. E. 1: Effect of bradykinin on permeability

<u>pretreatment/treatment</u>	<u>normalized permeability coefficient \pm sem</u>	
none/bradykinin	1.4 \pm 0.20	(n=11)
ethanol/bradykinin	0.99 \pm 0.37	(n=4)
aspirin/bradykinin	0.69 \pm 0.16	(n=11)

Agonist concentrations were: bradykinin, 1 μ M; ethanol, 0.0345%; and aspirin, 5 μ M in 0.0345% ethanol solvent. Normalized PC were not significantly different from normalized baseline PC. Non-normalized baseline PC (cm/sec) for each group are: none/ bradykinin, $6.6 \times 10^{-6} \pm 9.5 \times 10^{-7}$ (n=11); ethanol/bradykinin, $9.4 \times 10^{-6} \pm 1.3 \times 10^{-6}$ (n=4); and aspirin/bradykinin, $6.6 \times 10^{-6} \pm 1.1 \times 10^{-6}$ (n=11). The groups of baseline PC are not significantly different from each other by ANOVA.

concentrations of these samples were not determined. Third, the chambers are of unequal volume; therefore, the concentrations can not be compared directly.

3. F. Cyclic Nucleotide Analog/Phosphodiesterase Inhibitor Permeability Alterations

Cyclic AMP analogs, dibutyl cAMP and 8-bromo-cAMP, in conjunction with either IBMX or theophylline, significantly decreased permeability (Fig. 3. F. 1). IBMX alone also significantly decreased permeability to an extent indistinguishable from IBMX in the presence of dibutyl cAMP or 8-bromo cAMP. These decreases were maximum within 10 minutes after monolayer treatment and persisted in the dibutyl cAMP/theophylline system after a one hour incubation of washed monolayers in complete medium. Neither theophylline nor dibutyl cAMP significantly altered permeability unless supplemented by complementary agents. In contrast, dibutyl cGMP alone significantly reduced permeability (0.667 ± 0.122 (n=6)).

3. G. Inhibition of Thrombin-Induced Permeability Increases

Thrombin-induced permeability increases were inhibited in monolayers pretreated with iloprost. Normalized PC for thrombin challenged, iloprost pretreated monolayers was 1.6 ± 0.31 (n=7) compared to 9.6 ± 3.0 (n=9) for thrombin stimulated, non-pretreated monolayers. Since PGI_2 increases cAMP in endothelial cells, the effect of cAMP analog/phosphodiesterase inhibitor combinations on thrombin-induced permeability increases were investigated. All cAMP analog/phosphodiesterase inhibitor combinations reduced the full expression of

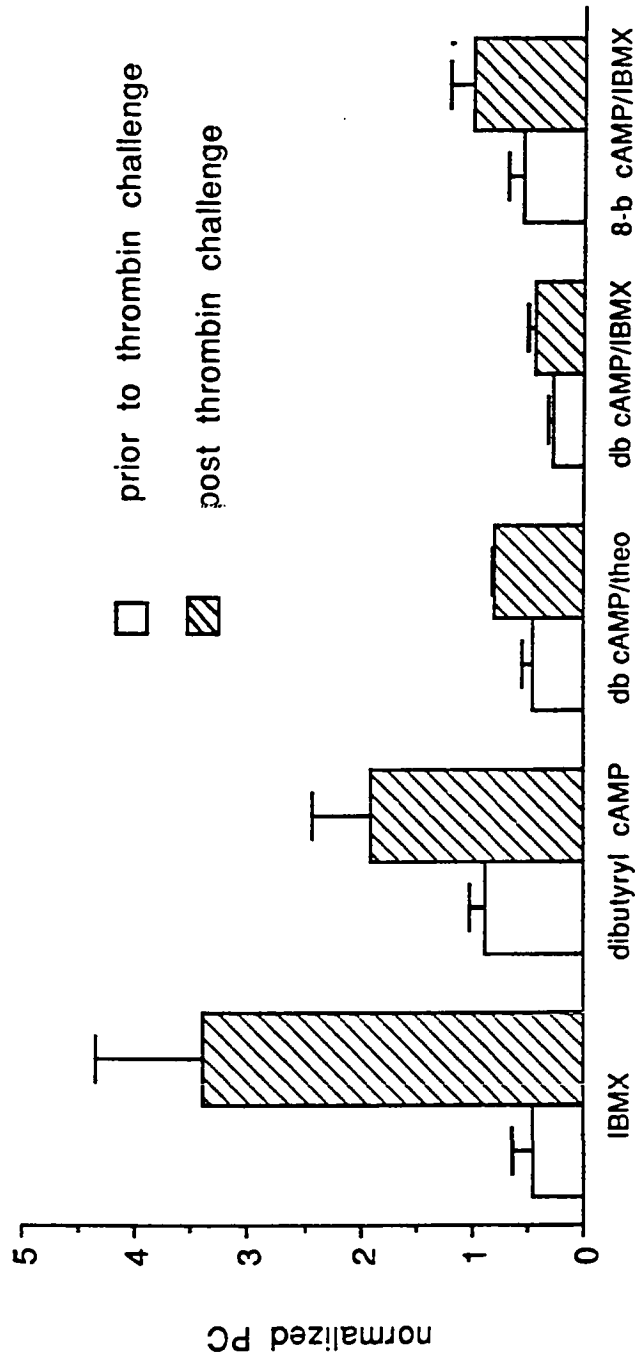


Figure 3. F. 1: The effect of cAMP analogs and phosphodiesterase inhibitors on permeability and on inhibition of thrombin-induced permeability increases. Normalization for all data is to untreated baseline PC, with normalized baseline PC for each group equal to 1. The unshaded columns show normalized PC in the presence of IBMX (0.1 nM), dibutyl cAMP (0.5 mM), dibutyl cAMP/theophylline (0.5mM) [db cAMP/theo], dibutyl cAMP/IBMX [db cAMP/IBMX], and 8-bromo cAMP (0.5mM)/IBMX [8-b cAMP/IBMX]. All agent combinations, except for dibutyl cAMP alone, significantly reduced permeability. The shaded columns represent the same treated monolayers after challenge with 0.15 U/ml thrombin. In all groups thrombin increased permeability but not significantly above baseline values. Thrombin causes a 9.6-fold permeability increase in non-pretreated monolayers (Fig. 3. D. 1). The non-normalized baseline PC (cm/sec) for each group are: IBMX, $7.3 \times 10^{-6} \pm 1.4 \times 10^{-6}$ (n=6); dibutyl cAMP, $9.4 \times 10^{-6} \pm 8.0 \times 10^{-7}$ (n=5); dibutyl cAMP/theophylline, $3.2 \times 10^{-6} \pm 9.4 \times 10^{-7}$ (n=8); dibutyl cAMP/IBMX, $3.8 \times 10^{-6} \pm 4.9 \times 10^{-7}$ (n=6); and 8-bromo cAMP/IBMX, $2.7 \times 10^{-6} \pm 6.8 \times 10^{-7}$ (n=7).

thrombin-induced permeability increases (Fig. 3. F. 1). Post-thrombin-challenge normalized PC for each treatment group are not significantly greater than normalized baseline PC.

Pretreatment with 0.5mM dibutyryl cGMP also reduced the full expression of thrombin-induced permeability increases (2.84 ± 1.01 (n=6)).

3. H. Recovery of Albumin

In the static system, the percent of albumin radioactive tracer recovered was 95.20 ± 1.960 % (n=98) as calculated from equation 2. H. 6. In this system some of the albumin may have adsorbed onto the walls or membrane of the Transwell. Some adsorption probably also occurred onto the walls of the pipette tips used to obtain samples. Also, a small pipetting error in the final luminal sample could greatly affect results since the luminal albumin concentration was high. In the flow system, the percent recovery was 95.14 ± 3.46 % (n=5) as calculated from equation 2. H. 7. In addition to the effect of adsorption or calibration errors on percent recovery, the fluorescently labeled dye in the flow system undergoes some photobleaching during the normal course of the experiment. However, the amount of dye which diffuses into the manometer leg from the subluminal chamber is minimal. When detectable, this amounted to less than 0.1% of the total dye.

3. I. Shear Stress

Shear stress at 7 dynes/cm² increased permeability approximately 7-fold over baseline values (Fig. 3. I. 1). After a half hour recovery period, this increase was

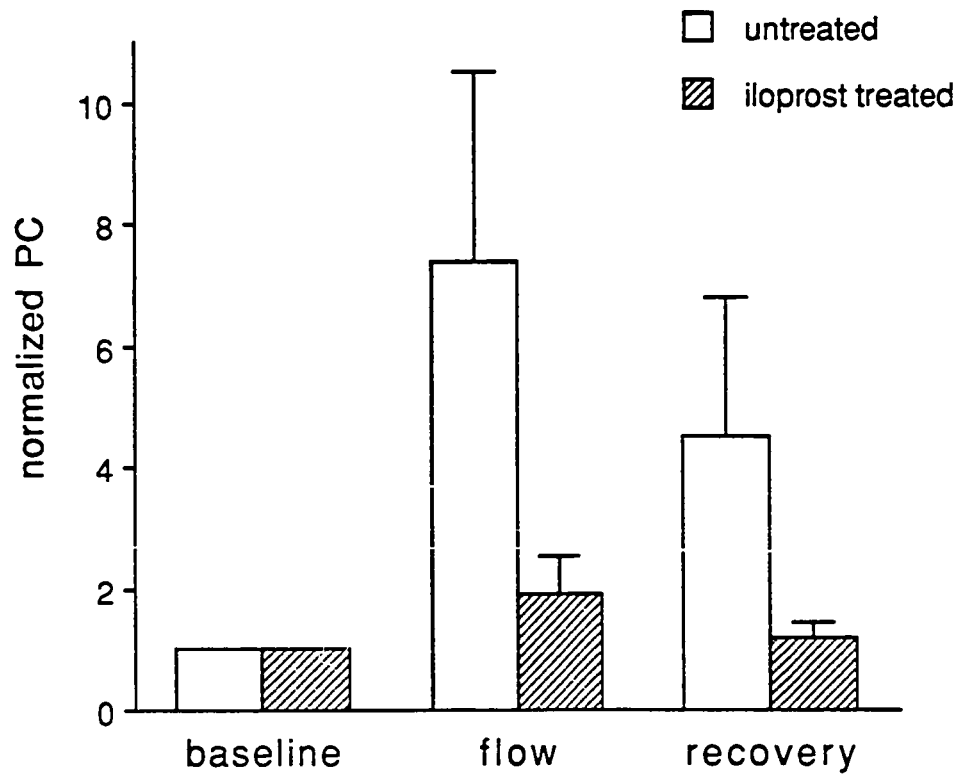


Figure 3. I. 1: Effect of 7 dynes/cm² shear stress on permeability. Normalized PC is plotted for the baseline, flow and recovery portions of the experiment. The unshaded columns show the response of untreated cells (n=3). The shaded columns show the response of monolayers pretreated with 6 nM iloprost (n=3).

partially reversed. When cells were pretreated with 6 nM iloprost, shear stress induced a 2-fold increase in permeability. Iloprost pretreatment also facilitated recovery to a level indistinguishable from baseline values.

No cell controls in the flow system showed that the permeability coefficients at each phase of the experiment were not significantly different from each other by ANOVA (Fig. 3. I. 2). Therefore, these values were averaged for a mean membrane PC of 4.6×10^{-5} cm/sec. As with the static system, the monolayer PC was calculated from equation 2. H. 2, after determination of the composite PC from equation 2. H. 5 (no-flow) or 2. H. 3 (flow).

3. J. Polarity of PGI₂ Expression

The luminal mass percent prostacyclin in response to 1 μ M bradykinin in the luminal chamber for each sampling time is shown in Fig. 3. J. 1. These values are not significantly different from 50%, indicating that prostacyclin is not preferentially secreted. When the cells are stimulated with 1 μ M bradykinin in the subluminal chamber (Fig. 3. J. 1), the results are not significantly different. These agonist stimulated values are not significantly different from the constitutive secretion ($46.1 \pm 2.45\%$ (n=27)). These results indicate that although bradykinin increases the overall magnitude of prostacyclin production, it does so in a non-polarized manner. Permeability coefficients for albumin, post bradykinin stimulation, were not significantly different from baseline permeability coefficients ($4.617 \times 10^{-6} \pm 0.5684 \times 10^{-6}$ cm/sec (n=23) versus $5.398 \times 10^{-6} \pm 1.053 \times 10^{-6}$ cm/sec (n=23).

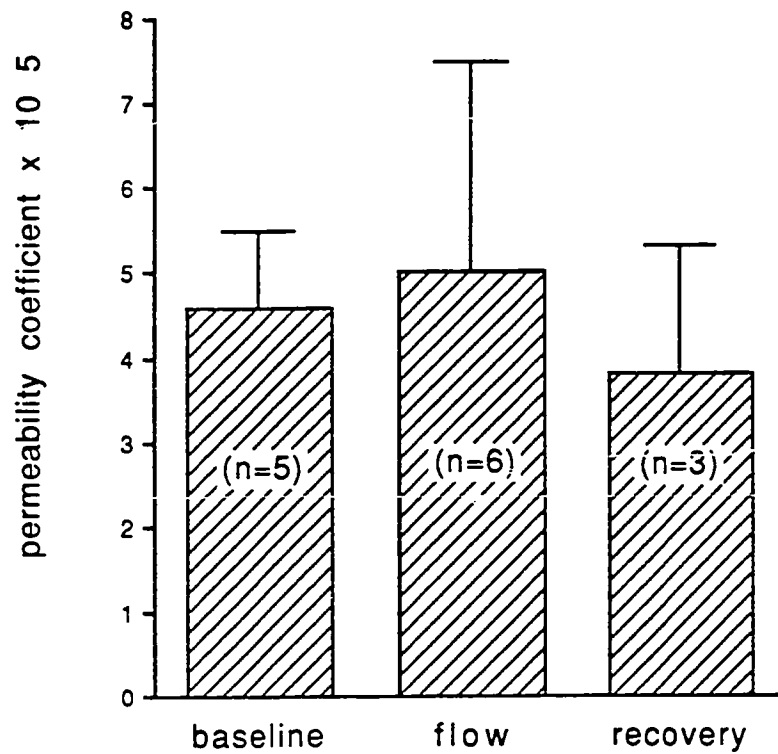


Figure 3. I. 2: Shear stress controls. The permeability coefficient for each phase of the experiment is plotted. These PC are not significantly different from each other by ANOVA.

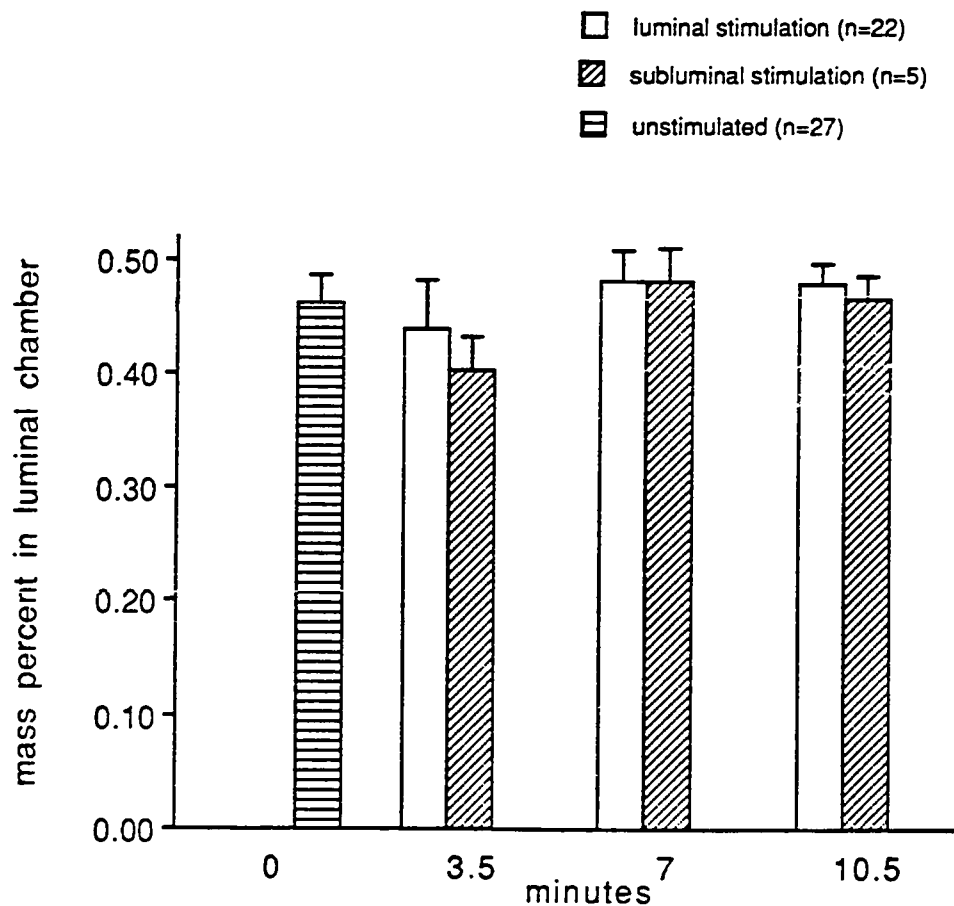


Figure 3. J. 1: Polarity of prostacyclin expression. At $t=0$, $1 \mu\text{M}$ bradykinin was added to the luminal or subluminal chamber. The mass percentages are corrected for the dilution effect due to sampling but not for diffusion of prostacyclin across the membrane. Control experiments demonstrated that diffusion was negligible during the 10.5 minute sampling period. All values are not significantly different from 50%, indicating that prostacyclin is not secreted in a polarized manner in response to bradykinin stimulation.

by paired students t-test.

Production averaged 2281 ± 299.9 (n=27) pg/well for the 10.5 minutes following bradykinin stimulation. This corresponds to approximately 14 ng/ 10^6 cells.

If the data are presented by cord pool (Fig. 3. J. 2), one cord pool (C) does appear to have polarized secretion in the subluminal direction. This apparent polarization may be a phenomenon of a specific drug treatment during delivery or handling/storage conditions of these particular umbilical cords.

Controls for these studies were run to determine the extent of iloprost diffusion during the 10.5 minute experimental period. Iloprost binds to albumin, and its transport is somewhat dependent on the albumin gradient across the membrane (Fig. 3. J. 3, 4%-0% versus 4%-4%). In a system with equal albumin concentrations in both chambers, the permeability coefficient for mass transfer in the subluminal to luminal direction is about one order of magnitude higher than that in the opposite direction. The physical significance of this difference is unclear. Based on mean PC from these control experiments (3.08×10^{-7} cm/sec luminal-to-subluminal and 2.21×10^{-6} cm/sec subluminal-to-luminal), the mass of prostacyclin which diffuses across the membrane during these 10.5 minutes experiments was <1% of the total mass; therefore, diffusion was ignored in the polarity calculations.

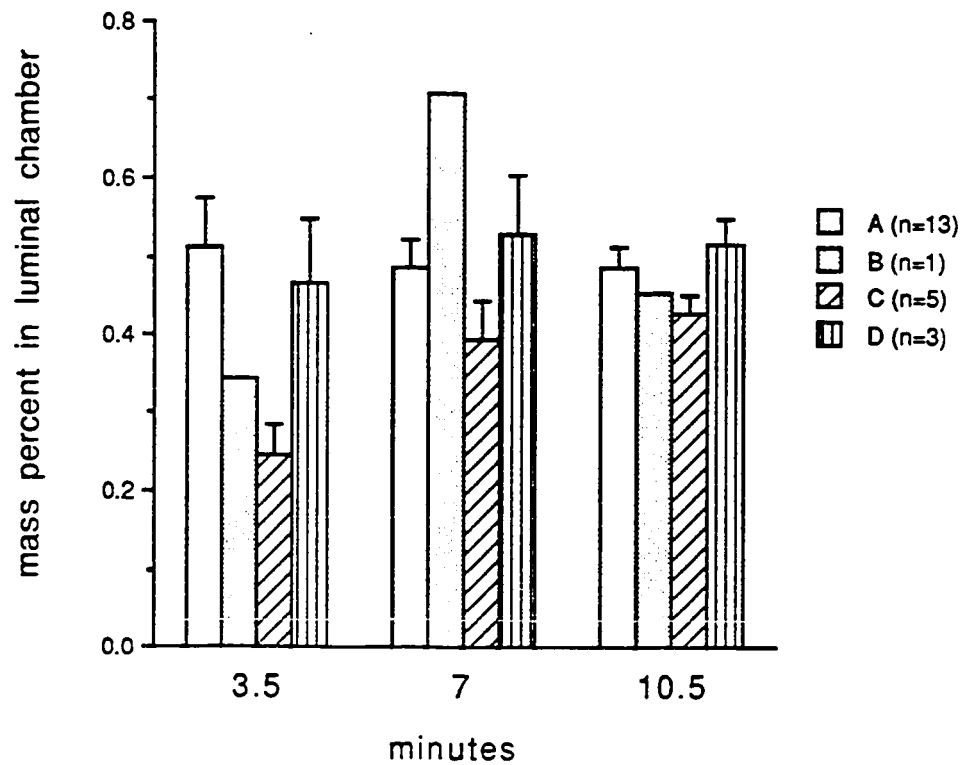


Figure 3. J. 2: Polarity of prostacyclin production by cord pool. The $n=22$ luminal bradykinin stimulation experiments from Fig. 3. J. 1 are reported here by cord pool. An apparent subluminal polarity is exhibited by cord pool C.

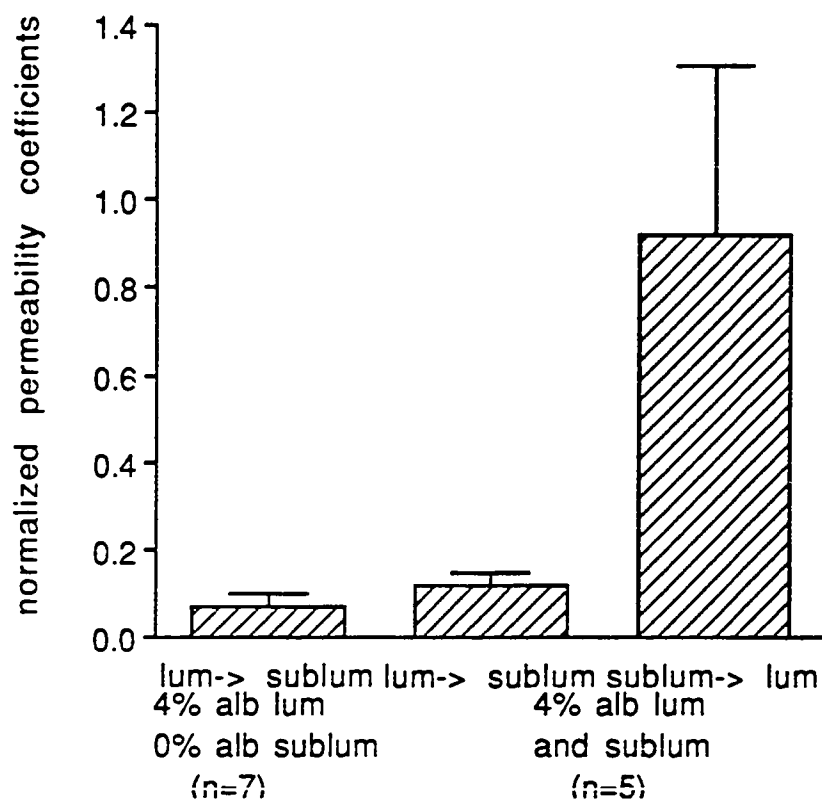


Figure 3. J. 3: Polarity controls were run with tritiated iloprost. The smaller molecule iloprost binds to the albumin in the experimental medium. Transport in the luminal to subluminal direction is somewhat dependent on the external albumin concentration gradient (4%-0% versus 4%-4%). In the presence of 4% albumin in both chambers, transport in the luminal to subluminal direction is much slower than in the subluminal to luminal direction.

CHAPTER FOUR: DISCUSSION

4. A. Model Verification and Application

This investigation was conducted using a permeability model consisting of endothelial cells cultured on a permeable polycarbonate membrane. This model provides the means to determine the relative contribution of a single cell type to the total vessel wall permeability. Although similar to other *in vitro* models, improvements were made through time course studies and permeability coefficient calculations. Time course studies demonstrated that 15-day post-seeding monolayers had the lowest baseline permeability coefficient for our system, and that baseline permeabilities varied the least at this time point (Fig. 3. B. 1b). Our permeability coefficient calculations accounted for the step changes in total system tracer mass due to sampling as well as the diffusion dependent increases in subluminal tracer concentrations. Permeability coefficient determinations also allowed for correction for the membrane contribution to the permeability barrier. Another advantage of reporting data as permeability coefficients is the ability to compare our data with other permeability models since PC normalize mass transfer with respect to concentration gradient across the monolayer, area of membrane, monolayer thickness, length of experiment, and chamber volumes.

Baseline permeability coefficients in our system are somewhat lower than those reported in other *in vitro* systems (Table 4. A. 1). A small osmotic pressure gradient

Table 4. A. 1: In vitro permeability coefficients of albumin for endothelial monolayers

Reference	PC (cm/sec)	Endothelial cell type
Cooper et al. (1987)	1.2×10^{-5}	Bovine pulmonary arterial
Garcia et al. (1986)	9.3×10^{-6}	Bovine pulmonary arterial
Albelda et al. (1988)	6.5×10^{-6}	Bovine fetal aortic
This study	4.8×10^{-6}	Human umbilical vein (static agonist experiments)

All studies used polycarbonate membranes of 0.4 μ M pore diameter (this study) or 0.8 μ M pore diameter (Cooper et al., 1987; Garcia et al., 1986; Albelda et al., 1988), with the same thickness (10 μ m) and porosity (15-20%). In addition, the coating procedures of Garcia et al., (1986) and Cooper, et al. (1987) are identical. Therefore, all permeability coefficients have been corrected for the membrane contribution of 3.9×10^{-5} cm/sec (this study, Cooper et al., 1987) according to equation 1. D. 5.

between luminal and subluminal chambers existed in two studies (Garcia et al., 1986; this study), but not in the others (Albelda et al., 1988; Cooper et al., 1987). The effect of the osmotic pressure gradient was undetectable in our system since baseline permeability coefficients were not significantly different in the presence or absence of an osmotic pressure gradient ($3.0 \times 10^{-6} \pm 3.1 \times 10^{-7}$ (n=27) cm/sec versus $3.5 \times 10^{-6} \pm 5.0 \times 10^{-7}$ (n=4), respectively). The lack of a significant effect based on the small oncotic pressure gradient is also predicted by an estimate of the volume flux using the Kedem-Katchalsky equations. A maximum 1% volume change in the subluminal chamber would occur based on the oncotic pressure gradient.

The difference between the mean baseline PC for agonist studies, 4.8×10^{-6} cm/sec (nine cell harvests), and the 15-day mean baseline PC for the time course study, 5.5×10^{-7} cm/sec (one cell harvest), is due to variability between cord pools. The 15-day time course PC can be compared directly to other time course data (as in Fig. 3. B. 1b), which are from matched cultures of HUVEC from the same cell harvest. However, because of the differences in baseline PC resulting from donor variability, the agonist study results were reported normalized to a baseline PC, using each monolayer as its own control. This normalized PC describes permeability effects of the various agonists by relating the permeability altering effect to the pre-stimulated permeability of the same monolayer.

In vitro permeability coefficients (10^{-5} to 10^{-7} cm/sec) can be compared to *in vivo* permeability coefficients which range from 10^{-6} to 10^{-9} cm/sec (Bratzler et al., 1977). The endothelial permeability barrier function of *in vitro* monolayers may be more similar to *in vivo* than the PC ranges indicate. *In vivo*, non-endothelial vessel

wall components or blood cells may metabolize tracer molecules, mediate the effect of agonists, and contribute to the vascular permeability barrier. The accumulation of tracer albumin molecules in the lymph system or vasa vasorum may alter the transmural concentration profiles by presenting an adventitial albumin concentration great enough to drive albumin flux back into the wall in the adventitia-to-media direction (Bratzler et al., 1977). This adventitial albumin concentration would result in reduced mass flux in the intima-to-media direction due to the flatter transmural concentration profile. Perfusion of vessels *in vivo* may result in altered permeability due to metabolic effects of shear stress, transmural pressure gradients, and pulsatile flow on the endothelium. For example, shear stress and pulsatile flow significantly increase endothelial production of PGI_2 (Frangos et al., 1985). Alternately, the permeability function of *in vitro* monolayers may be dependent on cell substrate and may require humoral factors released from other vascular cell types in order to realize the full permeability barrier function potential.

The advantage of *in vitro* permeability models is that they can provide information difficult to obtain directly from *in vivo* systems. Because of the complexity of *in vivo* permeability systems, the utility of *in vitro* models lies in the ability to study direct causal relationships between a single agonist and a single cell type. As these relationships are defined, the complexity of an *in vitro* system can increase to allow investigation of more complex interactions.

One important factor correlating with permeability may be cell density. *In vivo* cell surface areas for rabbit aorta have been reported as approximately $400 \mu\text{m}^2$.

proximal to a branch point and approximately $705 \mu\text{m}^2$ at the branch point (Nerem et al., 1981). From the cell areas the cell density may be calculated as 250,000 cells/cm² proximal to the branch point and 133,000 cells/cm² at the branch point. These differences in cell density may correspond to local differences in vascular permeability. For example, increased Evans blue dye-albumin uptake occurs at branch points (Fry, 1977). This hypothesis is partially supported by our permeability time course study with BAEC. The 3-day post-seeding cell density of 5×10^4 cells/cm² was essentially the same as the seeding density. Permeability did not significantly decrease from initial seeding to 3 days in culture. At 7 days, the cell density was approximately 1×10^5 cells/cm², which corresponds to a confluent density in tissue culture flasks. The permeability decreased significantly from 3 to 7 days post seeding. At 11 days, the cell density was approximately 1.5×10^5 cells/cm², with a corresponding significant decrease in permeability from the previous time point. At 15 days there was another significant decrease in permeability from the previous time point, and the density had increased to 3×10^5 cells/cm². The difference in cell density relative to *in vivo* position may account for regional patterns of increased permeability in areas of complex flow patterns or high shear stress, and may correspond to areas of increased cell turnover. In this manner, complex flow may affect *in vivo* permeability in a long term manner by stimulating increased turnover of endothelial cells (Davies et al., 1986). This discussion highlights an issue the model developed herein cannot address, which is determination of regional variations in vascular permeability. This determination is best done *in vivo* (Bell et al., 1974) or can be done *in vitro* (Bottaro et al., 1986a) if the permeability barrier function of all cell lines is independently

optimized.

The regulation and expression of cell products is dependent on the cell substrate. Cultured capillary endothelium exhibit differing phenotypes dependent on the subendothelial matrix components (Madri and Williams, 1983). If this aspect of cellular metabolism is substrate dependent, regulation of the cytoskeleton, an important determinant of endothelial permeability, may also be substrate dependent. As endothelial time in culture increases, the rate of secretion of glycosaminoglycans increases, and the relative proportions of heparin sulfate to chondroitin sulfate to dermatan sulfate are altered (Wang et al., 1985; Robinson and Gospodarowicz, 1983). Alterations in the composition of the basement membrane may modulate cell metabolism with respect to the permeability barrier function. Basement membrane alterations are another way in which time in culture may influence endothelial permeability.

A potential simple test for monolayer integrity is transendothelial electrical resistance (TEER); however, there is some discrepancy in the literature regarding the applicability of this test. TEER correlates with transfer of small ions across the endothelium, and some investigators report that this electrical resistance also correlates with macromolecular transport. Furie et al. (1984), using bovine microvascular endothelial cells cultured on human amnion, showed that transendothelial electrical resistance was greatest when permeability to wheat germ agglutinin-horseradish peroxidase conjugate was lowest. However, in a system of rabbit aortic endothelial cells cultured on polycarbonate membranes (Navab et al., 1986), TEER did not correlate with permeability to macromolecules. In an epithelial cell line, Sertoli cells, electrical resistance correlates with macromolecular transport

(Dr. A. Steinberger, personal communication), and the same laboratory reports decreased inulin transport corresponding with the appearance of tight junctions in their cultures (Janecki et al., 1987). Perhaps TEER is a useful indicator of monolayer integrity in cultures with mature junctions. Such a simple test for structural integrity of endothelial monolayers would be welcomed, if it can be used as an indication of macromolecular transport.

The cell culture *in vitro* methods of characterizing endothelial permeability described in this thesis do so in a controlled, well-defined manner. Perhaps even more importantly, these studies were accomplished without sacrifice of animal models. A test such as the Miles permeability assay (A.A. Miles and E.M. Miles, J. Physiol. (London), 118: 228, 1952), which involves Evans' blue injections into anesthetized hairless guinea pigs for observation of blue spots on the animals' backs, seems an unnecessary use of animals in research, as well as a relatively uncontrolled, unquantifiable assay. It is my personal belief that animal studies should be reserved for investigations which can not be accomplished in any other manner.

A word of caution must be mentioned here regarding comparison of *in vitro* data. Our initial studies with BAEC have clearly shown that endothelial cells migrate through 3 μm pores. However, several permeability studies have been conducted with larger (5 μm) pore diameter membranes (Navab et al., 1986; Rotrosen and Gallin, 1986; Shasby et al., 1982; Zerwes and Risau, 1987). These studies have the potential for pore blockage by cells, development of a second layer of cells on the underside of the membrane, and a monolayer of cells in the bottom well. If these phenomena occur undetected by the investigators, both permeability and metabolic studies may give

misleading results.

4. B. The Effect of Biochemical Agonists on Permeability

i. Prostacyclin and cAMP altering agents

The effect of PGI_2 on endothelial permeability was determined using the stable PGI_2 analog iloprost because of the short half life of PGI_2 compared to the length of the permeability assay. In the presence of iloprost, permeability decreased to 33% of baseline. Prostacyclin and PGI_2 analogs have been reported to reduce permeability of porcine arterial endothelial monolayers (Mizuno-Yagyu et al., 1987). In other vascular cell types, responses to PGI_2 are mediated through cAMP; for example, PGI_2 causes vasodilation and inhibition of platelet aggregation by activating smooth muscle and platelet adenylate cyclase, respectively. PGI_2 and PGI_2 analogs also increase endothelial intracellular cAMP (Dembinska-Kiec et al., 1980; Hopkins and Gorman, 1981; Makarski, 1981; Mizuno-Yagyu et al., 1987). Raising endothelial intracellular cAMP levels by incubation with cAMP analogs/phosphodiesterase inhibitors resulted in decreased permeability, suggesting that the permeability effect of iloprost, and therefore PGI_2 , may be mediated by intracellular cAMP.

Since endothelial PGI_2 production increases in response to bradykinin or thrombin stimulation, we investigated whether the permeability effects of these agonists might be modulated by monolayer production of PGI_2 . Response to bradykinin and thrombin challenge was indistinguishable in cyclooxygenase inhibited monolayers compared to

non-inhibited monolayers. This result is not unexpected due to the relatively small concentration of PGI_2 produced by our cells in response to these agonists (P2 HUVEC, cultured in the presence of heparin, do not maximally secrete PGI_2 (Ingberman-Wojenski and Silver, 1988; Hasegawa et al., 1988)), the instability of PGI_2 (length of permeability assay is an order of magnitude greater than the half life of PGI_2), and the corresponding absence of a phosphodiesterase inhibitor (to sustain PGI_2 -induced elevated cAMP concentrations). Also, thrombin and bradykinin stimulation of other metabolic pathways in the endothelial cells could potentially overpower the permeability effect of a low concentration of PGI_2 . Therefore, there was no discernable effect of thrombin or bradykinin stimulated PGI_2 production on the permeability modulating capacity of these two agonists.

It is not known how PGI_2 and increased intracellular cAMP result in decreased permeability, although cytoskeletal alterations may play a role. Weinbaum et al. (1985) have demonstrated mathematically that monolayer permeability coefficients are very sensitive to small changes in surface coverage of cells. Lloyd et al. (1987) report no detectable morphological changes in confluent monolayers of bovine aortic endothelial cells (BAEC) treated with dibutyryl cAMP (10 μM - 1 mM) or IBMX (10 μM - 0.1 mM) (presumably by visual inspection under light microscopy). However, PGI_2 incubation of subconfluent BAEC is reported to increase numbers of stress fibers and increase surface area of cells as determined with a digital image analyzer (Welles et

al., 1985a). More recent work by the same laboratory (Alexander et al., 1988) has shown that phalloidin, which induces actin polymerization, has similar morphological and permeability altering effects as PGI_2 . Phalloidin decreased permeability and reduced permeability increases induced by other agonists in post-confluent BAEC monolayers. In addition, phalloidin increased surface area, numbers of stress fibers and perimeter measurements in subconfluent BAEC. These cytoskeletal changes may augment intercellular junctions and enhance the permeability barrier function. However, increased numbers of stress fibers are probably not solely responsible for decreasing permeability since long-term exposure to flow is reported to increase stress fibers (Dewey et al., 1981) and increase permeability. PGI_2 and increased intracellular cAMP may decrease permeability through cytoskeletal alterations, possibly mediated by a cAMP-dependent protein kinase. The decrease in permeability produced by cAMP is not rapidly reversible. Permeability coefficients significantly less than control were observed one hour after washout (longer time periods were not tested), and Mizuno-Yagyu et al. (1987) report decreased permeability two hours following washout.

The possible role of the cytoskeleton in maintenance of the endothelial permeability barrier function has been investigated by Shasby et al. (1982). Using microfilament disrupting agents cytochalasin B or D and the fluorescent F-actin stain NBD phalloidin, they observed endothelial cell retraction and disorientation of the microfilaments. Corresponding studies with cells cultured on permeable polycarbonate membranes demonstrated a reversible increase in monolayer permeability in the

presence of cytochalasin B or D. This finding was verified *in vivo* with cytochalasin B perfused isolated rabbit lungs. Also, long-term (3 days) hyperoxia increases permeability in a manner associated with disruption of dense peripheral bands (Phillips and Tsan, 1988).

Analagous to the functional and morphological effects of PGI₂ are the effects of serotonin and norepinephrine on permeability, stress fibers and surface area. Serotonin and norepinephrine are platelet-derived agonists. These agonists decrease permeability (Bottaro et al., 1986b), and increase numbers of stress fibers and cell surface area (Welles et al., 1985b). These phenomena may also be cAMP-dependent, as both serotonin and norepinephrine stimulate increases in cAMP (Buonassissi and Venter, 1976). In contrast, histamine increases permeability (Bottaro et al., 1986b; Killlacky et al., 1986), and decreases numbers of stress fibers (Rotrosen and Gallin, 1986; Welles, 1985b).

In vivo and *in vitro* experiments with platelets are not inconsistent with the *in vitro* work with serotonin and norepinephrine. Lo et al. (1988) report decreased cultured monolayer permeability in the presence of washed platelets; however, the same concentration of red blood cells had no effect on permeability. In addition, treatment of thrombocytopenic sheep with platelet rich plasma resulted in decreased pulmonary permeability. The mechanism(s) underlying the permeability-reducing phenomena of platelets were not investigated, leaving no explanation for the observed results. It would be interesting to determine if platelet-derived serotonin and norepinephrine mediated the reported permeability reducing effects of platelets. The

possibility that platelets acted as "plugs" in areas of reduced endothelial integrity by deposition onto the subendothelium should be investigated.

Ethanol in small concentrations significantly reduced permeability. Acute ethanol has been shown to stimulate cAMP production in S49 mouse lymphoma cells and NG108-15 neuroblastoma x glioma cells through an extracellular adenosine mediated mechanism (Nagy et al., 1989). Therefore, permeability reductions in the presence of ethanol may be mediated by cAMP. Low concentrations of ethanol also inhibit platelet aggregation on collagen coated coverslips under flow conditions (Owens et al., 1990). This effect may also be mediated by cAMP, as cAMP increasing agents are known anti-platelet aggregating agents.

Several steps in the cAMP-mediated permeability modulation pathway have been elucidated by Stelzner et al. (1989). They have shown that cholera toxin stimulation of G_s protein (mediated by GTPase inhibition), forskolin stimulation of adenylate cyclase, dibutyryl cAMP, and cAMP-dependent protein kinase stimulation with Sp-cAMPS all result in decreased permeability of bovine pulmonary artery endothelial monolayers. Furthermore, the forskolin effect was partially reversed by treatment with Rp-cAMPS, an antagonist of cAMP-dependent protein kinase. These results were partially correlated with increased actin polymerization, as both cholera toxin and forskolin led to increased F-actin fluorescence as well as endothelial spreading. Since thrombin decreases adhesion plaques and increases permeability, it would be interesting to determine the effect of cAMP on the quality/integrity of adhesion plaques.

Since the initial discovery of EDRF by Furchgott and Zawadzki in 1980, its

chemical identity remained unknown for the better part of the past decade. Identification was difficult due to its small size and particularly due to its short half-life. Then in 1987 Palmer et al. reported that nitric oxide had the same biological activity as EDRF, similar stability, and the release of nitric oxide from endothelial cells was potentiated and inhibited by known mediators of EDRF. Later it was shown that EDRF/NO had anti-platelet aggregating activity (Radomski et al., 1987a) and that EDRF/NO and prostacyclin act synergistically to inhibit platelet aggregation (Radomski et al., 1987b). The remaining question of how cells make nitric oxide has been at least partially elucidated by Palmer et al. (1988). In experiments using ^{15}N -labelled L-arginine, they have shown that this is the precursor molecule for endothelial synthesized nitric oxide.

Since the effects of prostacyclin were mimicked by treating the cells with cAMP analog/phosphodiesterase inhibitor combinations, the attempt was made to mimic the effect of EDRF by treating the cells with a cGMP analog. This hypothesis is speculative, since although EDRF is known to increase cGMP concentrations in platelets and smooth muscle cells, this cGMP increase has not been verified in endothelial cells. Our finding of decreased permeability in the presence of dibutyryl cGMP may indicate that EDRF modulates endothelial permeability. The coupling of vasodilatory activity with reduction of endothelial permeability may indicate a mechanism to maintain structural integrity of the endothelium during mechanical stretching of the substratum or during periods of increased blood flow (and therefore increased wall shear stress).

In platelets, cGMP and cAMP increasing agents inhibited thrombin-induced formation of diacylglycerol (a product of the phosphatidylinositol response), release of

serotonin, and aggregation of platelets (Kawahara et al., 1984; Imai et al., 1983). Our studies show that treatment of endothelial cells with a cGMP analog also reduced thrombin-induced HUVEC permeability increase.

The effect of thrombin on endothelial permeability and morphology is also inhibited by atriopeptin (Baron et al., 1989). Atriopeptin is a peptide hormone which promotes increased cGMP synthesis in endothelial cells, although little else is known about its role in regulating the endothelium. In cells pretreated with atriopeptin thrombin does not increase mass transport of albumin, nor does it disrupt the integrity of the monolayer or reduce the number of stress fibers. These data further indicate that cGMP as well as cAMP may regulate endothelial permeability, although atriopeptin alone did not modulate permeability.

ii. Bradykinin

The vasodilator bradykinin had no effect on HUVEC permeability in our system. A similar finding was reported (Killackey et al., 1986) for HUVEC cultured on microcarrier beads. However, another study (Alexander et al., 1988) showed that BAEC cultured on microcarrier beads increased permeability in response to bradykinin, and *in vivo* increases in vascular permeability are well documented (Mullins, 1986). The differences between BAEC and HUVEC *in vitro* results could be a species dependent difference in response to bradykinin. Although BAEC (Hong, 1980) and HUVEC (Alhenc-Gelas et al., 1982) both respond to bradykinin by increasing prostacyclin production, calcium efflux and cytosolic calcium measured in response to bradykinin stimulation are greatly diminished in HUVEC as compared to BAEC (Dr. W. P. Shilling, personal communication). The intracellular calcium ion concentration may

have an important role in the integrity of endothelial monolayers. Chelation of extracellular calcium reversibly increased transendothelial albumin transport, reduced transendothelial electrical resistance (TEER), disrupted monolayer integrity, and produced retraction of the peripheral dense band (Shasby and Shasby, 1986). However, this effect may also be due to reduced adhesion to the substrate in low calcium medium. *In vivo* increases in vascular permeability in response to bradykinin may be a secondary effect of bradykinin on another vascular cell (i.e. histamine-producing mast cells), or may be most prominent in postcapillary venules and therefore difficult to detect in HUVEC. Considering the mediating role of cAMP in permeability alterations, it is interesting that bradykinin has been reported (Makarski, 1981) to have no effect on BAEC cAMP levels.

iii. Thrombin: native and modified forms

In our system, thrombin induced a 9.6-fold increase in permeability. This increase was not reversible within one hour after washout and required the proteolytic activity of thrombin, since DIP- and PPACK- α -thrombins had no effect on permeability. In addition, α -thrombin treatment of monolayers preincubated with DIP- α -thrombin or PPACK- α -thrombin did not alter permeability. The inactivated thrombins bind to cultured endothelial cells with equal affinity as α -thrombin (Awbrey et al., 1979), which provides a possible explanation for the inability of α -thrombin to elicit a permeability response in PPACK- α -thrombin preincubated monolayers. Also, γ -thrombin, which is proteolytically active, but with reduced binding capability, did not have a significant effect on permeability in our system.

Other investigators (Garcia et al., 1986; Killackey et al., 1986) reported cell

shape changes resulting in decreased substrate surface area coverage in the presence of thrombin, which may account for the increased permeability that we also observed. However, the extent of response to thrombin in our system is greater than in these other in vitro systems, which also report reversibility of cell shape changes within two hours of washing the monolayers free of thrombin and a corresponding decrease in permeability to albumin. In addition, Garcia et al. (1986) report significant increases in bovine endothelial permeability in the presence of PPACK- and DIP- α -thrombin.

Many analagous studies were performed by Laposata et al. (1983) with endothelial cells cultured on tissue culture plastic. Treatment of monolayers with 0.01 U/ml thrombin caused significant shape changes resulting in a reduction in surface area coverage of the cells to 20% of the prestimulated cell surface area within 15 minutes. This effect was reversed, as determined visually, within two hours of thrombin inactivation by hirudin. (Our results did not show complete reversibility; however, the permeability coefficient determination is a more sensitive indicator of monolayer integrity than visual inspection). This effect was inhibited by pretreating the cells with 2mM dibutyryl cAMP and was not observed with proteolytic inactive thrombin. There was a correlation between cell density and surface area uncovered, with more dense monolayers having the least extent of response to thrombin. Since the amount of thrombin binding to endothelial cells is dependent on confluency, with 20 times more thrombin binding to non-confluent monolayers as confluent monolayers (Isaacs et al., 1981), the dependency on cell density may be a dose dependent phenomenon related to the amount of thrombin bound per cell. This result is consistent with our observation that binding and proteolytic activity are both required for the effect of thrombin on

endothelial permeability to be realized.

One major factor accounting for differences in extent and reversibility of response in this system versus other *in vitro* systems may be time in culture. Morphologically similar monolayers can have significantly different permeability characteristics. For example, our time-course studies demonstrated significantly lower permeability coefficients for confluent 11- and 15-day monolayers versus confluent 7-day monolayers. We observed a similar dependence on post-seeding culture time with BAEC cultures. This decrease in permeability with increasing time in culture may be attributable to maturation of cell junctions (Larson and Sheridan, 1982; Furie et al., 1984). The increased extent of response to thrombin in our system may be due to an effect on cell junctions which may not be as readily reversible as change in cell shape. Increased culture time may also affect the composition and quantity of the extracellular matrix, which has been reported to provide some resistance to macromolecular transport (Albelda et al., 1988; Boiadjieva et al., 1984).

Differences in proteolytically inactivated thrombin results may be explained by potential species dependent differences (bovine (Garcia et al., 1986) versus human (Casnocha et al., 1989)) and differences in thrombin concentration. On a molar basis, our thrombin concentrations are three orders of magnitude less than those of Garcia et al. (1986). Residual proteolytic activity (0.1% of native active thrombin) in the higher concentration of inactivated thrombins is approximately equal to the active thrombin concentration which caused a permeability increase in our system. Recently the same group of investigators verified that their earlier positive results with proteolytic inactivated thrombins were due to residual proteolytic activity of

contaminating α -thrombin (DeMichele et al., 1989).

iv. Interactions between cAMP increasing agents and thrombin

The dramatic 9.6-fold thrombin-induced permeability increase was inhibited in monolayers pretreated with cAMP analog/phosphodiesterase inhibitor combinations, IBMX, dibutyryl cAMP, and iloprost. Inhibition of the thrombin-induced permeability increase appears to correlate with the extent of increase in intracellular cAMP, with cAMP analog/phosphodiesterase inhibitor combinations exhibiting the greatest inhibition. Hopkins and Gorman (1981) report a greater intracellular cAMP increase in HUVEC treated with PGI₂ and IBMX than PGI₂ alone, and similar results have been reported for BAEC (Dembinska-Kiec et al., 1980).

v. Possible mechanisms involved.

These studies with cAMP/thrombin and proteolytically inactive thrombins reveal important information about the mechanism of the effect of thrombin on permeability. First, proteolytic activity of thrombin is required to increase permeability. The role of proteolytic activity of thrombin in permeability alterations is unknown, but it is unlikely due to indiscriminant proteolytic degradation of the monolayer. LDH activity of supernatants from thrombin treated monolayers was indistinguishable from that of non-thrombin treated monolayers, indicating that thrombin treatment did not cause a detectable level of cell lysis. In addition to proteolytic activity, binding of the active thrombin to the endothelial cell seems to be required since α -thrombin did not increase permeability of PPACK- α -thrombin or DIP- α -thrombin pretreated monolayers, and γ -thrombin did not increase permeability. For this reason, it appears possible that

increased intracellular cAMP results in reduced thrombin binding. In platelets, elevated cAMP levels have been shown to result in decreased thrombin binding to receptors (Lerea et al., 1987). Elevated endothelial cAMP may decrease thrombin binding by direct phosphorylation of a membrane thrombin-binding protein through activation of a cAMP-dependent protein kinase (Sibley et al., 1987). Alternatively, cAMP may indirectly inhibit thrombin binding or thrombin-induced shape changes through cytoskeletal alterations. These cytoskeletal events may also be mediated by a cAMP-dependent protein kinase. However, cAMP inhibition is probably not specific for thrombin since increased intracellular cAMP has also been reported to inhibit histamine-induced permeability increases in HUVEC (Killackey et al., 1986) and increased cGMP also inhibits thrombin induced permeability increases. Also, as will be discussed in section 4. D, cells pretreated with iloprost show a reduced response to the permeability increasing effect of shear stress.

4. C. Polarity of Prostacyclin Expression

It was found that prostacyclin was released equally in both directions in response to bradykinin stimulation if the concentration of albumin was the same in both chambers. This condition doesn't exactly mimic the *in vivo* condition where the luminal concentration may be relatively constant around 4%, but the subluminal concentration may be affected by the lymph system, the vasa vasorum, and local alterations in vascular permeability. Our data are consistent with the observation that PGI_2 is not found within the cell, but rather is secreted as it is produced. PGI_2 transport within

the cell appears not to be regulated or directed. If differences are seen in the sidedness of the expression, one must be sure that this polarity is not due to rapid transport of prostacyclin across the monolayer due to external albumin gradients. Since hydrolyzed prostacyclin is unassociated from albumin, the kinetics of hydrolysis can also influence the transport of prostacyclin.

Bradykinin stimulated increased PGI_2 production without altering endothelial permeability and without deviating from the lack of polarity observed in constitutive secretion. However, this does not indicate that the same effect would be observed *in vivo*. Bradykinin increases *in vivo* vascular permeability, and increased permeability may lead to increased transport of PGI_2 into the blood vessel wall, resulting in an apparent polarity of expression.

Control studies with iloprost revealed an order of magnitude difference between luminal-to-subluminal permeability (3.1×10^{-7} cm/sec) versus subluminal-to-luminal permeability (2.2×10^{-6} cm/sec). The reason for this difference is unclear. Perhaps iloprost-endothelial surface interactions occur to a greater extent during the luminal-to-subluminal transport studies, and these interactions may hinder the diffusion of iloprost in this direction.

4. D. The Effect of Flow on Permeability

Shear stress, in the absence of convective flux, caused a 7-fold increase in permeability which was partially reversible after 30 minutes. These results are consistent with those of Jo et al. (1989), who report a dose-dependent increase in

permeability of BAEC monolayers exposed to 1 or 10 dynes/cm² shear stress.

The effect of flow on permeability of endothelial monolayers is not directly attributable to the morphological alterations such as elongation with the axis of flow, cell migration, or disappearance of dense peripheral bands, since these events are observed after shear stress stimulation of higher magnitude for many hours to a day. However, the length scale of these morphological alterations does not rule out a role of short-term permeability altering morphological modulations as an initial event in the progression leading to elongation or migration. Random motility would not account for the observations in our flow system. At an average rate of 30 $\mu\text{m/hr}$, significant migration off the membrane would not occur in 2-3 hours.

The effect of shear stress on endothelial permeability may be mediated by calcium. Endothelial cells respond to shear stress with increased cytosolic Ca^{2+} (Ando et al., 1988). In contrast, cAMP levels are unchanged in response to shear stress (Dr. J.A. Frangos, personal communication). Treatment of monolayers with histamine or calcium ionophore ionomycin caused increased intracellular calcium which was associated with increased permeability and decreased F-actin content (Rotrosen and Gallin, 1986). A shear stress-induced rise in cytosolic Ca^{2+} may elicit a cytoskeletal change responsible for the observed increase in permeability. Elevated cytosolic Ca^{2+} activates proteins responsible for nucleating, severing and filament end-blocking of actin filaments (Stossel, 1989).

The mechanism by which iloprost inhibits shear stress-induced permeability increases remains to be elucidated. There are at least two possible theories. First, the increased cAMP levels associated with iloprost treatment may stabilize the endothelial

cytoskeleton against shear stress modulation. (Even though cells grown on solid, transparent substrates appear morphologically unaltered in response to shear stress of this magnitude and duration, we have shown that gross morphology does not correlate with baseline permeability coefficients). A similar hypothesis was proposed for cAMP inhibition of thrombin-induced permeability increases. A second explanation is that iloprost may inhibit the shear stress-induced pinocytosis reported by Davies et al. (1984), although this effect has not been verified in our cell type or system. This theory seems unlikely for a number of reasons. In the system of Davies et al. (1984) a shear stress of 8 dynes/cm² increased uptake of horseradish peroxidase by a factor of two during the first two hours of flow. In our system a 7-fold increase in albumin uptake was seen after one hour of exposure to 7 dynes/cm² shear stress. Pinocytosis of albumin as the dominant transport mechanism is also inconsistent with the junctional transport theory proposed by Bottaro et al. (1986a). This theory is supported by cytoskeletal alteration induced permeability modulations (Alexander et al., 1988; Shasby et al., 1982). Also, pinocytosis is inhibited by microfilament disassembly with agents such as cytochalasins, in contrast to the permeability increasing effects of cytochalasins. It is interesting that cAMP increasing agents (PGE₁ and theophylline) also inhibit shear stress-induced activation of platelets (Hellums and Harwick, 1981).

When Bell et al. (1974) conducted studies to correlate areas of increased Evans blue dye accumulation with increased LDL uptake, they postulated that the focal areas of increased endothelial permeability corresponded with areas of hemodynamic injury, which in turn may correspond to areas of increased cell turnover. In addition, cells

accustomed to static culture conditions may respond more dramatically to the onset of flow.

In addition to producing metabolic and microscopic morphological responses to shear stress, it is interesting that the endothelium also produces macroscopic changes in the blood vessel wall. Langille and O'Donnell (1986) showed that the endothelium mediates a reduction in arterial inner and outer diameters following chronic (2 week) reductions in flow. This reduction in diameter could not be attributed to contraction of the smooth muscle; however, contraction could have been an initiating event leading to this dramatic change. Denuded arteries did not significantly change diameter under the same experimental conditions.

These flow rate and diameter alterations affect shear stress in a defined manner. Assuming a cylindrical geometry for the arteries, the shear stress is described by the equation:

$$\tau = \frac{4 \mu Q}{\pi r^3}$$

with Q equal to the volumetric flow rate and r equal to the radius of the artery. Langille and O'Donnell's experimental flow rate and radius reductions are summarized on the following page along with the corresponding changes in wall shear stress.

	<u>Q (ml/min)</u>	<u>radius</u>	<u>shear stress</u>
initial conditions	26.5	r_{initial}	τ_{initial}
immediately post-reduction	8	r_{initial}	0.30 τ_{initial}
2 weeks post-reduction	8	0.79 r_{initial}	0.61 τ_{initial}

A reduction in the volumetric flow rate from 26.5 to 8 ml/min, resulted in reduced shear stress to approximately 30% of the initial value. After two weeks of reduced flow, the radius decreased to 79% of the initial value, meaning that the shear stress increased to 61% of the initial value.

This endothelial-dependent response to alterations in blood flow raises the possibility that the endothelium regulates its own shear stress environment. Perhaps the acute and relatively acute responses to shear stress which we observe in our laboratory with cultured cells ultimately enable the endothelium to maintain a "normal" level of shear stress. In the simplest sense, considering endothelium derived vasoactive compounds, this regulation occurs when prostacyclin production increases in response to increases in shear stress (Frangos et al., 1985) and endothelin (a vasoconstrictor) production decreases in response to increases in shear stress (S.L. Diamond, personal communication).

4. E. *In Vivo* Implications

The endothelium may alter its permeability downward as a means of protecting the vascular bed from vasoconstrictors, while at the same time producing relaxing factors

such as EDRF and PGI_2 . The endothelium is known to mediate the effects of many vasoactive agonists; for example, acetylcholine causes constriction in deendothelialized vessels and relaxation (via EDRF) in vessels with intact endothelium. As discussed in the previous section, the endothelium regulates vessel diameter, both long and short term, and these responses are mediated by flow (shear stress). We propose that the endothelium regulates its hydrodynamic environment through acute and chronic changes in vessel diameter at least in part through permeability modulations. In this way, the endothelium can regulate transport of vasodilators and vasoconstrictors into the vessel wall.

While it is difficult to directly compare *in vitro* results with *in vivo* situations, it appears that the permeability modulations we observed act in a complementary manner to the hemostatic function of the agonists tested. For example, the effect of thrombin on platelet aggregation would be enhanced by the observed disruption of the integrity of the endothelial monolayer, as this would expose the thrombogenic subendothelium. Conversely, the antiplatelet aggregating activity of prostacyclin would be enhanced by decreased endothelial permeability which would limit transendothelial prostacyclin transport, and by the accompanying postulated morphological change of flattening of the cells, which may reduce the surface area of any exposed subendothelium. These effects would, at best, be difficult to observe *in vivo* because of the dynamic nature of the morphological changes and because of the localized nature of these effects (due to the hydrolysis of prostacyclin and the redundant systems to clear thrombin from the circulation).

What is the role of cAMP in the permeability barrier function of the endothelium? Increased intracellular cAMP concentrations are associated with contact inhibited, non-migrating, non-mitotic cells (Hackett et al., 1987; Pastan, 1975; Stout, 1982). *In vivo*, areas of slow cell turnover (with presumably higher cAMP concentrations), may be less permeable than regions containing mitotic cells (with presumably lower cAMP concentrations), which are considered "leaky" (Weinbaum et al., 1985). Therefore, cAMP may mediate *in vivo* endothelial permeability to the extent that cAMP concentrations inversely correlate with cell turnover.

Although atherosclerosis was not specifically studied in this thesis, the same principles of mass transport can be used to study permeability to LDL as were used to study permeability to albumin. Two major factors contributing to atherosclerotic lesion formation are increased serum LDL and hemodynamics. Both factors may lead to an increase in endothelial permeability or otherwise alter LDL transport to ultimately result in increased cholesterol deposition in the blood vessel wall.

Hennig et al. (1984) modeled triglyceride hydrolysis of lipoproteins by treating cultured endothelium with linoleic and oleic acids. In the presence of these fatty acids permeability to albumin increased. Navab et al. (1986) reported that very low density lipoproteins reversibly caused increases in transendothelial LDL and albumin transport. The same results were found with endothelial cells derived from Watanabe heritable hyperlipidemic rabbits (which do not have LDL receptors due to a genetic defect), indicating that this increased LDL transport is not receptor mediated. Similar results have been reported *in vivo*, in which cholesterol-fed rabbits exhibited increased permeability to albumin to an extent greater than that which could be

attributed to disruption of the endothelium caused by atherosclerotic lesions on the intimal surface (Chobanian et al., 1983).

Atherosclerotic lesions *in vivo* are found focally in areas of low shear stress or oscillatory shear stress such as the outer walls of major bifurcations or the inner wall of curved segments (Caro et al., 1971). Areas of high shear, such as flow dividers, are spared. It is unknown how low flow or disturbed flow patterns ultimately cause the onset of atherogenesis. Regions prone to atherosclerotic lesion formation may display intimal thickening, smooth muscle proliferation, and platelet adhesion. These morphological responses are probably related to endothelial metabolic responses to the low shear environment. For example, increased uptake and degradation of LDL occurs in BAEC subjected to high shear stress (30 dynes/cm²) versus low shear stress (1 dyne/cm², Sprague et al., 1987).

Understanding the mechanisms of serum LDL-dependent and flow-induced lesion formation will lead to a better understanding of the prevention and treatment of atherosclerosis. One potential agent to reduce the onset of atherogenesis is cAMP. Cyclic AMP can effectively inhibit the atherosclerotic related phenomena of increased endothelial permeability and smooth muscle proliferation. An intact endothelium provides a permeability barrier, and this function *in vitro* is enhanced by increased intracellular cAMP concentrations. Smooth muscle cell proliferation *in vitro* is reduced in cells with elevated intracellular cAMP (Stout, 1982). Therefore, prostacyclin secretion by the endothelium may influence more than smooth muscle tone; it may also regulate smooth muscle proliferation.

To summarize the work presented herein, the PGI₂ analog iloprost or cAMP analog/phosphodiesterase inhibitor combinations decrease monolayer permeability and provide protection against thrombin-induced and shear stress-induced permeability increases. Cyclic GMP also decreased permeability and inhibited thrombin-induced permeability increases. Cyclic AMP associated permeability decreases persist for at least an hour. Through cAMP mediation, PGI₂ may produce long-term permeability effects even though it is rapidly hydrolyzed in the circulation. In this manner, PGI₂ and other unstable vasoactive agonists have the potential to cause local alterations in endothelial permeability, thereby regulating macromolecular transport in the blood vessel wall.

CHAPTER FIVE: POTENTIAL FUTURE WORK

5. A. Co-culture Systems

Monolayers of cultured endothelial cells have been used to study the endothelial permeability barrier function. By optimizing culture conditions we have been able to improve this function by an order of magnitude over some other *in vitro* systems, as assessed by determining a permeability coefficient for albumin. However, another order of magnitude improvement may be necessary to attain *in vivo* permeabilities. Because *in vivo* endothelial cells are in close proximity to and in constant communication (Davies et al., 1988) with smooth muscle cells, and because *in vitro* co-culture experiments have shown that endothelial cells and smooth muscle cells communicate with each other in ways that alter cell metabolism and growth (Davies et al., 1985; Castellot et al., 1982; Gajdusek et al., 1980), the *in vitro* endothelial permeability barrier function may be enhanced by co-culture with smooth muscle cells. The same type of interdependence has been shown for brain microvascular endothelium with glial cells (Stewart and Wiley, 1981) and with pericytes (Orlidge and D'Amore, 1987). A related issue is that of the endothelial monolayer substrate, which may influence optimal permeability barrier function.

The increase of vascular permeability in the presence of bradykinin *in vivo* has been well documented (Mullins, 1986); however, *in vitro* this agonist has no effect on endothelial permeability. Co-culture of endothelial cells with other vascular components may implicate an interdependence of two or more cell types for this effect

to be observed *in vitro*. It has been proposed that bradykinin causes *in vivo* increases in permeability by causing release of histamine from mast cells (Killacky et al., 1986). This hypothesis could be tested in an appropriate co-culture system.

A related project would be the development of a membrane suitable for co-culture which would be compliant, and allow for detection of contraction/relaxation of smooth muscle cells in response to agonists which stimulate the co-cultured endothelial cells. A concomitant effort would have to be phenotypic manipulation of the cultured smooth muscle cells, since currently culture of these cells results in rapid loss of the contractile phenotype. With this type of system, one may also study the effect of the mechanical changes associated with alterations in smooth muscle tone on endothelial permeability to determine if there is a coupling of smooth muscle tone and regulation of endothelial permeability. This hypothesis is suggested by the strong effect of the vasodilator prostacyclin on endothelial permeability and earlier *in vivo* work indicating a role of smooth muscle tone in vascular permeability (Caro and Lever, 1983).

Another facet of a co-culture system is culturing endothelium in the presence of platelets. Lo et al. (1988) reported that platelet rich plasma infusion of thrombocytopenic sheep reduced vascular permeability; also, platelets, but not red blood cells, added to *in vitro* monolayers decreased permeability. This work could begin by treating endothelial monolayers with physiological concentrations of platelet granule release products and progress to a system where platelets are perfused in the permeable membrane flow chamber. In addition, platelet release products serotonin and norepinephrine enhance the endothelial permeability barrier (Bottaro et al., 1986b).

5. B. EDRF

It has been shown that prostacyclin production increases in response to onset of shear stress and to pulsatile shear stress (Frangos et al., 1985 and 1988). Prostacyclin in many ways is similar to EDRF (nitric oxide). Both have the same biological activity in platelets and smooth muscle cells, both are short half-life compounds, and both act through increasing cyclic nucleotide production in their target cells. Do shear stress and pulsatile flow also increase production of EDRF? If so, does this increased production of EDRF (as determined by a bioassay, i.e. smooth muscle cGMP accumulation, anti-platelet aggregating activity, or smooth muscle relaxation activity) correspond to increased release of nitric oxide by the endothelial cells? If not, is there perhaps a shear dependent EDRF and a non-shear dependent EDRF (nitric oxide)?

Since EDRF has biological activity in both directions, is EDRF expressed by the endothelium in both directions? The polarity issue is particularly important for EDRF due to its extremely short half life. Are there different rates of transport in the luminal to subluminal direction versus subluminal to luminal direction? The effective diffusion of EDRF is important because it is unknown how NO is transported from the endothelium to the smooth muscle cells. A slow rate of transport humorally would provide incentive for the study of possible gap junctional-direct contact transport of EDRF between the endothelium and smooth muscle cells.

Does EDRF modulate endothelial permeability? There is very preliminary evidence that it might because we have shown that cGMP decreases permeability. It

should also be determined if EDRF increases cGMP concentrations in endothelial cells. Both native EDRF and NO could be tested for their ability to modulate endothelial permeability. The use of both native EDRF and NO may provide information regarding potential additional forms of EDRF; however, it would be difficult to generate pure native EDRF uncontaminated by other endothelial products.

In a related issue, does gap junctional communication within the endothelium occur to such an extent that treatment of endothelial cells with PGI₂ or EDRF at a discrete location results in response to this agonist farther away in the plane of the endothelial cells where the EDRF or PGI₂ could not possibly have acted humorally?

5. C. More Flow Studies

The studies completed so far with the permeable membrane flow system are initial studies in this area of research. The effects of a range of shear stresses should be investigated. Also long term effects of shear stress on permeability should be investigated, especially since shear stress is known to affect gene expression. This would encompass long term exposure to flow which may ultimately cause discernable changes in the cytoskeleton (Herman et al., 1987), and elicit expression of factors responsible for controlling vessel diameter (not vasoactive substances) (Langille and O'Donnell, 1986).

From the work of Langille and O'Donnell (1986) we have seen that chronic reductions in flow cause dramatic changes in arterial diameter in an endothelial dependent manner. It would be interesting to determine the metabolic and

morphological responses of the endothelium to reductions in shear stress. Since endothelin production decreases in response to increased shear stress, would endothelin production increase in response to decreased shear stress?

Once the response to a range of shear stresses is characterized, the permeable membrane flow chamber could be used to study the effects of shear stress in the presence of convective flux. This work would require characterization of the hydraulic conductivity of endothelial monolayers at each transmural pressure used in the convective flux studies.

5. D. Morphology and Polarity

Since we have proposed that the cytoskeleton plays a major role in permeability modulations, a detailed study of the effects of prostacyclin, cAMP and thrombin on the cytoskeleton would add insight to mechanism of activity of these agents. This work would be best done with confluent monolayers grown on transparent permeable membranes using fluorescently labeled antibodies for cytoskeletal proteins. Actin would be the first choice to study since others have shown that microfilament polymerization is altered with permeability altering agents (Rotrosen and Gallin, 1986; Shasby et al., 1982).

We observed no polarity of prostacyclin expression when the cells were treated with bradykinin. However, other agonists may elicit polarized expression. In particular, is shear stress-induced prostacyclin production polarized? Since endothelial protein products have been shown to exhibit polarized secretion (Sporn et al., 1989; Zerwes and Risau, 1987), is the vasoconstrictor peptide endothelin secreted

in a polarized manner?

5. E. Practical Applications

Modulations in vascular permeability may be exploited for enhanced drug delivery. This type of drug delivery may be particularly effective using site specific antibodies conjugated to drugs which would ordinarily have low and non-specific uptake rates. The drug-antibody conjugate could be targeted for a specific organ utilizing organ specific endothelial surface glycoproteins (Belloni and Nicolson,1988).

Permeability of endothelial or epithelial cell monolayers may also be used in an industrial setting. In a reactor configuration suitable for anchorage dependent cells, such as a chemostat with microcarrier beads or a hollow fiber reactor, the cells may be genetically engineered to secrete their product in a polarized fashion, i.e. basolaterally, resulting in enhanced recovery schemes. The permeability barrier function of a monolayer of cells would serve as an additional molecular sieve to trap product in the lumen of hollow fibers or inside microcarrier beads. Harvesting of the product could then be accomplished, for example, by treating the beads with a reversible permeability modulating agent. This arrangement would allow the release of product without destroying the cells or beads.

REFERENCES

Albelda, S.M., P.M. Sampson, F.R. Haselton, J.M. McNiff, S.N. Mueller, S.K. Williams, A.P. Fishman and E.M. Levine. Permeability characteristics of cultured endothelial cell monolayers. *J. Appl. Physiol.* 64 (1): 308-322, 1988.

Alexander, J.S., H.B. Hechtman and D. Shepro. Phalloidin enhances endothelial barrier function and reduces inflammatory permeability in vitro. *Microvasc. Res.* 35: 308-315, 1988.

Alhenc-Gelas, F., S.J. Tsai, K.S. Callahan, W.B. Campbell and A.R. Johnson. Stimulation of prostaglandin formation by vasoactive mediators in cultured human endothelial cells. *Prostaglandins* 24 (5): 723-742, 1982.

Ando, J., T. Komatsuda and A. Kamiya. Cytoplasmic calcium response to fluid shear stress in cultured vascular endothelial cells. *In Vitro Cell. Dev. Biol.* 24(9): 871-877, 1988.

Awbrey, B.J., J.C. Hoak and W. G. Owen. Binding of human thrombin to cultured human endothelial cells. *J. Biol. Chem.* 254 (10): 4092-4095, 1979.

Baron, D.A., C.E. Lofton, W.H. Newman and M.G. Currie. Atriopeptin inhibition of thrombin-mediated changes in the morphology and permeability of endothelial monolayers. *Proc. Natl. Acad. Sci. USA* 86: 3394-3398, 1989.

Bassenge, E., R. Busse and U. Pohl. Abluminal release and asymmetrical response of the rabbit arterial wall to endothelium-derived relaxing factor. *Circ. Res.* 61 (suppl. II): II-68 - II-73, 1987.

Behar, D.M., M. Juszynski, N. Ben Hur, J. Golan, A. Eldad, Y. Tuchman, N. Sterenberg and B. Rudensky. Omiderm, a new synthetic wound covering: physical properties and drug permeability studies. *J. Biomed. Mat. Res.* 20: 731-738, 1986.

Bell, F.P., I.L. Adamson and C. Schwartz. Aortic endothelial permeability to albumin: Focal and regional patterns of uptake and transmural distribution of ¹³¹I-albumin in the young pig. *Exp. Mol. Pathol.* 20: 57-68, 1974.

Belloni, P.N. and G.L. Nicolson. Differential expression of cell surface glycoproteins on various organ-derived microvascular endothelia and endothelial cell cultures. *J. Cell. Physiol.* 136(3): 398-410, 1988.

Bhagyalakshmi, A. and J.A. Frangos. Mechanism of shear-induced prostacyclin production in endothelial cells. *Biochem. Biophys. Res. Commun.* 158(1): 31-37, 1989.

Boiadjieva, S., C. Hallberg, M. Hogstrom and C. Busch. Exclusion of trypan blue from microcarriers by endothelial cells: an in vitro barrier function test. *Laboratory Investigation* 50 (2): 239-246, 1984.

Bottaro, D., D. Shepro and H.B. Hechtman. Heterogeneity of intimal and microvessel endothelial cell barriers in vitro. *Microvasc. Res.* 32: 389-398, 1986a.

Bottaro, D., D. Shepro, S. Peterson and H.B. Hechtman. Serotonin, norepinephrine, and histamine mediation of endothelial barrier function in vitro. *J. Cell. Physiol.* 128: 189-194, 1986b.

Bratzler, R.L., G.M. Chisolm, C.K. Colton, K.A. Smith, D.B. Zilversmit and R.S. Lees. The distribution of labeled albumin across the rabbit thoracic aorta in vivo. *Circ. Res.* 40 (2): 182-190, 1977.

Bucana, C.D., J. Trial, A.C. Papp and K.K. Wu. Bovine aorta endothelial cell incubation with interleukin 2: morphological changes correlate with enhanced vascular permeability. *Scanning Microscopy* 2 (3): 1559-1566, 1988.

Buonassisi, V. and J.C. Venter. Hormone and neurotransmitter receptors in an established vascular endothelial cell line. *Proc. Nat. Acad. Sci. USA* 73: 1612-1616, 1976.

Burgess, W.H., T. Mehlman, R. Friesel, W.V. Johnson and T. Maciag. Multiple forms of endothelial cell growth factor: rapid isolation and biological and chemical characterization. *J. Biol. Chem.* 260(21): 11389-11392, 1985.

Caro, C.G., J.M. Fitz-Gerald and R.C. Schroter. Atheroma and arterial wall shear: observation, correlation and proposal of a mass transfer mechanism for atherogenesis. *Proc. R. Soc. Lond. (Biol.)* 177: 109-159, 1971.

Caro, C.G. and M.J. Lever. Effect of vasoactive agents and applied stress on the albumin space of excised rabbit carotid arteries. *Atherosclerosis* 46: 137-146, 1983.

Casnocha, S.A., S.G. Eskin, E.R. Hall, L.V. McIntire. Permeability of human endothelial monolayers: effect of vasoactive agonists and cAMP. *J. Appl. Physiol.* 67(5): 1997-2005, 1989.

Castellot, J.J., L.V. Favreau, M.J. Kamovsky and R.D. Rosenberg. Inhibition of vascular smooth muscle cell growth by endothelial cell-derived heparin. *J. Biol. Chem.* 257(19): 11256-11260, 1982.

Castronovo, V., C. Colin, B. Parent, J.M. Foidart, R. Lambotte and P. Mahieu. Possible role of human natural anti-Gal antibodies in the natural anti-tumor defense system. *J. Natl. Cancer Inst.* 81(3): 212-216, 1989.

Cho, M.J. and M.A. Allen. Chemical stability of prostacyclin (PGI_2) in aqueous solutions. *Prostaglandins* 15: 943-954, 1978.

Chobanian, A.V., J.O. Menzoian, J. Shipman, K. Heath and C.C. Haudenschild. Effects of endothelial denudation and cholesterol feeding on in vivo transport of albumin, glucose, and water across rabbit carotid artery. *Circ. Res.* 53:805-814, 1983.

Clarkson, T.W., P.R. Sager and T.L.M. Syversen, eds. *The cytoskeleton: a target for toxic agents.* 3-21, Plenum Press, New York, 1986.

Cole, O.F., T-P.D. Fan and G.P. Lewis. Isolation, characterization, growth and culture of endothelial cells from the rat aorta. *Cell Biol. Internat. Reports* 10(6): 399-405, 1986.

Cooper, J.A., P.J. Del Vecchio, F.L. Minnear, R.F. Burhop, W.M. Selig, J.G.N. Garcia and A.B. Malik. Measurement of albumin permeability across endothelial monolayers in vitro. *J. Appl. Physiol.* 62 (3): 1076-1083, 1987.

Davies, P.F., C.F. Dewey, Jr., S.R. Bussolari, E.J. Gordon and M.A. Gimbrone, Jr. Influence of hemodynamic forces on vascular endothelial function: in vitro studies of shear stress and pinocytosis in bovine aortic cells. *J. Clin. Invest.* 73: 1121-1129, 1984.

Davies, P.F., G.A. Truskey, H.B. Warren, S.E. O'Connor and B.H. Eisenhaure. Metabolic cooperation between vascular endothelial cells and smooth muscle cells in co-culture: changes in low density lipoprotein metabolism. *J. Cell Biol.* 101: 871-879, 1985.

Davies, P.F., A. Remuzzi, E.J. Gordon, C.F. Dewey, Jr., M.A. Gimbrone, Jr. Turbulent shear stress induces vascular endothelial cell turnover in vitro. *Proc. Natl. Acad. Sci. USA* 83: 2114-2117, 1986.

Davies, P.F., S-P. Olesen, D.E. Clapham, E.M. Morrel and F.J. Schoen. Endothelial communication: state of the art lecture. *Hypertension* 11: 563-572, 1988.

Dembinska-Kiec, A., W. Rucker and P.S. Schonhofer. Effects of PGI_2 and PGI analogues on cAMP levels in cultured endothelial and smooth muscle cell derived from bovine arteries. *Naunyn-Schmiedeberg's Arch. Pharmacol.* 311: 67-70, 1980.

DeMey, J.G. and P.M. Vanhoutte. Heterogeneous behavior of the canine arterial and venous wall. *Circ. Res.* 51: 439-447, 1982.

DeMichele, M.A.A., D.G. Moon, J.E. Kaplan, J. Fenton III and F.L. Minnear. Thrombin increases permeability of pulmonary artery endothelial cell monolayers by an enzymatic rather than a receptor binding mechanism. *Thrombosis and Haemostasis* 62(1): 1403, 1989.

Dewey, C.F., S.R. Bussolari, M.A. Gimbrone Jr., and P.F. Davies. The dynamic response of vascular endothelial cells to fluid shear stress. *J. Biomech. Eng.* 103: 173-185, 1981.

Diamond, S.L., S.G. Eskin and L.V. McIntire. Fluid flow stimulates tissue plasminogen activator secretion by cultured human endothelial cells. *Science* 243: 1483-1485, 1989.

Diamond, S.L., L.V. McIntire, J.B. Sharefkin, C. Dieffenbach, K. Frasier-Scott and S.G. Eskin. Tissue plasminogen activator messenger RNA levels increase in cultured human endothelial cells exposed to laminar shear stress. *J. Cell. Physiol.*, in press, 1990.

Doukas, J., D. Shepro, and H.B. Hechtman. Vasoactive amines directly modify endothelial cells to affect polymorphonuclear leukocyte diapedesis in vitro. *Blood* 69 (6): 1563-1569, 1986.

Eskin, S.G., H.D. Sybers, L. Trevino, J.T. Lie, J.E. Chimoskey. Comparison of tissue-cultured bovine endothelial cells from aorta and saphenous vein. *In Vitro* 14: 903-, 1978.

Eskin, S.G., C.L. Ives, L.V. McIntire and L.T. Navarro. Response of cultured endothelial cells to steady flow. *Microvasc. Res.* 28: 87-94, 1984.

Eskin, S.G., F.M. Strickland and J.P. Heath. Effects of shear stress on the migration and cell-substratum adhesion of cultured endothelial cells. *J. Cell Biol.* 109 (4(2)):394, 1989.

Exton, J.H. Role of calcium and phosphoinositides in the actions of certain hormones and neurotransmitters. *J. Clin. Invest.* 75: 1753-1757, 1985.

Frangos, J.A., S.G. Eskin, L.V. McIntire and C.L. Ives. Flow effects on prostacyclin production by cultured human endothelial cells. *Science* 227: 1477-1479, 1985.

Frangos, J.A., L.V. McIntire and S.G. Eskin. Shear stress induced stimulation of mammalian cell metabolism. *Biotenol. Bioeng.* 32: 1053-1060, 1988.

Franke, W.W., M. Grafe, H. Schnittler, C. Mittermayer and D. Drenckhahn. Induction of human vascular endothelial stress fibers by fluid shear stress. *Nature (Lond.)*. 307: 648-649, 1984.

Fry, D.L. Aortic Evans blue dye accumulation: its measurement and interpretation. *Am. J. Physiol.* 232(2): H204-H22, 1977.

Furchgott, R.F. and J.V. Zawadzki. The obligatory role of endothelial cells in the relaxation of arterial smooth muscle by acetylcholine. *Nature* 288: 3733-376, 1980.

Furie, M.B., E.B. Cramer, B.L. Naprstek and S.C. Silverstein. Cultured endothelial cell monolayers that restrict the transendothelial passage of macromolecules and electrical current. *J. Cell Biol.* 98: 1033-1041, 1984.

Furie, M.B. and D.D. McHugh. Migration of neutrophils across endothelial monolayers is stimulated by treatment of the monolayers with interleukin-1 or tumor necrosis factor-alpha. *J. Immunol.* 143(10): 3309-3317, 1989.

Gajdusek, C., P. Dicorleto, R. Ross and S.M. Schwartz. An endothelial cell-derived growth factor. *J. Cell Biol.* 85: 467-472, 1980.

Garcia, J.G.N., A. Siflinger-Birnboim, R. Bizios, P.J. Del Vecchio, J.W. Fenton II and A.B. Malik. Thrombin-induced increase in albumin permeability across the endothelium. *J. Cell Physiol.* 128: 96-104, 1986.

Gilman, A.G. G proteins and dual control of adenylate cyclase. *Cell* 36(3): 577-579, 1984.

Gimbrone, M.A. Culture of vascular endothelium. *Prog. Hemostasis. Thromb.* 3: 1-28, 1976.

Grabowski, E.F., E.A. Jaffe and B.B. Weksler. Prostacyclin production by cultured endothelial cell monolayers exposed to step increases in shear stress. *J. Lab. Clin. Med.* 105: 36-43, 1985.

Hackett, S.F., Z. Friedman and P.A. Campochiaro. Cyclic 3',5'-adenosine monophosphate modulates vascular endothelial cell migration in vitro. *Cell Biol. Internat. Reports* 11(4): 279-287, 1987.

Hasegawa, N., M. Yamamoto, and K. Yamamoto. Stimulation of cell growth and inhibition of prostacyclin production by heparin in human umbilical vein endothelial cells. *J. Cell. Physiol.* 137: 603-607, 1988.

Hellums, J.D. and R.A. Hardwick. Response of platelets to shear stress - a review. *The Rheology of Blood, Blood Vessels and Associated Tissues.* D.R. Gross and N.H.C. Hwang, eds. Sijhoff and Noordhoff, Amsterdam. 160-183, 1981.

Hennig, B., D.M. Shasby, A.B. Fulton and A.A. Spector. Exposure to free fatty acid increases the transfer of albumin across cultured endothelial monolayers. *Arteriosclerosis* 4: 489-497, 1984.

Herman, I.M., A.M. Brant, V.S. Warty, J. Bonaccorso, E. Klein, R.L. Kormos, and H.S. Borovetz. Hemodynamics and the Vascular Endothelial Cytoskeleton. *J. Cell Biol.* 105: 291-302, 1987.

Hong, S.L. Effect of bradykinin and thrombin on prostacyclin synthesis in endothelial cells from calf and pig aorta and human umbilical cord vein. *Thromb. Res.* 18: 787-795, 1980.

Hopkins, N.K. and R.R. Gorman. Regulation of endothelial cell cyclic nucleotide metabolism by prostacyclin. *J. Clin. Invest.* 67: 540-546, 1981.

Imai, A., H. Hattori, M. Takahashi and Y. Nozawa. Evidence that cyclic AMP may regulate Ca^{2+} -mobilization and phospholipases in thrombin-stimulated human platelets. *Biochem. Biophys. Res. Commun.* 112(2): 693-700, 1983.

Ingerman-Wojenski, C.M. and M.J. Silver. Prostacyclin synthesis by endothelial cells from human umbilical veins: Effect of cumulative population doublings. *Prostaglandins* 36(2): 127-137, 1988.

Isaacs, J., N. Savion, D. Gospodarowicz and M.A. Shuman. Effect of cell density on thrombin binding to a specific site on bovine vascular endothelial cells. *J. Cell Biol.* 90: 670-674, 1981.

Ives, C.L., S.G. Eskin, L.V. McIntire and M. E. DeBaakey. The importance of cell origin and substrate in the kinetics of endothelial cell alignment in response to steady flow. *Trans. Am. Soc. Artif. Intern. Organs* 29: 269-274, 1983.

Jaffe, E.A., R.L. Nachman, G.C. Becker and C.R. Minick. Culture of human endothelial cells derived from umbilical veins. *J. Clin. Invest.* 52: 2745-2756, 1973.

Janecki, A., A. Jakubowiak and A. Steinberger. Study of the dynamics of Sertoli cell secretions in a new superfusion, two-compartment culture system. *In Vitro Cell. Develop. Biol.* 23(7): 492-500, 1987.

Jo, H., R.O. Dull, J.M. Tarbell and T.M. Hollis. Hydraulic conductivity and shear dependent albumin permeability of cultured endothelial cell monolayers. *Proceedings of the Second International Symposium on Biofluid Mechanics and Biorheology.* Munich, West Germany. 255-266. June 25-28, 1989.

Kawahara, Y., J. Yamanishi and H. Fukuzaki. Inhibitory action of guanosine 3',5'-monophosphate on thrombin-induced calcium mobilization in human platelets. *Thrombosis Res.* 33: 203-209, 1984.

Killackey, J.J.F., M.G. Johnston and H.Z. Movat. Increased permeability of microcarrier-cultured endothelial monolayers in response to histamine and thrombin. *Am. J. Pathol.* 122: 50-61, 1986.

Knuckel, R., J. Feichtinger, A. Recktenwald, H.G. Hollweg, P. Franke, G. Jakse, E. Rammel and F. Hofstadter. Interactions between bladder tumor cells as tumor spheroids from the cell line J82 and human endothelial cells in vitro. *J. Urol.* 139 (3): 640-645, 1988.

Langille, B.L. and F. O'Donnell. Reductions in arterial diameter produced by chronic decreases in blood flow are endothelium-dependent. *Science* 231: 405-407, 1986.

Laposata, M., D.K. Dohnarsky and H.S. Shin. Thrombin-induced gap formation in confluent endothelial cell monolayers in vitro. *Blood* 62(3): 549-556, 1983.

Larson, D.M. and J.D. Sheridan. Intercellular junctions and transfer of small molecules in primary vascular endothelial cultures. *J. Cell Biol.* 92: 183-191, 1982.

Lawrence, M.B., C.W. Smith, S.G. Eskin and L.V. McIntire. Effect of venous shear stress on CD18-mediated neutrophil adhesion to cultured endothelium. *Blood* 75(1): 227-237, 1990.

Leitman, D.C., R.R. Fiscus and F. Murad. Forskolin, phosphodiesterase inhibitors, and cyclic AMP analogs inhibit proliferation of cultured bovine aortic endothelial cells. *J. Cell. Physiol.* 127: 237-243, 1986.

Lerea, K.M., J.A. Glomset and E.G. Krebs. Agents that elevate cAMP levels in platelets decrease thrombin binding. *J. Biol. Chem.* 262 (1): 282-288, 1987.

Levin, E.G., U. Marzec, J. Anderson and L.A. Harker. Thrombin stimulates tissue plasminogen activator release from cultured human endothelial cells. *J. Clin. Invest.* 74: 1988-1995, 1984.

Levine, J.D., J.M. Harlan, L.A. Harker, M.L. Joseph and R.B. Counts. Thrombin-mediated release of factor VIII antigen from human umbilical vein endothelial cells in culture. *Blood* 60: 531-534, 1982.

Levitzki, A. From epinephrine to cyclic AMP. *Science* 241: 800-806, 1988.

Lloyd, C.J., D.A. Cary and F.A.O. Mendolsohn. Angiotensin converting enzyme induction by cyclic AMP and analogues in cultured endothelial cells. *Mol. Cell. Endocrinol.* 52: 219-225, 1987.

Lo, S.K., K.E. Burhop, J.E. Kaplan and A.B. Malik. Role of platelets in maintenance of pulmonary vascular permeability to protein. *Am. J. Physiol.* 254 (Heart Circ. Physiol. 23): H763-H771, 1988.

Lum, H., P.J. Del Vecchio, A.S. Schneider, M.S. Goligorsky and A.B. Malik. Calcium dependence of the thrombin-induced increase in endothelial albumin permeability. *J. Appl. Physiol.* 66(3): 1471-1476, 1989.

Machovich, R. Choices among the possible reaction routes catalyzed by thrombin. *Ann. NY Acad. Sci.* 485: 170-183, 1986.

Madri, J.A. and S.K. Williams. Capillary endothelial cell cultures: phenotypic modulation by matrix components. *J. Cell Biol.* 97: 153-165, 1983.

Majno, G. and G.E. Palade. Studies on inflammation I. The effect of histamine and serotonin on vascular permeability: An electron microscopic study. *J. Biophys. Biochem. Cytol.* 11: 571-605, 1961.

Makarski, J.S. Stimulation of cyclic AMP production by vasoactive agents in cultured bovine aortic and pulmonary artery endothelial cells. *In Vitro* 17(5): 450-458, 1981.

Menzoian, J.O., C.C. Haudenschild, J.L. Shipman, C.J. Nickerson, R.M. Fuller and A.V. Chobanian. Correction of enhanced endothelial permeability by cessation of cholesterol feeding. *J. Vasc. Surg.* 5(2): 336-341, 1987.

Miller, V.M., L.L. Aarhus and P.M. Vanhoutte. Modulation of endothelium-dependent responses by chronic alterations of blood flow. *Am. J. Physiol.* 251 (Heart Circ. Physiol. 20): H520-H527, 1986.

Mizuno-Yagyu, Y., R. Hashida, C. Mineo, S. Ikegami, S. Ohkuma and T. Takano. Effect of PGI_2 on transcellular transport of fluorescein dextran through an arterial endothelial monolayer. *Biochem. Pharmacol.* 36 (22): 3809-3813, 1987.

Muller, W.A. and M.A. Gimbrone, Jr. Plasmalemmal proteins of cultured vascular endothelial cells exhibit apical-basal polarity: analysis by surface-selective iodination. *J. Cell Biol.* 103 (6 (1)): 2389-2402, 1986.

Mullins, R.J. Bradykinin causes a prolonged increase in skin microvascular permeability. *J. Surg. Res.* 40: 540-549, 1986.

Nagy, L.E., I. Diamond, K. Collier, L. Lopez, B. Ullman, and A.S. Gordon. Adenosine is required for ethanol-induced heterologous desensitization. *Mol. Pharmacol.* 36: 744-748, 1989.

Navab, M., G.P. Hough, J.A. Berliner, J.A. Frank, A.M. Fogelman, M.E. Haberland and P.A. Edwards. Rabbit beta-migrating very low density lipoprotein increases endothelial macromolecular transport without altering electrical resistance. *J. Clin. Invest.* 78: 389-397, 1986.

Nerem, R.M., M.J. Levesque and J.F. Cornhill. Vascular endothelial morphology as an indicator of the pattern of blood flow. *J. Biomechanical Engineering* 103: 172-176, 1981.

Nollert, M.U., E.R. Hall, S.G. Eskin and L.V. McIntire. The effect of shear stress on the uptake and metabolism of arachidonic acid by human endothelial cells. *Biochim. Biophys. Acta* 1005: 72-78, 1989a.

Nollert, M.U., L.V. McIntire, S.G. Eskin and E.R. Hall. Flow effects on human endothelial cell arachidonic acid metabolism and second messenger generation. *Extended Abstracts, AIChE Annual Meeting*, 711, 1989b.

Olesen, S-P, D.E. Clapham and P.F. Davies. Haemodynamic shear stress activates a K⁺ current in vascular endothelial cells. *Nature* 331: 168-170, 1988.

Orlidge, A. and P.A. D'Amore. Inhibition of capillary endothelial growth by pericytes and smooth muscle cells. *J. Cell Biol.* 105: 1455-1462, 1987.

Orr, F.W., M.R. Buchanan, V.A. Tron, D. Guy, D. Lauri and D.N. Sauder. Chemotactic activity of endothelial cell derived interleukin 1 for human tumor cells. *Cancer Res.* 48(23): 6758-6763, 1988.

Owens, C.K., L.V. McIntire and A. Lasslo. Ethanol inhibition of thrombus formation on collagen-coated glass. *Thrombosis and Haemostasis*, in press, 1990.

Palmer, R.M.J., D.S. Ashton and S. Moncada. Vascular endothelial cells synthesize nitric oxide from L-arginine. *Nature* 333:664-666, 1988.

Palmer, R.M.J., A.G. Ferrige and S. Moncada. Nitric oxide release accounts for the biological activity of endothelium-derived relaxing factor. *Nature* 327: 524-526, 1987.

Pastan, I. Regulation of cellular growth. *Adv. Metab. Disorders* 8: 7-16, 1975.

Phillips, P.G. and M-F. Tsan. Hyperoxia causes increased albumin permeability of cultured endothelial monolayers. *J. Appl. Physiol.* 64 (3): 1196-1202, 1988.

Radomski, M.W., R.M.J. Palmer and S. Moncada. Comparative pharmacology of endothelium-derived relaxing factor, nitric oxide and prostacyclin in platelets. *Br. J. Pharmac.* 92: 181-187, 1987 a.

Radomski, M.W., R.M.J. Palmer and S. Moncada. The anti-aggregating properties of vascular endothelium: interactions between prostacyclin and nitric oxide. *Br. J. Pharmac.* 92: 639-646, 1987 b.

Ramirez, C.A., C.K. Colton, K.A. Smith, M.B. Stemerman and R.S. Lees. Transport of ¹²⁵I-albumin across normal and deendothelialized rabbit thoracic aorta in vivo. *Arteriosclerosis* 4: 283-291, 1984.

Robinson, J. and D. Gospodarowicz. Glycosaminoglycans synthesized by cultured bovine corneal endothelial cells. *J. Cell. Physiol.* 117: 368-376, 1983.

Rotrosen, D. and J.I. Gallin. Histamine type-1 receptor occupancy increases endothelial cytosolic calcium, reduces f-actin, and promotes albumin diffusion across cultured endothelial monolayers. *J. Cell Biol.* 103 (6(1)): 2379-2387, 1986.

Rubanyi, G.M., J.C. Romero and P.M. Vanhoutte. Flow-induced release of endothelium-derived relaxing factor. *Am. J. Physiol.* 250 (Heart Circ. Physiol. 19): H1145-1149, 1986.

Schafer, A.I., M.A. Gimbrone, Jr. and R.I. Handin. Endothelial cell adenylate cyclase: activation by catecholamines and prostaglandin I₂. *Biochem. Biophys. Res. Commun.* 96(4): 1640-1647, 1980.

Schlichting, H. *Boundary Layer Theory*. McGraw-Hill, New York. 178. 1968.

Shasby, D.M. and S.S. Shasby. Effects of calcium on transendothelial albumin transfer and electrical resistance. *J. Appl. Physiol.* 60: 71-79, 1986.

Shasby, D.M., S.S. Shasby, J.M. Sullivan and M.J. Peach. Role of endothelial cell cytoskeleton in control of endothelial permeability. *Circ. Res.* 51: 657-661, 1982.

Sibley, D.R., J.L. Benovic, M.G. Caron and R.J. Lefkowitz. Regulation of transmembrane signalling by receptor phosphorylation. *Cell* 48: 913-922, 1987.

Silberberg, A. Structure of the interendothelial cell cleft. *Biorheology* 25: 303-318, 1988.

Sporn, L.A., V.J. Marder and D.D. Wagner. Differing polarity of the constitutive and regulated secretory pathways for von Willebrand Factor in endothelial cells. *J. Cell Biol.* 108: 1283-1289, 1989.

Sprague, E.A., B.L. Steinbach, R.M. Nerem and C.J. Schwartz. Influence of a laminar steady-state fluid-imposed wall shear stress on the binding, internalization, and degradation of low-density lipoproteins by cultured arterial endothelium. *Circulation* 76(3): 648-656, 1987.

Stelzner, T.J., J.V. Weil and R.F. O'Brien. Role of cyclic adenosine monophosphate in the induction of endothelial barrier properties. *J. Cell. Physiol.* 139: 157-166, 1989.

Stewart, P.A. and M.J. Wiley. Developing nervous tissue induces formation of blood brain barrier characteristics in invading endothelial cells: a study using quail-chick transplantation chimeras. *Dev. Biol.* 84: 183-192, 1982.

Stoll, L.L. and A.A. Spector. Lipid transfer between endothelial and smooth muscle cells in coculture. *J. Cell. Physiol.* 133: 103-110, 1987.

Stossel, T.P. From signal to pseudopod: how cells control cytoplasmic actin assembly. *J. Biol. Chem.* 264 (31): 18261-18264, 1989.

Stout, R.W. Cyclic AMP: a potential inhibitor of DNA synthesis in cultured arterial endothelial and smooth muscle cells. *Diabetologia* 22: 51-55, 1982.

Tournier, J.F., A. Lopez, N. Gas and J. F. Tocanne. The lateral motion of lipid molecules in the apical plasma membrane of endothelial cells is reversibly affected by the presence of cell junctions. *Exp. Cell Res.* 181: 375-384, 1989.

Thornton, S.C., S.N. Mueller and E.M. Levine. Human endothelial cells: use of heparin in cloning and long-term serial culture. *Science* 222: 623-625, 1983.

Unemori, E.N., K.S. Bouhana and Z. Werb. Vectorial secretion of extracellular matrix proteins, matrix-degrading proteinases, and tissue inhibitor of metalloproteinases by endothelial cells. *J. Biol. Chem.* 265 (1): 445-451, 1990.

van Buul-Wortelboer, M.F., H.J.M. Brinkman, K.P. Dingemans, Ph. G. DeGroot, W.G. van Aken and J.A. van Mourik. Reconstitution of the vascular wall in vitro: a novel method to study interactions between endothelial and smooth muscle cells. *Exp. Cell Res.* 162: 151-158, 1986.

Voyta, J.C., D.P. Via, C.E. Butterfield and B.R. Zetter. Identification and isolation of endothelial cells based on their increased uptake of acetylated-low density lipoprotein. *J. Cell Biol.* 99: 2034-2040, 1984.

Wang, Z-W., T. Irimura, M. Nakajima, P.N. Belloni and G.L. Nicolson. Characterization of extracellular matrix-associated glycosaminoglycans produced by untransformed and transformed bovine corneal endothelial cells in culture. *Eur. J. Biochem.* 153: 125-130, 1985.

Weinbaum, S., G. Tzeghai, P. Ganatos, R. Pfeiffer and S. Chien. Effect of cell turnover and leaky junctions on arterial macromolecular transport. *Am. J. Physiol.* 248 (Heart Circ. Physiol. 17): H945-H960, 1985.

Weksler, B.B., C.W. Ley and E.A. Jaffe. Stimulation of endothelial cell prostacyclin production by thrombin, trypsin, and ionophore A23187. *J. Clin. Invest.* 62: 923-930, 1978.

Welles, S.L., D. Shepro and H.B. Hechtman. Eicosanoid modulation of stress fibers in cultured bovine aortic endothelial cells. *Inflammation* 9 (4): 439-450, 1985a.

Welles, S.L., D. Shepro and H.B. Hechtman. Vasoactive amines modulate actin cables (stress fibers) and surface area in cultured bovine endothelium. *J. Cell Physiol.* 123: 337-342, 1985b.

White, G.E., K. Fujiwara, E.J. Shefton, C.F. Dewey, Jr. and M.A. Gimbrone, Jr.. Fluid shear stress influences cell shape and cytoskeletal organization in cultured vascular endothelium. *Fed. Proc.* 41: 321, 1982

Yanagisawa, M., H. Kurihara, S. Kimura, Y. Tomobe, M. Kobayashi, Y. Mitsui, Y. Yazaki, K. Goto and T. Masaki. A novel potent vasoconstrictor peptide produced by vascular endothelial cells. *Nature* 332: 411-415, 1988.

Zerwes, H-G. and W. Risau. Polarized secretion of a platelet-derived growth factor-like chemotactic factor by endothelial cells in vitro. *J. Cell Biol.* 105: 2037-2041, 1987.

APPENDIX

```

dimension dpm(20,4,10),tp(4,10),time(10),ss(4,10),q(4,10),
+ qr(4,10),qrl(4,10),x(4,10),dpmia(20),ippp(1)
open (unit=8,file='cal.dat',status='unknown')
open (unit=7,file='con.dat',status='unknown')
write(6,50)
50 format(/,5x,'enter date of experiments(mmddyy)')
read(5,*)idate
write(6,100)
100 format(/,10x,'enter no of experiments (1 - 20)')
read(5,*)nie
write(6,110)
110 format(/,5x,'enter no of plots per experiment (1,2,3 or 4)')
read(5,*)np
write(6,120)np
120 format(/,5x,'for ',il,' plots,enter no of points for each')
read(5,*)(ippp(1),i=1,np)
read(7,*)(dpmia(x),x=1,nie)
a=4.524
samvol=0.2
nsam=isp
sint=8
write(8,190)idate
190 format(/,/,/,10x,'date of experiments = 'i6)
do 500 jj=1,nie
vl=1.0
vs=4.0
write(8,200)jj
200 format(/,/,/,15x,'experiment no ',i2)
do 495 io=1,np
nipp=ippp(io)
if(io .eq. 2) vl=vl+0.015
if(io .eq. 2) vs=vs+0.060
if(io .eq. 3) vl=vl+0.015
if(io .eq. 3) vs=vs+0.060
if(io .eq. 4) vl=vl+0.015
if(io .eq. 4) vs=vs+0.060
read(7,*)(dpm(jj,io,nn),nn=1,nipp)
tp(1,1)=dpmia(jj)
tp(1,2)=tp(1,1)
do 400 ii=1,nipp
time(ii)=(ii*sint) - 0.0
if(ii .eq. 1)go to 390
if((ii .eq. 2) .and. (io .eq. 1))go to 390
iii=ii-1
tp(io,ii)=tp(io,iii)-(samvol*dpm(jj,io,iii))
390 continue
q(io,ii)= 1 -(vl+vs)*dpm(jj,io,ii)/tp(io,ii)
qr(io,ii)=1/q(io,ii)
if(qr(io,ii) .le. 0) go to 393
qrl(io,ii)=alog(qr(io,ii))
go to 394
393 qrl(io,ii)=0.0
394 x(io,ii)=(60*a*(vs+vl)*time(ii))/(vs*vl)
write(8,395) time(ii),dpm(jj,io,ii),tp(io,ii),
+ qrl(io,ii),x(io,ii)
395 format(/,5x,f6.1,3x,f9.2,3x,f10.1,3x,
+ f8.5,3x,f9.1)
400 continue

```

```

if(io .eq. np) go to 410
ion = io + 1
tp(ion,1) = tp(io,nippp) - (samvol*dpm(jj,io,nippp))
410  ym=0.0
      xm=0.0
      syic=0.0
      sxic=0.0
      rn= 1.0 + nippp
      sxy=0.0
      sxs=0.0
      sys=0.0
      do 450 ic=1,nippp
        sxic=sxic + x(io,ic)
        syic= syic + qrl(io,ic)
        sxy=sxy + x(io,ic)*qrl(io,ic)
        sxs=sxs + x(io,ic)**2
        sys=sys + qrl(io,ic)**2
450  continue
      xm=sxic/rn
      ym=syic/rn
      betal = (rn*sxy - sxic*syic)/(rn*sxs - sxic**2)
      beta0 = ym - betal*xm
      cc=(rn*sxy-sxic*syic)/sqrt((rn*sxs-sxic**2)*(rn*sys-syic**2))
      write(8,475) betal,beta0,cc
475  format(/,7x,'PC = ',e10.3,'cm/sec',3x,'y-int = ',f6.3,3x,'cc = ',
+i7.4)
      recip = 1/betal - 1.0/0.0000352
      pcec = 1/recip
      write(8,480) pcec
480  format(/,12x,'PCec = ',e10.3)
495  continue
500  continue
      close(unit=9)
      close(unit=7)
      stop
      end

```

date of experiments = 61789

experiment no 1

0.0	0.00	251221.0	0.00000	0.0
8.0	961.36	251221.0	0.01932	2714.4
16.0	2450.84	251028.7	0.05005	5428.8
24.0	2866.30	250538.6	0.05890	8143.2

PC = $0.764E-05$ cm/sec y-int = 0.001 cc = 0.9813

PCec = $0.976E-05$

0.0	5615.58	249965.2	0.12105	0.0
8.0	6711.53	248842.2	0.14720	2674.3
16.0	6487.23	247499.9	0.14274	5348.6
24.0	7639.15	246202.4	0.17134	8022.9

PC = $0.547E-05$ cm/sec y-int = 0.124 cc = 0.9165

PCec = $0.648E-05$

0.0	9036.15	244674.6	0.18530	0.0
8.0	8401.12	243067.4	0.19601	2635.3
16.0	8510.28	241387.1	0.20036	5270.7
24.0	8407.75	239685.1	0.19925	7906.0

PC = $0.175E-05$ cm/sec y-int = 0.188 cc = 0.8677

PCec = $0.194E-05$

0.0	9816.70	238003.5	0.24272	0.0
8.0	9698.72	236040.2	0.24140	2597.5
16.0	10806.50	234102.4	0.27601	5195.0
24.0	11617.60	231941.1	0.30342	7792.5

PC = $0.834E-05$ cm/sec y-int = 0.232 cc = 0.9427

PCec = $0.109E-04$